



# **DEVELOPMENT OF PLANTS REPORTING ER STRESS IN REAL TIME**

## **MASTER'S THESIS**

Submitted by  
**Janet BAKALARZ**

October 2019

Department of Applied Genetics and Cell Biology  
University of Natural Resources and Life Sciences, Vienna

### **Supervised by:**

Univ. Prof. Mag. Dr.rer.nat. Eva STÖGER  
and Stanislav MELNIK, PhD

Department of Applied Genetics and Cell Biology  
University of Natural Resources and Life Sciences, Vienna

### **Co-supervised by:**

Prof. Snježana KEREŠA, PhD  
Department of Plant Breeding, Genetics and Biometrics  
University of Zagreb - Faculty of Agriculture

## **Affidavit**

I hereby swear that I have compiled this Master's Thesis without external help and without using sources and aides other than those permitted and that the sources have been cited verbatim or quoted textually in the places indicated. This work has not been submitted in the same or similar form to any other examiners as a form of examination. I am aware that offenders may be punished ('use of unauthorized assistance') and that further legal action may ensue.

Date

Signature

## Acknowledgement

First of all, my deepest gratitude goes to my primary supervisor and group leader Dr. Eva Stöger. When I was reaching out to numerous professors for thesis topics, she offered me to contribute to a project fitting my background and interest without hesitations. I highly appreciate the received trust enabling me to work in the trending field of molecular farming with my favorite test subject, being *N. benthamiana*. Despite the medley of different ideas, I came along with knocking at Eva's door, she always had an open ear for my concerns. She was patient with me while providing me with helpful input to keep me on the right path.

As second, I would like to thank Dr. Stanislav Melnik for not only being my practical supervisor but also for becoming my mentor. I had the great opportunity to profit from his endless knowledge about seemingly every method and technique ever developed by humanity, or at least in molecular biology. Combined with continuously sharing his wisdom, he provided me with the necessary skill-set and the confidence to succeed with my own cloning adventures. Despite being always busy, he showed me his proper lab manners and taught me how to approach different research questions. He left me enough room for my own plans encouraging me to find solution for given problems. In though phases, Stani was always available for any question at any time and kept me motivated. With his endless pool of information, he did not only supervise me but is constantly helping and supporting fellow researchers and other students. I was very lucky with such a knowledgeable supervisor who also became a good friend of mine.

My next acknowledgements go to Dr. Julia Hilscher and Dr. Elsa Arcalis. Juli is not only a fun person, I had many good laughs with, she is also a good teacher giving me many insights in her methodology with *A. thaliana*. In particular, she supported the generation of transgenic plants for this thesis. The microscopy expert in the group, Elsa taught me to prepare leaf samples, as well as how to use epifluorescence and confocal microscopes. Thanks to her, this thesis includes some beautiful confocal pictures.

Furthermore, I would like to thank the whole group where I was welcomed by not only highly skilled but lovely people with a great team spirit. Hereby, I would like to mention Dr.rer.nat. Eszter Kapusi, Mag. Ulrike Hörmann-Dietrich, DI Marc Tschofen, DI Jennifer Schwestka and Lukas Zeh. Together with the numerous Bachelor students, the easy-going work environment provides the feeling that no difficulty has to be faced alone.

In addition, I have to thank Dr. Snježana Kereša to take up the co-supervision of my thesis on a short notice. I highly appreciate her cooperation and diligence.

Last but not least, I owe a debt of gratitude to my family and friends. My parents' emphasis on hard work and perseverance during my youth taught me that I can achieve any goal, no matter what I intend. In this case, I have finished a prolonged Master's thesis. During this busy year, I was allowed to air my frustrations, while making myself rare. Nevertheless, my friends kept inquiring about my well-being and my whereabouts keeping my spirits and motivation up.

## Abstract

Plant molecular farming stands for the production of recombinant pharmaceutical proteins using genetically modified plants. This advancing technology exploits plants, such as tobacco, to produce medically relevant proteins. Most of these proteins are directly translated into the ER lumen when produced in plant cells. However, heterologous protein overexpression can lead to ER stress, so-called UPR. When UPR is unresolved, it causes PCD observable as necrosis on plant tissue. UPR constitutes an obstacle in molecular farming, but its regulatory mechanisms in plants are not well known yet. Therefore, the idea rose to develop a molecular tool enabling the visualization of UPR *in planta*. In this thesis, advantages were taken from elaborated studies on UPR in different organisms. One branch of plant UPR is transduced by an interesting mechanism: unconventional splicing of *bZIP60* mRNA. To exploit this activation mechanism, bZIP60 was taken as basis for a molecular sensor. GFP was fused to the C-terminus while considering frameshift caused by previous splicing. The initial sensor constructs were transiently tested in *N. benthamiana*. The fluorescent reporting system of the sensor was designed to emit a signal upon UPR induction. The signal was observable with a microscope making the sensor a convenient *in planta* tool for UPR detection. Different parts for the sensor were in investigation: necessary bZIP60 domains, inducible promoters and later optimized FP. It was proved that both the intron region and the HR domain are necessary for efficient unconventional splicing and in turn activation of the bZIP60-based sensor. The preliminary drawback of the first sensor variants was a relatively low signal to background ratio, which was approached by testing different UPR-inducible promoters. One outcome was a sensor prototype being already functional in plants. However, concrete improvements are needed to enable dynamic studies of UPR on cellular level *in planta*.

## List of Abbreviations

'	Seconds
"	Minutes
A	Adenine
<i>A. thaliana</i>	<i>Arabidopsis thaliana</i>
<i>A. tumefaciens</i>	<i>Agrobacterium tumefaciens</i>
B cell	B lymphocyte
BAG7	B-cell lymphoma-2-associated athanogene 7
BiPs	Binding Proteins
bp	Base pairs
BrBlue	Bromophenol Blue
bZIP	Basic Leucine Zipper
C	Cytosine
CaMV	Cauliflower mosaic virus
cDNA	Complementary deoxyribonucleic acid
CHO	Chinese Hamster Ovary
DARPA	Defense Advanced Research Projects Agency
DNA	Desoxyribonucleic acid
dNTPs	Desoxynucleoside triphosphate
dpi	Days post-infiltration
dT	Desoxythymidine
DTT	Dithiothreitol
<i>E. coli</i>	<i>Escherichia coli</i>
EDTA	Ethylenediaminetetraacetic acid
eGFP	Enhanced green fluorescent protein
ER	Endoplasmic reticulum
ERSE	ER stress responsive cis-elements
EU	European Union
Fab	Antigen-binding fragment
EFM	Epi-fluorescence microscope
FP	Fluorescent protein
G	Guanine
gDNA	Genomic deoxyribonucleic acid
GM	Genetically modified
GMP	Good Manufacturing Practice
h	Hours
HAC1	Homologous to Atf/Creb1
HC	Heavy chain
HIV	Human immunodeficiency viruses
hpi	Hours post-infiltration
HR	Hydrophobic region
Ig	Immunoglobulin
IRE1	Inositol-requiring enzyme 1
LanYFP	Yellow fluorescent protein from <i>B. lanceolatum</i>
LB media	Lysogenic broth
LB	Left border
LC	Light chain
mAbs	Monoclonal antibodies
MCS	Multiple cloning site

MES	2-morpholin-4-yl-ethanesulfonic acid
mRNA	Messenger Ribonucleic acid
MS	Murashige and Skoog
<i>N. benthamiana</i>	<i>Nicotiana benthamiana</i>
<i>N. tabacum</i>	<i>Nicotiana tabacum</i>
NAC	No apical meristem (NAM), Arabidopsis transcription activation factor (ATAF), and Cup-shaped cotyledon (CUC)
NOS	Nopaline synthase
nt	Nucleotides
OD	Optical density
ORF	Open reading frame
PCD	Programmed cell death
PCPs	Plant Cell Packs
PCR	Polymerase chain reaction
PHU	Phusion polymerase
PMPs	Plant-made pharmaceuticals
qPCR	Quantitative polymerase chain reaction
RB	Right border
R-RNC	mRNA-ribosome-nascent chain
RT	Reverse Transcriptase
<i>S. cerevisiae</i>	<i>Saccharomyces cerevisiae</i>
SAR	Scaffold attachment region
T	Thymine
Ta	Annealing temperature
T-DNA	Transferable deoxyribonucleic acid
TM	Tunicamycin
TMD	Transmembrane domain
UPR	Unfolded Protein Response
UV	Ultraviolet
V	Volt
VFU	Vertical Farming Units
XBP1	X-box binding protein 1
YEB	Yeast Extract Beef

## Table of contents:

Affidavit.....	1
Acknowledgement.....	2
Abstract .....	3
List of Abbreviations.....	4
Introduction .....	7
1. Plant molecular farming .....	7
2. Technical aspects of production systems using tobacco and friends .....	14
3. Bottlenecks of recombinant protein expression.....	19
Research Aim .....	24
1. Problem statement: The link between plant UPR and molecular farming.....	24
2. Scope of this thesis: Development of an UPR reporting tool in plants.....	24
3. Objective: bZIP60-based sensor visualizing UPR with FP .....	25
Materials and Methods.....	26
1. Design of primers for bZIP60 sensor .....	26
2. Preparations of primers, vectors and genomic material .....	27
3. Cloning protocols for isolation and modifications of <i>NbZIP60</i> .....	29
4. Agroinfiltration experiments .....	35
5. Protein extraction .....	35
6. Solutions and Buffers .....	36
7. Floral dip of <i>Arabidopsis</i> after Zhang et al. 2006.....	37
Results and Discussion.....	38
1. Design of sensor variants on basis of endogenous <i>NbZIP60</i> with FP reporter .....	38
2. Transient testing of sensor variants .....	43
3. Further development of sensor for better sensitivity.....	51
4. Next steps in sensor development regarding reporter.....	59
5. Generation of transgenic plants carrying a sensor construct.....	61
6. Co-expression experiments .....	63
Conclusion .....	66
Appendix.....	68
1. Sequencing results from <i>bZIP60</i> isolation.....	68
2. Plasmid maps.....	71
3. Pictures of false positive signals emitted from leaf tissue under UV lamp .....	72
4. Structure of JBE22s - the second positive control sensor variant.....	73
5. Pictures from confocal microscopy .....	73
List of Figures and Tables .....	74
Publication bibliography .....	75

# Introduction

## 1. Plant molecular farming

### 1.1. Tobacco for health

Tobacco smoking affects the respiratory tracts, eventually leading to cancer and premature deaths. The consumption of tobacco products still constitutes a major global health threat. The harmfulness of the tobacco smoking is due to the inherent nicotine content with extremely high addictive potential (West 2017). Nevertheless, this plant entered the focus of researchers in order to exploit its potential for solving public health issues. In 2008, the pharma-chemical company Bayer announced under the provocative slogan “Tobacco for Health” its new research venture in the area of plant-made vaccines. Together with ICON Genetics, they reached the clinical phase for such a vaccine in 2010, a premise for the future market launch of tobacco deriving health products. The underlying technology enables efficient production of pharmaceuticals from tobacco plant (Icon Genetics 1/28/2010). Bayer’s directive promoted the development of plant-made pharmaceuticals (PMPs) world-wide. A particular collaboration with BOKU led to the generation of tobacco plants capable of producing human-like antibodies. These genetically engineered plants were then used by MAPP Biopharmaceuticals to produce an antibody cocktail upon agroinfiltration (Castilho et al. 2011; Zeitlin et al. 2011). Within weeks, these tobacco plants grown in greenhouses were infiltrated to produce sufficient amounts of the active components for ZMapp, a drug against the Ebola virus. This plant-derived vaccine was approved as an experimental drug by the FDA during the Ebola outbreak in 2014 (Largent 2016). Currently, the EU-funded project NEWCOTIANA has the intention to exploit two tobacco species, the cultivated *Nicotiana tabacum* and its wild relative *Nicotiana benthamiana*. The objective is to use New Plant Breeding Techniques to genetically engineer these plants to be better suited for the production of valuable substances for medicine and cosmetics. Thereby, tobacco plants should evolve from primary smoking products with nicotine, to pharmaceutical crops (<https://newcotiana.org>).

### 1.2. Molecular farming: Origins and milestones

These undertakings fall under the technological umbrella term: plant molecular farming. It stands for the production of recombinant pharmaceutical proteins using genetically modified (GM) plants (Stoger et al. 2014). Plants meant for molecular farming fall into the third generation of GM plants. Instead of generating food crops, the aim of those engineered plants is to produce proteins and other small molecules with medical relevance, or for industrial needs. Crop plants as tobacco, which are not meant for human consumption, constitute ideal candidates to avoid competition with food (Buiatti et al. 2012). The term molecular farming, or former molecular pharming, came in use due to its original objective to become an alternative in pharmaceutical manufacturing (Martinis et al. 2016). Its story began in 1986 with a functional human growth hormone being produced in tobacco and sunflower (Barta et al. 1986). A few years later, full-size antibodies being functional in humans were reported to be successfully produced in plants (Hiatt et al. 1989). This achievement was followed a year later by the first recombinant protein, serum albumin, being expressed in potato and tobacco (Sijmons et al. 1990). These studies paved the way for further developments to exploit the potential in plant genetic engineering for molecular farming. In the 2010s, a variety of proteins proved to be producible in transgenic plants; many were reaching clinical trials and the first plant-made proteins had entered the market. In Europe, the development of a monoclonal HIV-neutralizing antibody produced in tobacco was in focus. In the field of HIV therapeutic production, a great economic potential was expected from plant-based platforms. Current manufacturing of HIV antibodies is very costly and as a consequence, preventive measures or therapies against HIV are non-accessible for many people world-wide (Ma et al. 2013). A consortium of researchers proved that plant-based



production of pharmaceuticals is compatible with pharmaceutical manufacturing standards. They had established GMP guidelines for producing antibodies in tobacco leading to the first approval for clinical trials of a plant-derived monoclonal antibody against HIV, paving the way for more PMPs (Ma et al. 2015). Since GMP is the global standard in the pharmaceutical industry, this was an important step to acquire the necessary regulatory approval for the commercialization of PMPs (Stoger et al. 2014). Meanwhile, on the other side of the Pacific, the American Defense Advanced Research Projects Agency (DARPA) supported the advancement of molecular farming by backing the funding of a large-scale plant-production system. The target was to enable the rapid production of antigens against influenza virus to accommodate the American population in case of need (Paul et al. 2015). Vaccines against the highly mutagenic virus are ideal candidates to be produced through plant production systems. The production of recombinant antibodies through transient expression in *N. benthamiana* plants grown in greenhouses proved to be efficiently and readily scalable to meet sudden demands (Sack et al. 2015). As a result, in 2015, one of the world's largest facilities manufacturing PMPs allowed the production of 10million doses of vaccines per month in case of an epidemic (Holtz et al. 2015). In the same period, the Israeli company Protalix Biotherapeutics had developed a plant-made drug to treat a rare genetic disorder, type 1 Gaucher's disease. The drug is a recombinant enzyme deriving from a human lysosomal enzyme. The recombinant protein was named taliglucerase alfa and was approved for the American market by the FDA under the trade name ELELYSO (Rub et al. 2017). This was the first plant derived protein receiving the commercial approval by a regulatory agency (Mor 2015; Donini and Marusic 2019). These milestones fueled further progress in molecular farming, leading to the exploitation of unique opportunities deriving from plant systems.

### 1.3. Initial farming for recombinant antibodies

#### 1.3.1. Quick revision on antibodies

Antibodies are glycoproteins of the immunoglobulin (Ig) superfamily, having diverse sugar residues, called glycans. As part of the mammalian immune system, they are secreted by B cells upon detection of foreign antigens from pathogens. Antibodies constitute of two light and two heavy chains, each with hypervariable regions forming together the antigen-binding site. The hypervariable regions alone are designated as fragment antigen-binding domain (Fab) and specifically bind to antigens. The constant domains are responsible for effector functions. During an immune response in animals, antibodies of polyclonal nature are generated, targeting multiple antigens. In the 1970s, researchers produced for the first time monoclonal antibodies (mAbs) *in vitro* by using murine cell cultures, known as hybridoma (Buss et al. 2012). In contrast to polyclonal antibodies, mAbs have all the same Fab recognizing only one epitope, but with greater specificity. The homogenous nature of mAbs allows precise prediction of binding characteristics, making them useful tools for immunological studies. Over the years, the main application of mAbs was in diagnostics. Their high specificity allows the detection and identification of any given substance, from blood and cellular markers, to pathogens (Nelson et al. 2000). While polyclonal antibodies are produced in animals, mAbs can only be synthesized in cell cultures, such as hybridoma. Bacteria, most famously *Escherichia coli*, are also common expression hosts to generate recombinant proteins. In the case of antibodies, it was shown that the respective genes for the light and heavy chain can be combined in a vector followed by successful expression in *E. coli*. However, the chain peptides turned out to be insoluble, hence non-functional and had to undergo further processing to achieve the same antigen-binding activity comparable to antibodies derived from hybridoma (Boss et al. 1984). Therefore, bacteria are limited to the production of simple polypeptide structures, such as insulin, simple antibodies and antibody fragments, which fold spontaneously. Most antibodies have a complex structure requiring glycosylation, chaperone-guided folding and catalyzation of disulfide bonds. The necessary post-translational machinery is naturally missing in prokaryotes. Therefore, mammalian cell systems are the favored production platform for recombinant antibodies over bacteria (Tschofen et al. 2016).

### 1.3.2. *Plant-made recombinant antibodies*

Recombinant antibodies and their fragments advanced as key players in modern medicine, composing a large portion of available therapeutic proteins. For instance, their application is of great importance in cancer diagnosis, immunotherapy and gene therapy (Hudson 1999). The early goal of plant molecular farming was to become an alternative to produce such medically relevant proteins to fight public health issues. Besides antibodies, also recombinant enzymes, growth factors, cytokines, as well as antigens are manufactured in plants for the purpose of treating or preventing infectious and chronic diseases (Stoger et al. 2014). Since its beginnings, plant molecular farming has been described as a promising vehicle to advance the manufacturing of recombinant antibodies for pharmaceutical applications. These recombinant proteins are traditionally produced in fermenters using mammalian cells, a production system with high demands regarding sterility and containment (Donini and Marusic 2019). The golden standard platform nowadays, to produce antibodies, remains Chinese hamster ovary (CHO) cells cultured in bioreactors. The installation of appropriate containers and their maintenance is cost-intensive. The economic factor was the initial driver of the exploitation of plant-based platforms (Kunert and Reinhart 2016). Nowadays, many plant-based production platforms have been established, complementing conventional manufacturing systems in the pharmaceutical field. To date, plant systems proved to have many technical advantages (Donini and Marusic 2019). Plants allow controlled glycosylation, increasing biosafety for human applications. Moreover, past cases demonstrated the rapid scalability, lowering costs compared to other production systems discussed below in more detail.

## 1.4. Specific advantages of plants

### 1.4.1. *Glycosylation and controlling factors*

Higher eukaryotic organisms have the cellular make-up, including specialized enzymes for a secretory pathway allowing post-translational modifications of glycoproteins, such as antibodies. Besides correct folding and disulfide bonds, the key modification, which determines the quality of antibodies, is glycosylation. Glycosylation is the addition of various glycans to proteins through glycosyltransferases. Glycans influence the stability, structure and immunogenicity, while having an impact on function and activity of antibodies (Stoger et al. 2014). N-glycosylation processes in the ER lumen are conserved among all eukaryotes. The subsequent modifications in the Golgi apparatus differ among plant and animal cells, leading to distinct glycan structures, called glycoforms. Plant-specific glycans carry the potential to induce immune responses in humans. Therefore, the glycoforms in plants differing from mammals were considered as the major limitation for PMPs (Gomord et al. 2010). In the 1990s, it was shown with transgenic tobacco plants that the glycosylation machinery in plant cells is appropriate for the expression and assembly of complex recombinant proteins (Ma et al 1995). Advances in the areas of protein targeting and glycoengineering enabled controlled glycosylation. Thus, the production of recombinant antibodies with custom-made glycans became reality in plants. *N. benthamiana* proved to be exceptionally receptive for glycoengineering, making it a promising host plant in molecular farming. On the one hand, using tags for subcellular targeting can directly control glycosylation. Undesired glycosylation processes are avoided by targeting recombinant proteins to certain cell compartments. On the other hand, glycoengineering is another multiverse strategy to manipulate glycosylation. The deletion or gain of genes encoding glycosyltransferases can directly modulate the glycosylation, allowing to generate glyco-optimized proteins, which naturally could never be produced in plants (Strasser et al. 2014). In regards to controlling glycosylation processes, plants provide an inherent advantage in comparison with animal cells. Hundreds of N-linked glycoforms are reported in mammals, indicating that their N-glycosylation machinery is more complex compared to plants, where only few N-glycans are found. The high heterogeneity of glycoforms in mammalian cells provokes inconsistencies between glycoprotein batches. This is a huge drawback, since highly specific recombinant antibodies with a high degree of homogeneity are a requisite for most applications. Moreover, a complex system is more difficult

to modify, making glycoengineering more straightforward in plants. Through optimization of glycosylation pathways in plants, it became possible to produce glycoforms with great homogeneity suitable for human applications (Castilho et al. 2011; Zeitlin et al. 2011). Controlled glycosylation reduces biosafety risks, which may facilitate regulatory approval. Moreover, glycoengineering in plants allow to significantly improve the functionality of produced mAbs (Montero-Morales and Steinkellner 2018). The famous ZMapp therapeutic was composed of three neutralizing antibodies produced in a glycoengineered *N. benthamiana* strain missing certain glycosyltransferases (Donini and Marusic 2019).

#### 1.4.2. *Encapsulation enables edible vaccines*

One innovative product idea using the potential of molecular farming was the production of edible vaccines in plant organs, such as bananas (Menassa et al. 2012). Plant tissues are digestible and hence suitable for oral uptake by animals and humans. This fact opens the opportunity for new delivery strategies of therapeutic proteins. Oral delivery is in many cases, more convenient than subcutaneous injections. Especially in cases of drugs that require daily administration, oral uptake of vaccines would be beneficial due to lower hygiene premises. Moreover, the harsh conditions for proteins in the gastrointestinal tract are one of the main considerations for orally delivered therapies. Protective coatings for drugs are an established tool to ensure the arrival at the destination site. When plants store proteins in cell organelles, the encapsulating membrane of the latter serves as a protective layer (Sack et al. 2015). The approach to encapsulate therapeutic proteins in plant matrix for oral delivery is also economically interesting regarding the potential to reduce expensive downstream processes. Encapsulated proteins in certain plant matrices can be easier to formulate, while being effective as oral vaccines. For instance, encapsulated antigens in plant cells taken up by mucosal cells conferred systemic and active immunity similar to vaccine injections (Kwon et al. 2013). Furthermore, the exploitation of edible plant organs, such as fruits, leaves, seeds, tubers, or roots opens the possibility of „edible vaccines.“ The possibility of producing recombinant proteins, such as antibodies, in edible tissues would enable direct oral uptake, minimizing processing (Virdi and Depicker 2013). Recombinant protein production cannot only be limited to particular plant cells or tissues, but also to different cellular compartments. Evolution of plants resulted in many different storage organelles, whereas cereal seeds and potato tubers show excellent stability features. While seeds are long term storable and insensitive to temperature changes, they are digestible, allowing the release of their content. Therefore, special storage organelles in seeds deriving from the endomembrane system and the endoplasmic reticulum (ER) itself are often targeted for the production of encapsulated recombinant proteins (Stoger et al. 2014).

#### 1.4.3. *Promises regarding production costs and scalability*

Besides the drawbacks of conventional systems on a molecular level compared to plant cells, plant production systems are promised to lower the costs for biopharmaceutical manufacturing. Despite molecular farming being a young field and the limited commercial applications yet, the investment costs for plant-based production platforms are assumed to be significantly lower, more than 50%, than their mammalian counterparts (Nandi et al. 2016). Nevertheless, not all initial promises could be kept since field cultivation turned out to be unfeasible. The original idea of molecular farming was growing plants in open fields and the biomass achieved by closely grown tobacco plants is indeed significant. The nutrient requirements for plant based systems are minimal compared to mammalian cell based systems because plants need mostly only water and light (Stoger et al. 2014). However, pharmaceutical production standards require controlled conditions, which are only attainable under containment. The solution is greenhouses where plants grow in contained conditions complying with GMP without the need of stringent sterility. The development of vertical farming units (VFU) in fully automated plant-handling facilities enables simple scaling of plant production to large biomasses. The scalability compensates the initial investment costs. The golden standard of recombinant antibody production in CHO cells is a rigid

system difficult to upscale. The scalability limitations derive from the necessity of sterile and high-tech bioreactors, requiring high investments. Furthermore, plant cell systems as biofactories comparable to CHO cultures are common to produce PMPs. Plant biofactories require simpler nutrients than animal cell cultures with the advantage of animal components and pathogens being absent (Buyel et al. 2017). A promising platform is transient expression in *N. benthamiana* plants leading to high yields in short time. The sufficient amounts of recombinant antibodies for ZMapp were manufactured within weeks in *Nicotiana* leaves. This event highlighted the potential of plant production platforms, enabling rapid manufacturing of pharmaceuticals to respond efficiently to public health emergencies (Sack et al. 2015). While producing large biomasses is considered straightforward with plants, practice over time demonstrated that downstream purification from whole plant biomass is often difficult. It is much easier to purify secreted proteins from liquid media than proteins from heterogeneous tissues. In addition, plant matter includes fibers, oils, insoluble proteins, as well as secondary metabolites which all can intervene with physical or chemical processes hindering the overall downstream process. Thus, the cost-savings from the upstream production are nullified by the complex downstream processings. This is another reason for the current trend towards minimally processed topical and oral formulations (Stoger et al. 2014).

## 1.5. Status quo and challenges

### 1.5.1. Plant-manufactured pharmaceuticals

To date, plant systems proved to have many technical advantages regarding safety and rapid scalability, leading to lower production costs compared to other systems (Donini and Marusic 2019). These advantages make plants interesting production platforms for manufacturing pharmaceuticals, which meet global health issues. Numerous PMPs are in the development pipeline with the objective to tackle major diseases. These include degenerative conditions or infectious diseases, such as Alzheimer's respectively Malaria (Moustafa et al. 2016). Furthermore, recombinant antibodies are promising tools in cancer therapy (Hudson 1999). Besides Bayer, other companies and research institutions have been focusing on PMPs for oncological purposes (Pujol et al. 2007; Tusé et al. 2015). In addition to vaccines against influenza, also antigens for immunizations against Human Papilloma Virus and Hepatitis B Virus are reported to be efficiently expressed upon agroinfiltration in *N. benthamiana* (Menassa et al. 2012). Thus, the potential of molecular farming was demonstrated numerous times. The proof of concept of plant-based production systems for therapeutic proteins was set in various plant species and tissues. This versatility is a strength of molecular farming, but the great diversity in plant systems hindered the early development of a standardized plant production platform. Without a standardized platform, there was no common basis to advance plant productions for pharmaceutical industry. However, the concentration on product-specific needs allowed molecular farming to replace traditional technologies in niche productions. Initial regulatory obstacles regarding GMP and specifically GM plants are overcome in the area of molecular farming. As a result, numerous research ventures regarding PMPs became commercially interesting (Fischer et al. 2013). The molecular farming technology experienced several milestones over the past thirty years and PMPs have received worldwide interest. Multiple PMPs underwent clinical trials or are currently under testing, but only a few have reached market readiness. Hampering aspects for PMP commercialization are remaining biosafety concerns and downstream processes, such as protein extraction and purification (Yao et al. 2015). The protein yields achieved in established mammalian systems, such as CHO cells, are still significantly higher and protein purifications from whole plants is still challenging. Consequently, technical barriers in plant-based production, such as processing, mask the initial financial advantages. Thus, the conventional systems are still the dominant production platform for recombinant proteins due to their robustness, profitability and regulatory compliance. The pharmaceutical industry focused its efforts to maximize the performance of established platforms, such as the golden standard CHO cells or well-known *E. coli*, leading to high yields of quality recombinant proteins at low

costs. While mammalian cells are capable of manufacturing complex protein structures, such as glycoproteins, bacterial cultures have lower requirements in terms of growth conditions. This fact explains why prokaryotes are the expression system of choice for simple polypeptides. These are the reasons that mostly plant-made protein products with unique properties for niche markets are reaching the commercial pipeline. This includes antibodies, vaccine agents and replacement proteins, whereas recombinant antibodies and their fragments are the biggest group of plant derived pharmaceuticals (Schillberg et al. 2019). Besides human medicine, molecular farming is also interesting for veterinary therapeutics. The overuse of antibiotics in livestock production is considered one of the main drivers for resistance developments. Therefore, plant production systems constitute a promising alternative manufacturing platform, profiting from the same advantages as production for human purposes (Topp et al. 2016). Owczarek and colleagues published an overview in 2019 of the current production systems for pharmaceuticals to date (Tab. 1).

#### 1.5.2. *Non-pharmaceutical industry*

While the original potential in molecular farming was seen in biopharmaceuticals, more non-pharmaceutical plant-made products are currently available on the market. They constitute mostly of components for diagnostics and research, such as growth factors needed for cell culture, for biosensors, for biocatalysts to facilitate bioremediation, and for cosmetics. In addition, enzymes digesting lignocellulose used in manufacturing paper, biofuel and feed are commercially plant-made. These industrial products do not underlie to as high regulatory requirements as their pharmaceutical counterparts do. The industry, apart from the biopharmaceutical sector, can profit from the same advantages of plant production platforms regarding costs and scalability. Raw materials for production and subsequent processing are inexpensive. While upscaling is not a technical issue and only depends on equipment investments, most plant-derived products are manufactured on a small or medium-scale. The absence of any animal or microbial contaminations is another key feature of plant-derived products. Nonetheless, the advancement of plant-made non-pharmaceutical products is tightly linked the technical development of the plant-engineering field. The latter underlies restrictive regulations due to the peculiar status of GM organism (Tschofen et al. 2016).

#### 1.6. Future perspectives and sustainability

Hence, molecular farming is advancing in various industrial areas. The focus of biopharmaceutical industry lies on the improved protein functions through glycosylation, the potential for oral vaccines and on the possibilities of rapid production to respond efficiently to global health demands. The technical aspect of animal-free production excludes relevant contaminations increasing biosafety. Moreover, cosmetic products deriving from plants are inherently animal-free and in turn, are more often socially acceptable. Plant-derived products are also assumed to be more natural and manufactured in more environment-friendly processes (Schillberg et al. 2019). Lately in the field of molecular farming, an innovative approach to exploit the sustainable character of plant systems has emerged. Plant-based manufacturing or “biomanufacturing” systems are being explored for possible side streams. Due to their biodegradability, plants are essentially single-use bioreactors. In general, the use of plants generates neglectable amounts of toxic waste compared to mammalian systems. In addition, plants fixate carbon dioxide in their tissues through photosynthesis. Thus, farming plants can compensate extensive carbon emissions from other industrial productions. Plants are natural biofactories for many different molecules with particular properties, most famously secondary metabolites. The current plant production systems focus on the harvest of one specific protein, while discarding the plant biomass during purification. Instead, several production side streams could be established allowing to extract valuable plant metabolites and to utilize the remaining biomass as biofuel. While waste streams from mammalian platforms are noxious in most cases, side streams in plant production systems can significantly contribute

to the economy of the whole production (Buyel 2018). Regarding the positive impact on society and the environment, plant production systems with similar costs to conventional systems are making molecular farming a sustainable technology.

Platform/host	Overall costs	Production time	Scale-up capacity	Propagation	Product quality	Contamination risk	Purification cost
Transgenic plants	very low	medium	very high	easy	high	low	high
Plant cell culture	medium	medium	medium	easy	high	very low	medium
Plant viruses	low	low	high	feasible	medium-high	very low	high
Microalgae	low	high	high	easy	high	very low	medium
Yeast	medium	medium	high	easy	medium	low	medium
Bacteria	low	low	high	easy	low	medium (e.g., endotoxins)	high
Mammalian cell culture	high	high	very low	hard	high	very high (e.g., virus, prions, oncogenic DNA)	high
Transgenic animals	high	high	low	feasible	high	very high (e.g., virus, prions, oncogenic DNA)	high
Insect cell culture	medium	medium	high	feasible	medium	very low	medium
Filamentous fungi	low	high	high	easy	medium	low	low

Tab. 1: General overview of different production systems for recombinant proteins and their respective production features adopted from Owczarek et al. 2019.

## 2. Technical aspects of production systems using tobacco and friends

In the period when the first molecular farming endeavors were undertaken, several gene transfer techniques had already been established and many plant species were well-studied subjects in different research areas. Naturally, the large pool of available engineering methods drove the development of a vast range of plant production systems. Common strategies in molecular farming are the use of whole plants, cell suspensions or tissue cultures as platforms, whereas different expression techniques are employed, such as stable transformation, transient or inducible expression, as well as protein targeting (Schillberg et al. 2019). The choice of the production platform is a critical factor in molecular farming. Every plant species harbors unique features, which can greatly impact the recombinant protein yields, post-translational modifications, stability of polypeptides and foremost the total production costs (Leite et al. 2019). The following section describes some of the prevailing platforms and production strategies used in molecular farming. Besides plant systems, also other photosynthetic species are briefly introduced as molecular farming hosts.

### 2.1. Stable transformation of and transient expression in whole plants

#### 2.1.1. *Agrobacterium-mediated plant transformation*

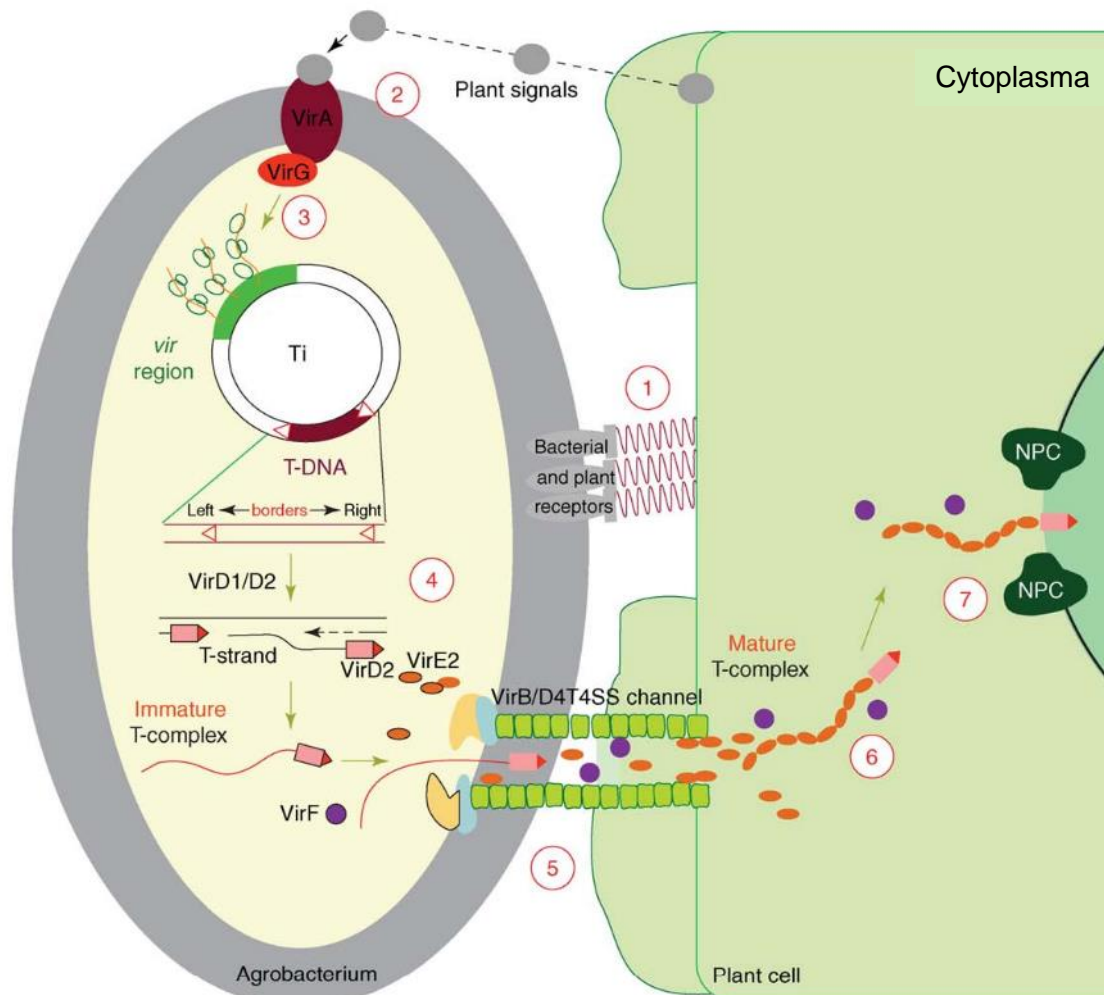


Fig. 1: Schematic representation of the T-DNA transfer by Agrobacteria into plant host cells (adjusted from Hwang et al. 2017).

Plants used in molecular farming undergo genetic transformation in order to express a recombinant protein of interest. Since over three decades, plant transformation is commonly mediated with

*Agrobacterium tumefaciens*. The popularity of this phytopathogen as a transformation tool comes with the vast knowledge about its interactions with plant cells on molecular level. This bacterium has the unique ability to readily introduce genes of interests into many plant species. Therefore, agrobacterium-mediated plant transformation is considered as the most efficient method for gene transformation being responsible for much advancement in plant breeding and biotechnology (Niazian et al. 2017). As described before, the natural ability of this bacterium to transfer DNA to plants is exploited for molecular farming. This phytopathogen occurs in the soil and infects plants upon wound detection, leading to tumor development. The *Agrobacterium* genus was discovered as the infectious agent of many plant diseases, such as crown gall tumor or hairy root. *A. tumefaciens* carries a virulence plasmid, which is responsible for tumor-induction. In the case of *Agrobacterium rhizogenes*, its plasmid induces abnormal root growth. The oncogenes causing the diseases symptoms reside on the so-called transferred DNA, short T-DNA, easily replaceable with genes of interests. Agrobacteria transfer the T-DNA into the host cell nucleus through a bacterial secretion system. In the case of transgenic plants, the genes on the T-DNA stably integrate into the plant genome. In transient expression, these foreign genes also enter the nucleus, becoming available for transcription, however not modifying the host's genome (Hwang et al. 2017). The process of agrobacterium-mediated plant genetic transformation is illustrated in more detail in Fig. 1. In most labs, the method of choice for transient expression is agrobacterium-mediated transformation of leaf tissue applying syringe infiltration (Menassa et al. 2012). While *Agrobacteria* are also widely used for stable transformation to generate of transgenic plants, the other method commonly in practice for plant transformation is particle bombardment using coated DNA microprojectiles (Keshavareddy et al. 2018).

#### 2.1.2. Stable transformation

During stable transformation, the gene of interest is stably integrated in the plastidial or nuclear genome. In consequence, the new protein becomes an inheritable phenotypic trait of the transplastomic or transgenic plant. The peptide is continuously expressed locally in a specific plant organ or systemically in the whole plant. This strategy is commonly applied in molecular farming being suitable for many plant species (Leite et al. 2019). Typical transgenic plant hosts are *N. tabacum* and *N. benthamiana*. For instance, transgenic *N. tabacum* served as a production platform for the first clinically tested PMP and is the leading host for recombinant antibody production. Besides, the model plant *Arabidopsis thaliana*, crop plants, such as lettuce, potato and maize, or aquatic plants, such as duckweed, are utilized as farming hosts (Donini and Marusic 2019).

#### 2.1.3. Transient expression system

In contrast, the transient transformation of a plant does not lead to the stable integration of exogenous sequences in the genome. A possible progeny generation of the transiently transformed host plant would not inherit any transgenes. This circumstance lowers the risk of accidental release of transgenes in the environment, which results in higher biosafety compared to transgenic plants. Moreover, high expression levels are achieved within days to weeks with transient expression systems conveying greater yields of recombinant proteins than expression through stable transformation could ever achieve (Komarova et al. 2010). Bacterial or viral infective vectors are used as shuttles to confer transient expression of genes of interests. Their expression efficiency and the functionality of the resulting proteins can quickly be confirmed through transient expression experiments. In molecular farming, leaf tissues are often transiently transformed in order to achieve high expression levels of the desired proteins (Leite et al. 2019). For plant transformation, modified plasmids deriving from *A. tumefaciens* serve as vectors already carrying T-DNA gene cassettes. For overexpression, the gene of interest is inserted into the T-DNA cassette, together with a strong constitutive promoter (Donini and Marusic 2019). Additionally, a typical vector consists of multiple cloning sites, selection marker genes and replication origins (Ori) for *E. coli* and *A. tumefaciens* (Komori et al. 2007). Besides, vectors deriving from plant viruses have been



developed for efficient expression and are currently exploited. In particular, a deconstructed viral vector containing only necessary elements to express the gene of interest is the basis of the 'Magnifection' technique. This technique allows large-scale production, which dramatically increases protein yields up to hundred-fold. MAbs are commercially produced through this viral expression system in *N. benthamiana*. The three Ebola virus neutralizing mAbs from ZMapp were produced by applying 'Magnifection' on glycoengineered *N. benthamiana* plants (Leite et al. 2019). Besides *N. benthamiana* and *tabacum*, lettuce and tomato are successfully exploited as hosts for transient expression. Agrobacteria cultures carrying the vector with the gene of interest are infiltrated with the help of flat syringes or with vacuum into leave tissues. The bacteria permeate the intracellular spaces between the plant cells, allowing a simultaneous infection of the infiltrated tissue. This efficient method is called leaf agroinfiltration, providing a synchronous gene expression, which in practice results in high protein yields. Furthermore, co-expression strategies with plant viral gene silencing suppressors, such as p19, proved to enhance, in particular antibody production. Vacuum agroinfiltration can easily be automated for large-scale production under GMP, which is already exploited by biotech companies in the USA (Donini and Marusic 2019).

## 2.2. Biofactories: Another production platform on basis of cell and tissue cultures

Also, parts of plants, such as certain tissues or single cells are being exploited as production systems for heterologous proteins which are foreign to the host. The premises of strictly sterile conditions for cultures are beneficial for the overall requirements regarding contamination free production. All plant tissues have the inherent capability to be propagated endlessly. The key advantage of cell and tissue cultures is the secretion of synthesized proteins in the culture medium, simplifying subsequent purification steps. Unfortunately, current biofactories based on plant cells are providing mediocre quantities of protein yields (Donini and Marusic 2019).

### 2.2.1. Plant cell suspension cultures

Plant cells can be cultured as suspensions in containment, called plant biofactories. These platforms for large-scale production, in particular for PMPs, are the most promising in terms of economic aspects (Leite et al. 2019) and are in place since over twenty years. The plant cells derive from undifferentiated tissue, called callus, and are cultured as suspensions in flasks or in fermenters under constant shaking. The most prominent cell lines BY2 and NT1 originated from *N. tabacum*, but several cell lines are also established from rice, soybean, carrot and tomato plants. The recombinant protein production with cell suspensions is uncomplicated due to the low nutrient requirements and purification from liquid media. Plant cell systems seem to have insensitive expression machinery towards possible interference with foreign sequences, leading to constant protein secretions into the media. However, proteolytic enzymes in the culture media hamper yields. The first recombinant protein, human serum albumin, was produced in tobacco cell cultures already in 1990 (Sijmons et al. 1990). The success story of molecular farming, the plant made drug EYLEYO is being produced in carrot cells using the cost-effective platform ProCellEx (Rosales-Mendoza and Tello-Olea 2015). Furthermore, cell cultures are easier to genetically engineer with increased possibilities to control glycosylation processes (Donini and Marusic 2019). In the area of cell cultures for molecular farming, the newest developments are so-called Plant Cell Packs (PCPs). Instead of a loose suspension, PCPs consist of tightly packed, but still porous cell aggregates growing in absence of media. These culturing conditions positively influence the expression of proteins, which are still secreted and easily purified (Rademacher et al. 2019).


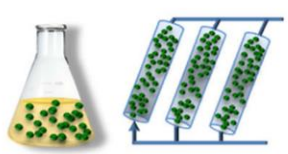


### 2.2.2. Novel platforms: Hairy root tissue, moss and microalgae cultures

Further tissues and organisms emerged as suitable production systems for recombinant proteins. Other photosynthetic species apart of plant cultures show similar production performances in bioreactors. A

famous example for tissue cultures is hairy roots, which have been applied in many systems for bioactive metabolite production since a long time. Hairy root cultures deriving from *N. benthamiana* are only explored recently as suitable platform for heterologous protein production. These plant roots are transgenic tissues that have been infected by *A. rhizogenes* and as a result can be stably cultured in sterile conditions. For example, mAbs for tumor targeting have been successfully expressed in hairy roots achieving high yields (Donini and Marusic 2019). Also, the moss species, *Physcomitrella patens*, is commonly used as a production host for biopharmaceuticals due to its ease for clone propagation and culturing under containment. It brings optimal requisites for simple genetic engineering via homologous recombination (Leite et al. 2019), while its genome is widely characterized. In particular, glycoengineering is possible in mosses and the absence of plant-specific sugar residues increases biosafety of synthesized pharmaceuticals. Despite of one production platform based on moss cultures already being introduced by a biopharmaceutical company, many barriers still need to be overcome to establish large scale productions (Donini and Marusic 2019). Another interesting host for recombinant proteins is microalgae. Those unicellular organisms show a high growth rate, leading to fast biomass accumulation. Prominently, the algae species *Chlamydomonas reinhardtii* is explored as an alternative pharmaceutical production platform. Such an algae system requires low cost and low-tech being ready for upscale in photobioreactors. Its fully characterized genomic make-up promoted the development of many genetic tools optimized for this species (Owczarek et al. 2019). Despite the presence of appropriate glycosylation machinery, controlled glycoprotein synthesis remains challenging in microalgae (Donini and Marusic 2019).

## 2.1. Summary of the different production platforms and systems

Overall, a variety of plants and their tissues, as well as a number of selected photosynthetic organisms have already been serving as production hosts for PMPs. The initial step is the gene transfer into the host cells through transformation. However, stably transformed systems provide, in practice, low yields of recombinant proteins. In the case of transient expression, leaf agroinfiltration induces high expression levels of the recombinant proteins in short time. In consequence, the achievable protein yields are much higher compared to other systems. Despite of low yields, bioreactor production offers ease for subsequent protein purification. Meanwhile, the complex biomass of whole plants still constitutes a challenge for downstream processes. The table above by Donini and Marusic from 2019 offers a simplified overview of the different production systems with their given advantages and disadvantages.

Whole plants		Cell / Tissue cultures	Moss / microalgae cultures
<b>Transgenic plants</b>	<b>Agroinfiltration</b>		
<b>Advantages</b>	 <ul style="list-style-type: none"> <li>✓ Production at very large-scale (tons of recombinant protein)</li> <li>✓ Competitiveness of costs at large-scale</li> <li>✓ Possibility of accumulating the recombinant protein in seeds (long-term protein stability without the need of the cold chain)</li> </ul>	 <ul style="list-style-type: none"> <li>✓ Rapid and flexible production platform</li> <li>✓ High protein expression yields</li> <li>✓ Scale-up with semi-automated systems in greenhouse</li> <li>✓ No environmental safety issues (production in greenhouse allows containment)</li> <li>✓ Use of glyco-engineered plants</li> </ul>	<ul style="list-style-type: none"> <li>✓ Growth in contained bioreactors (no contamination by pathogens)</li> <li>✓ Compliance with current regulatory standards</li> <li>✓ Easy downstream processing (protein secreted in the medium)</li> <li>✓ Drug produced in plant-cell cultures already on the market</li> <li>✓ Use of glyco-engineered cell/tissue lines</li> </ul>
	<ul style="list-style-type: none"> <li>✗ Environmental containment issues concerning GM plants in the open field</li> <li>✗ Low protein expression yields</li> <li>✗ Downstream processing issues related to extraction of proteins from leaves</li> <li>✗ Regulatory hurdles</li> </ul>	<ul style="list-style-type: none"> <li>✗ High investment costs required</li> <li>✗ Low protein expression yields</li> <li>✗ Difficulty in culture scale-up (especially for hairy roots)</li> </ul>	<ul style="list-style-type: none"> <li>✗ High investment costs required</li> <li>✗ Low expression yields are generally obtained</li> <li>✗ Culture scale-up is complex</li> <li>✗ Glycoengineering of microalgae is difficult</li> </ul>
<b>Challenges</b>			

Tab. 2: Comparison of advantages and challenges regarding different production platforms based on phototrophic organisms, table by Donini and Marusic 2019.

### 3. Bottlenecks of recombinant protein expression

#### 3.1. Recombinant protein yield and quality in plants

##### 3.1.1. Strategies to enhance protein expression

One main objective of molecular farming is to produce higher protein yields than comparable systems (Donini and Marusic 2019). As mentioned before, transient expression via agroinfiltration in *N. benthamiana* leaves is known to provide high yields. Plants for molecular farming are genetically engineered to become optimized hosts for improved protein production (Matoba et al. 2011). Besides the choice of host and platform, the key factor determining successful yields at the cellular level is the recombinant protein biosynthesis and stability. Various molecular strategies had been developed to increase protein yields, such as improved promoters (Ma et al. 2005), codon optimization or developing of novel expression vectors. Furthermore, co-expression approaches showed to successfully increase final yields including co-expression of post-transcriptional gene silencing (PTGS) inhibitor such as virus-derived RNA silencing suppressor p19 or co-expression of chaperones, which lowers the impact of the protein load on the ER homeostasis. When recombinant proteins are secreted outside the plant cell, they often undergo proteolysis due to proteases. Several methods are suitable to minimize proteolysis, such as generation of knock-out or RNA silenced plants. Also, co-expression with protease inhibitors is assumed to recover higher protein yields (Matoba et al. 2011). The common approach of using signal targeting enables the accumulation in subcellular compartments where some recombinant proteins are more stable (Ma et al. 2005). By adding signal peptides to the recombinant proteins, the latter can be targeted to many subcellular compartments, such as endoplasmic reticulum, apoplast, cytoplasm, chloroplast or vacuoles (Matoba et al. 2011).

##### 3.1.2. Secretory pathway in the cell: From synthesis to mature proteins

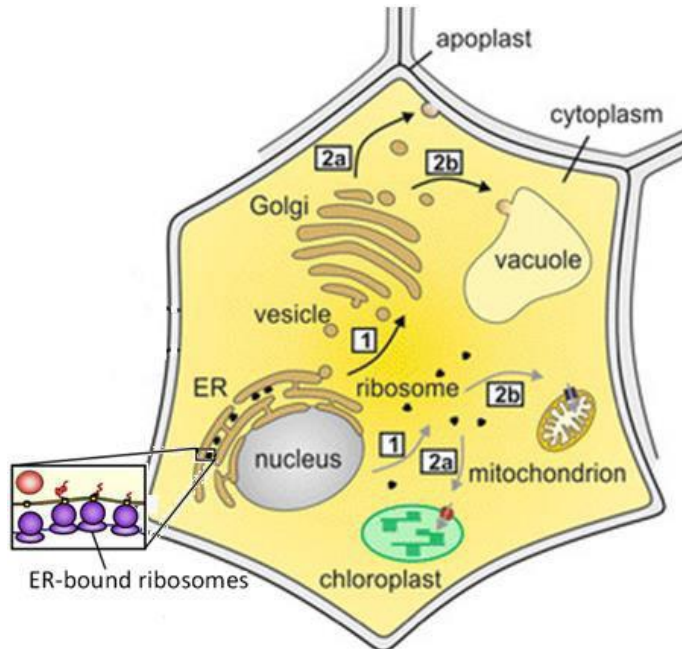


Fig. 2: Schematic overview of a plant cell with secretory pathways being illustrated. The first pathway begins with ribosomes (zoom box) translating and associating to ER, where the nascent peptide chain translocates into the ER lumen. Free ribosomes translate proteins following the second pathway to plastids or mitochondria. Figure adopted from Lambertz et al. 2014.

Recombinant protein expression in plants begins with the corresponding transgene in a gene cassette, such as a T-DNA, being transferred to the host cell into the nucleus via transformation. The plant cell expression machinery takes over transcribing and translating the transgene independently of genomic

integration (Hwang et al. 2017). When recombinant proteins are expressed, they can follow one of two secretory pathways passing different subcellular compartments (Fig. 2). In the first pathway, ribosomes associated to the endoplasmic membrane (ER) translate the nascent polypeptide chain of the recombinant protein, directly into the ER lumen. Subsequently, the proteins are transported to the Golgi apparatus, where they are modified and again packed in vesicles. These new vesicles are transferred to the vacuole or the apoplast and fuse with the respective membrane releasing the transported proteins. The second pathway consist of translation through free ribosomes followed by transport to mitochondria or chloroplasts for protein release (Lambertz et al. 2014).

### 3.1.3. *The ER as gateway of protein folding is susceptible to stress*

Recombinant proteins are frequently directed to compartments part of the secretory pathway and organelles derived thereof by adding protein tags to the recombinant gene cassette. The prominent strategy to target the ER lumen opens up many opportunities. The folding and post-translational modifications of recombinant proteins are mostly taking place in the ER lumen. Numerous storage compartments, such as protein storage vacuoles or protein bodies, are arising from the endomembrane system not only in seed but most plant cells (Stoger et al. 2014). The endoplasmic reticulum is the entry point to the secretory pathway and a cell organelle found in all eukaryotes. This membranous organelle is fundamental for cell development and functioning due to its machinery for protein maturation and secretion. The ER lumen is an oxidative environment beneficial for formation of disulfide bonds and N-glycosylation. Moreover, various chaperones are present in the ER facilitating the proper folding of new proteins through binding to hydrophobic regions. Since proteins are being synthesized, folded, and sorted for delivery to the subsequent compartment (Bravo et al. 2012), the ER represents the gateway of the protein secretory pathway. Hence, several molecular mechanisms ensure quality control, so that only correctly folded proteins leave the ER. As a result, misfolded (or unfolded) proteins can be accumulated in the ER leading to stress. Different molecular mechanisms have evolved to respond to ER stress in order to restore homeostasis and to overcome the aberrant protein overload (Cho and Kanehara 2017).

### 3.1.4. *ER stress leading to unfolded protein response: an overview*

The finely controlled conditions in the ER lumen provide the environment for proper protein folding. The ER microenvironment is very sensitive to stress conditions, since imbalances between in- and outflow of proteins disturb the regular protein secretory pathways. Protein folding can be affected by developmental conditions or environmental factors. Environmental stressors are sensed by plant cells with the help of ER stress responsive proteins to induce appropriate reactions to diminish of the adverse effects. Therefore, the ER stress mechanisms being crucial for maintaining cell homeostasis are conserved among all eukaryotes (Deng et al. 2013; Nawkar et al. 2018). When lumen homeostasis is disrupted, the accumulation of misfolded proteins is detected leading to transduction of the stress signal to the nucleus. Here, the expression of specific stress genes is regulated according to the signal in order to prevent harmful concentrations of misfolded proteins. This kind of stress signal transduction is called unfolded protein response (UPR). UPR leads to numerous cellular processes which can be summarized in three activities: (1) increasing overall protein folding capacity through upregulating the expression of chaperones and foldases expression; (2) limiting further protein inflow by repression of the translational machinery; (3) lowering overload through removal of misfolded proteins from ER lumen to proteasomes for eventual degradation. In cases of excessive ER stress exceeding a certain threshold, UPR activity can lead to programmed cell death (PCD). Cell death is the ultimate response in eukaryotes to cope with overwhelming signals. Initial research on ER stress was conducted in mammalian systems, because of its relevance in human health. Chronic UPR in mammals is linked to oxidative stress and the resulting cell death promotes the development of diseases, such as diabetes, hypoxia and neurodegenerative syndromes. As mentioned above, ER stress responses are conserved processes among eukaryotes.

Therefore, plants share many key features of ER stress responses with animals equally experiencing oxidative stress and PCD (Williams et al. 2014). In spite of its importance, UPR as a ER stress response mechanism has only recently stepped into the focus of plant researchers (Cho and Kanehara 2017).

### 3.2. UPR and its transducers in plants

#### 3.2.1. The two primary branches of UPR

Special sensors embedded in the ER membrane are detecting ER stresses and initiate UPR signaling. While mammals possess three sensors mediating each a different UPR signaling pathway, only two primary branches of UPR transduction have been identified in plants, so far (Williams et al. 2014). One branch is activated through inositol-requiring enzyme 1 (IRE1) splicing the mRNA of a basic leucine zipper domain (bZIP) transcription factor (illustrated in Fig. 3). The second branch involves the proteolytic processing of two other ER-membrane-associated bZIPs (Deng et al. 2013). IRE1 being expressed in all plant cells mediates the first main branch of UPR signaling. In plants, the transmembrane protein IRE1 is localized at the perinuclear ER and includes domains for ER sensing and ribonuclease activity. There are actually two isoforms, IRE1a and IRE1b, with the same function regarding ER stress. However, IRE1b mediates a further signaling pathway during starvation stress (Williams et al. 2014). During normal conditions, ER luminal Binding Proteins (BiPs) are bound to the luminal sensor domain of a monomeric IRE1 and its substrate, bZIP60, is integrated in the ER membrane facing the cytosol (Nawkar et al. 2018). BiPs are the biggest family of chaperones resident in the ER lumen with the purpose to promote proper folding of proteins by preventing protein aggregations (Cho and Kanehara 2017). When misfolded proteins accumulate in the ER, the BiPs dissociate from IRE1 to reinforce protein-folding processes (Fig. 3(A1)). This leads to the dimerization of the freed IRE1s and the IRE1 dimer in turn has active ribonuclease domains (Fig. 3(A2)). Meanwhile, the expression of bZIP60 is upregulated and the newly synthesized *bZIP60* mRNAs are recruited to the ER membrane in the proximity of IRE1 (Nawkar et al. 2018). When *bZIP60* mRNA docks to the activated IRE1, they recognize the special structure of the mRNA leading to its cleavage at two explicit sites (Fig. 3(A4)). The mRNA fragments are subsequently ligated back with the help of a tRNA ligase resulting in a spliced *bZIP60* transcript (Fig. 3(A5)). Then, the latter is translated to the active form of bZIP60 (bZIP60s), which translocates into the nucleus. There, activated transcription factor bZIP60s forms complexes and upregulates the expression of UPR-related genes (Nawkar et al. 2018). Several genes involved in UPR downstream activities have promoters containing ER stress responsive cis-elements (ERSE), which are the binding targets of bZIP60s. For instance, the expression of *BiP* genes is upregulated by bZIP60s to increase protein-folding capacity. In *A. thaliana*, three *BiP* genes are identified: *BiP1* (At5g28540), *BiP2* (At5g42020), and *BiP3* (At1g09080) (Iwata and Koizumi 2005; Sun et al. 2013). BiP1 and BiP2 proteins are almost identical in amino acid sequence and also expressed when stress is absent, albeit at significantly lower levels. The expression of the less conserved protein BiP3 seems to be induced only under stress conditions (Cho and Kanehara 2017). In addition, the plant-specific transcription factor NAC103 was identified to be expressed only during ER stress. The reason is the exclusive binding of bZIP60 to a particular ERSE sequence named UPRE-III (TCATCG or CGATGA) on the NAC103 promoter (Sun et al. 2013). For *in planta* experiments, dithiothreitol (DTT) and tunicamycin (TM) are commonly utilized to induce ER stress in plants through the IRE1-bZIP60 pathway. The other UPR branch in plants is elucidated by the two-transcription factors bZIP17 and bZIP28. Both are anchored in the ER membrane facing cytosol. Similar to IRE1, they are mobilized upon BiP dissociation when unfolded protein is accumulating in the ER lumen. Subsequently, the two bZIP proteins translocate into the Golgi apparatus. The Golgi resident proteases cleave the transcription factors to their active forms, which can enter the nucleus in order to upregulate certain UPR genes. In the case of bZIP17/bZIP28, chaperones and foldases are expressed to support the assembly of macromolecular structures respectively of proteins (Williams et al. 2014). There are also further UPR transducers identified in plants. Besides NAC103, also NAC017, NAC062 and NAC089, were shown to



be induced by ER stress by applying known UPR inducers, DTT and TM. NAC transcription factors are named after "No apical meristem (NAM), Arabidopsis transcription activation factor (ATAF), and Cup-shaped cotyledon (CUC)" and are plant specific. Moreover, recent studies found another UPR transducer: the plant co-chaperone called B-cell lymphoma-2-associated athanogene 7 (BAG7) active during heat stress in plants (Nawkar et al. 2018).

### 3.2.2. The unconventional splicing of bZIP60

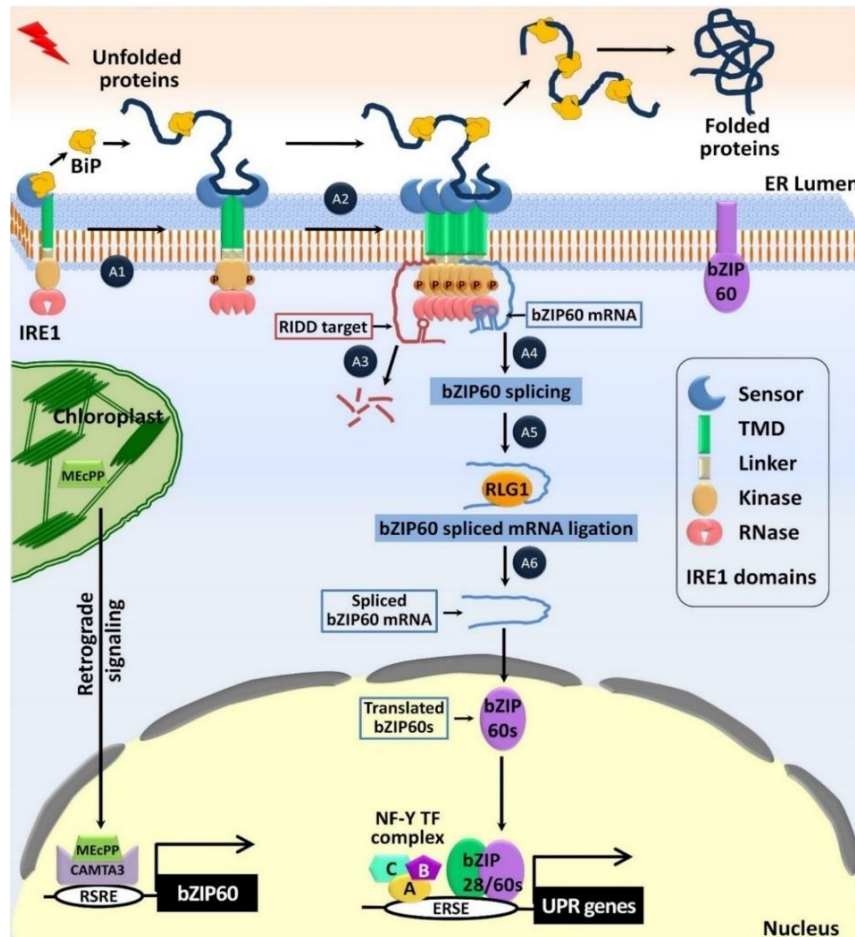


Fig. 3: Schematic UPR signaling pathway through IRE1-bZIP60 described in plant cells. The activation and transduction mechanism of this UPR branch is describe in the text above. Picture taken from Nawkar et al. 2018.

In plants, bZIP transcription factors are a large family of genes involved in the regulation of development, light perception, pathogen defense and stress signaling. The *bZIP60* gene greatly differs compared to the other bZIPs (Jakoby et al. 2002) indicating its unique role in UPR signal transduction. During UPR, the activated IRE1 dimer cleaves the *bZIP60* mRNA transcript in the cytosol. While the mRNA is re-ligated, a part of the sequence is lost leading to a frameshift in the transcript. This mechanism is called unconventional splicing since it occurs outside the nucleus (Nagashima et al. 2011). The IRE1-mediated unconventional splicing is the oldest branch of UPR among fungi, plants and animals. While the upstream processes of IRE1 activation are conserved, the downstream signaling components differ across kingdoms. The substrates of IRE1 are bZIP60 analogues, HAC1 or XBP1, in yeast respectively in animals. The three transcription factors, bZIP60, HAC1 and XBP1, have in common that a defined portion of their native mRNA is cut out during unconventional splicing. This intron region forms a characteristic double hairpin loop structure in the mRNA of all three transcription factors (Fig. 4B). Three bases (CGG) are conserved on each loop serving as recognition sites for splicing (Zhang et al. 2015). The removal of the intron leads to a frameshift changing the open reading frame (ORF). The translated HAC1s and

XBP1s acquire the necessary activation domain at the C-terminus for UPR signaling upon splicing. In plants, the native bZIP60u already possesses the activation domain at the N-terminus, which is not modified upon splicing. In order to prevent transcriptional activation of UPR genes, unspliced bZIP60 is excluded from the nucleus due to its transmembrane domain (TMD, also called hydrophobic region HR) targeting the native bZIP60 to the ER membrane. In the particular case of bZIP60, 23nt are removed from the mRNA and the shifted ORF encodes an early stop codon. As a consequence, the C-terminal TMD is lost in the truncated bZIP60s (Fig. 4A). Without the anchoring through TMD to the ER membrane, the activated bZIP60s translocates in the nucleus upregulating UPR genes (Nagashima et al. 2011). A study examined the precise course of the splicing event in mammalian cells. When the native transcription factor is initially translated, the mRNA-ribosome-nascent chain (R-RNC) complex is dragged to the ER membrane. This is due to the earlier translated hydrophobic region of the nascent protein anchoring the R-RNC complex to the ER membrane. A conserved sequence at the C-terminus was identified to provoke a translational pausing. The pausing allows sufficient exposure of R-RNC complex to the ER membrane where IRE1 resides. The exiting mRNA from the R-RNC comes in proximity to IRE1, allowing efficient recognition and effective splicing of the intron sequence. The now spliced mRNA sequence is translated again resulting in an activated transcription factor (Yanagitani et al. 2011) (Fig. 4C). Due to the homologies between animals and plants, it can be assumed that a similar pausing event facilitates the efficient splicing of *bZIP60* mRNA. All in all, bZIP60s is an active UPR transducer in plants transporting the signal from the ER to the nucleus. The interaction of various other ER stress-related genes and proteins is reported resulting in a complex gene expression network (Fig. 4D).

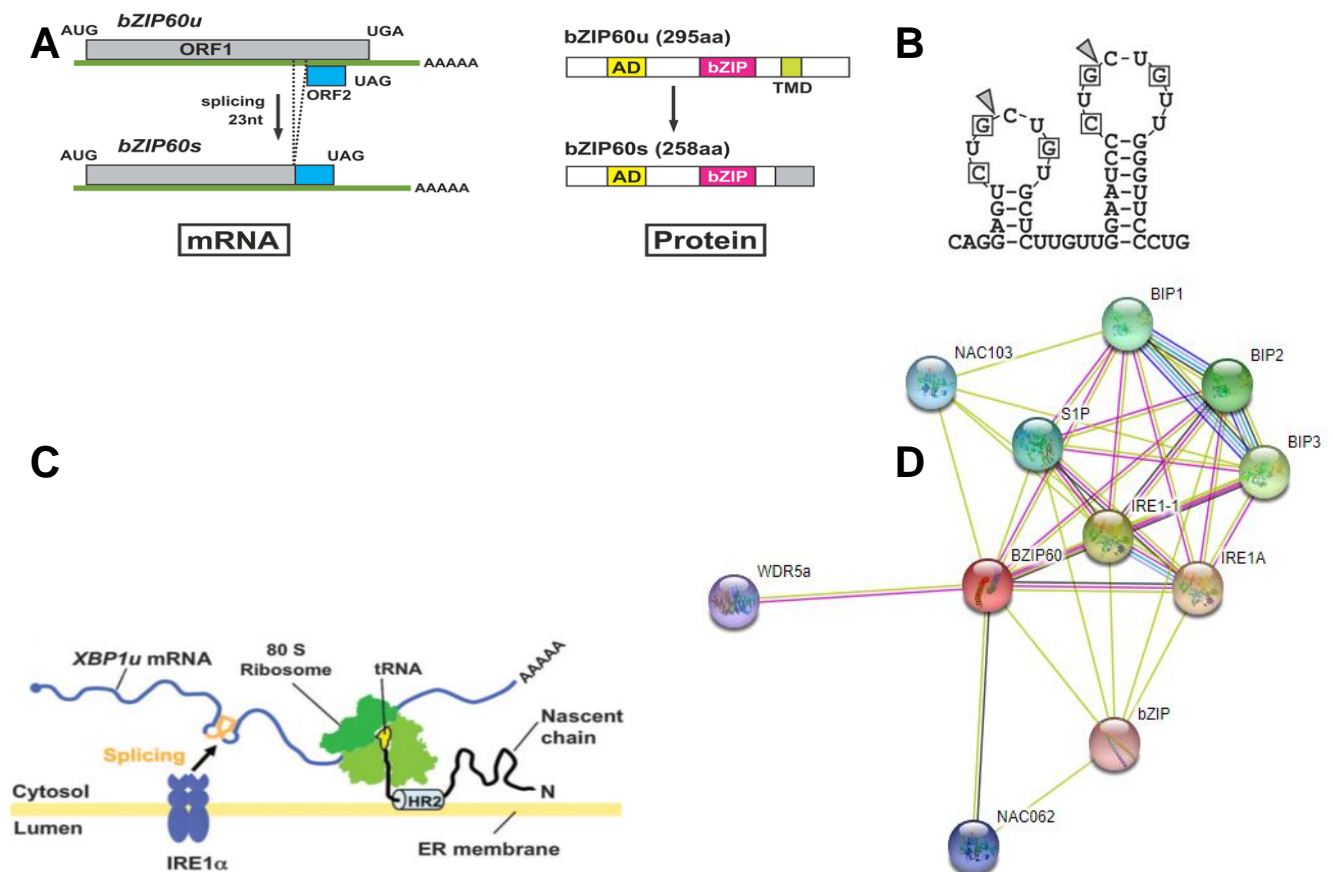


Fig. 4: A: The two mRNA isoforms of *bZIP60* in *A. thaliana*. The unconventional splicing of the mRNA results in a shortened protein (*bZIP60s*). B: conserved intron region of *bZIP60* mRNA with marked sequence motifs (in squares) and cleaving sites (grey arrows) (from Nagashima et al. 2011). C: Schematic description of unconventional splicing mechanism of mammalian XBP1 mRNA indicating the pausing event with HR2 at the ER membrane (from Yanagitani et al. 2011). D: Gene co-expression network of *bZIP60* in plants showing the described connections with other proteins (generated at <https://string-db.org/>).



# Research Aim

## 1. Problem statement: The link between plant UPR and molecular farming

When gene cassettes encoding for recombinant proteins are expressed, often necrosis can be observed (Hamorsky et al. 2015; Yokota et al. 2017; Song et al. 2018). Similar experiences were made in our lab group where upon agroinfiltration *N. benthamiana* plants would show necrosis signs. Regarding the role of the ER as secretory gateway, the overexpression of recombinant proteins might lead to an overload of the ER. If the continuous flow of synthesized proteins cannot be properly folded anymore, the UPR signaling is activated leading to PCD observed as necrosis. In molecular farming, plant-based production relies on the overexpression of recombinant proteins. The overall goal is to achieve high quantities of proteins (Leite et al. 2019). A stress mechanism, such as UPR, constitutes an obstacle to reach sufficient protein yields. Moreover, the protein tagging approach is often applied to target recombinant proteins to the endomembrane system (Stoger et al. 2014). However, there is a high probability that targeting to the ER affects the microenvironment favorable for protein folding or artificially overloads the ER machinery. The exact regulating mechanisms of UPR in plants are still a matter of research. The standard method to study UPR *in planta* is the analysis of UPR-related gene expression in qPCR assays (Gachon et al. 2004). QPCR is based on the amplification of present sequences in cDNA samples. The samples are taken from plant tissue pieces inevitably pooling numerous cells and the latter are destroyed to extract the genetic material. Samples can only be taken from different time points prohibiting the observation of temporal development of UPR. Also, qPCR is only an indirect method to confirm UPR by examining ER stress related genes. These genes are probably not expressed throughout whole UPR, but only during specific regulatory steps elucidated from one branch. Also, other events might regulate the expression of chosen marker genes providing great potential for biased conclusions. In summary, qPCR is an unprecise and destructive method for UPR studies, where cells are pooled leading to a resolution only on tissue level. An appropriate method for the holistic study of UPR signaling processes at the cellular level is currently missing. Moreover, there is no application described in plants, which would enable the observation of the temporal development of ER stress upon overexpression of proteins. The idea evolved to close this technical gap by developing a molecular tool which would allow the *in planta* visualization of UPR.

## 2. Scope of this thesis: Development of an UPR reporting tool in plants

As initial host plant, *N. benthamiana* was chosen because of its favorable properties in regards of protein expression commonly exploited in molecular farming (Goulet et al. 2019). Agroinfiltrations in the leaves of this plant species reaches up to 100% transformation efficiency (Hwang et al. 2017). In general, Agrobacterium-mediated transient transformation is the preferred production system for recombinant proteins in plants. Optimal expression parameters can be deduced through transient expression making it a valuable tool for research applications (Menassa et al. 2012). The advantages of syringe infiltration into leaves are evident making it ideal for recombinant protein expression on laboratory scale. This transformation technique is low-tech and low-cost allowing flexibility for overexpression and co-expression assays. In the first case, one target gene is introduced into leaf, while in the latter several genes are simultaneously infiltrated into the same leaf. Transient expression via agroinfiltration allows the quick comparison of different gene constructs or vectors for expression efficiency and / or protein production. For instance, the expression of fluorescent proteins (FPs), such as GFP or DsRed, provides robust yields (Leuzinger et al. 2013). While transient experiments allow quickly assessing promoter behavior, gene activity and protein function, the generation of stably transformed or transgenic lines can take months. A reporter construct within T-DNA in a binary vector transferred via *Agrobacterium* is naturally processed in the plant cell nucleus (Hwang et al. 2017). The non-integrated T-DNA is

transcriptionally competent leading to a short-lived burst in protein expression. As result, maximal protein yields can be reached within two to five days (Menassa et al. 2012). Moreover, a draft genome of *N. benthamiana* is available enabling the isolation of endogenous genes from this plant (Bombarely et al. 2012). In previous studies, UPR detection tools were examined and were developed in living cells of other species, such as yeast (*S. cerevisiae*), mammals (CHO) and insects (*Drosophila*). They commonly exploited the IRE1-mediated UPR signaling pathway by modifying the primary transducer (Sone et al. 2012; Lajoie et al. 2014; Roy et al. 2017). The homologue bZIP60 also underlies the same unconventional splicing, whereas the precise mechanism in plants is sparsely described in literature. The endogenous *bZIP60* gene can be isolated from *N. benthamiana* to confirm the draft genome data. Therefore, the transcription factor constitutes an interesting target for gene engineering by utilizing its coding sequence as basis for a molecular sensor. Due to its relevance regarding human chronic diseases, a system to monitor ER stress *in vivo* was developed already 25 years ago. Transgenic animals were expressing an „ER stress indicator“ composed of a green fluorescent protein being fused to XBP-1 (Iwawaki et al. 2004). This imaging approach exploiting FPs to visualize UPR in yeast and mammalian systems has also been published already (Lajoie et al. 2014). Moreover, GFP-fusions with bZIP60 were already applied in a previous study to follow the transcription factor's activity (Parra-Rojas et al. 2015). Recent advancements regarding signal stability of fluorescent reporters were achieved allowing dynamic studies on cellular and tissue level (Hostettler et al. 2017).

### 3. Objective: bZIP60-based sensor visualizing UPR with FP

In order to monitor possible UPR processes during development of various plant tissues in basic research studies, as well as UPR upon leaf agroinfiltration with recombinant genes for a more applied scenario, the aim was to design and to develop a molecular sensor reporting UPR *in planta*. Therefore, we took advantage of the extensive knowledge on UPR mechanisms in different organisms and reporting systems. The primary UPR signal transducer bZIP60 serves as basis for the sensor by exploiting its inherent activation mechanism. In a next step, the ER-stress inducible promoters of secondary transducers, such as BiPs and NACs (Nagashima et al. 2011; Sun et al. 2013), will serve to improve sensitivity of the sensor. The fusion of a FP, first eGFP, to the sensor construct enables the visualization of UPR *in planta*. For a sensor with advanced properties in regards of accurate quantification and capturing signal dynamics, the initial eGFP will be substituted by brighter FPs with altered half-life. In transient expression experiments, the generated sensor variants were evaluated for their UPR reporting performance. Overall, a fluorescent stress sensor will be developed, which produces a fluorescent signal in cells enduring UPR. One last goal was also to generate transgenic plants carrying the transgene of the UPR sensor confirming the functionality of the designed sensor constructs.

# Materials and Methods

## 1. Design of primers for bZIP60 sensor

### 1.1. Isolation and mutagenesis primers

The predicted sequence for *bZIP60* in *N. benthamiana* found in the draft genome on Sol Genomic Network was used as template to design two primer pairs to isolate the said gene in a Nested PCR approach. The outer forward primer bZIP60\_F1 is complement to the 5'-UTR-region just before ATG, while the outer reverse primer bZIP60\_R1 incorporates the stop codon TGA. Lu and colleagues have successfully used the same reverse primer in 2016 to isolate bZIP60. The inner forward primer bZIP60\_Aarl\_F2 included the start codon followed by an overhang enabling Golden Gate Cloning with Aarl. The inner reverse primer bZIP60\_Aarl\_R2 was equal to bZIP60\_R1 but with an overhang with Aarl recognition sites. Based on the later confirmed *NBbZIP60* sequence, a set of primers and primer pairs was designed for modifying the native sequence for our purpose: reporting UPR. The first primer pair, bZIP60\_splice\_F and bZIP60\_splice\_R, was extending outward from the native splicing motifs to remove the intron to imitate the unconventional splicing of bZIP60 mRNA during UPR in plants (Nagashima et al. 2011). The second pair of primers, bZIP6S0\_dS\_F and bZIP6S0\_dS\_R, was also extending in opposite directions. Each primer introduced a single mutation by a substituted cysteine respective guanine in place of the first thymine of the two stop codons. Both primer pairs were phosphorylated to later enable recircularization. Two additional primers, bZIP60\_Aarl\_F3 and bZIP60\_Aarl\_F4, were designed which would lead to 5' end truncations of bZIP60. The third pair, bZIP60\_GFP\_F and NLS\_GFP\_R, isolated eGFP from pEZLS-GFP (plasmid containing eGFP) and had an overhang to enable parallel fusion of GFP while generating the different length bZIP60 variants. This was done through overlap extension PCR using primers NLS\_GFP\_R and bZIP60\_F2/F3/F4 and two templates: isolated eGFP sequence and modified *NBbZIP60* sequence. In a last step, the Aarl (Thermo Scientific™ Aarl (2U/μl), ER1581) recognition sites were added with an overhang primer pair to the different length variants fused with GFP.

### 1.2. Primer list

Primer name	5'-Sequence-3'
bZIP60_F1	CTGGGTTGTAGAATAGGCG
bZIP60_R1 (Lu et al. 2016)	GAGTCACATAACAATTCCCAAAG
bZIP60_Aarl_F2	CACCTGCACTGAACAATGGTGGATGACATCGATG
bZIP60_Aarl_R2	CACCTGCTTCCGATCGAGTCACATAACAATTCCCAAAG
bZIP60_splice_F	P-GCTGTTGGGTTCCCTGCTTTG
bZIP60_splice_R	P-AGACTCCTGCTTGGTCATACAAG
bZIP6S0_dS_F	P-TCGGATTTTCGAGTTCCTGTCCTTCATGAT
bZIP6S0_dS_R	P-CCAGCCTTGTTTCCTCCCTTTATCGGAAC
GFP_bZIP60_R	CTCCTCGCCCTTGCTCACATAACAATTCCCAAAGAATG
bZIP60_GFP_F	TGGGAATTGTTATGTGAGCAAGGGCGAGGAG
bZIP60_Aarl_F3	CACCTGCACTGAACAATGGTTGATGATGACGACAAAGAC
bZIP60_Aarl_F4	CACCTGCACTGAACAATGACCAAGCAGGAGTCTG
NLS_GFP_R	TTAAACCTTACGCTTCTTCTTAGGCCCTGACTTGTACAGCTC GTCCATG
NLS_Aarl_R	CACCTGCGGTTCGATCTTAAACCTTACGCTTCTTCTTAGG
Ascl-AtBiP1P_F	AGGCGCGCCAGAGGAGGTTGAGAGAGAAGATAG

PstI-AtBiP1P_R	ACTGCAGACTGTTGAAACTTTTGC GTACGATCTCTC
Ascl-AtBiP2P_F	AGGCGCGCCTGATTGGGTACGAGTCATTC
PstI-AtBiP2P_R	ACTGCAGACTGTTGAAACTTTTGC GTACGATCTCTC
Ascl-AtBiP3P_F	AGGCGCGCCTCGAAGAGCAAACATAGCACC
PstI-AtBiP3P_R	ACTGCAGACTGTTGCGTTGTTGAGAACTCTTCTTCGATC
Jet_F	CGACTCACTATAGGGAGAGCGGC
LacZ-124-R	CTTCGCTATTACGCCAGCTG
ANAC103Pe_F	AGGCGCGCCTAGGGATATTTTGAAGGCTATTCATTTTC
ANAC103Pe_R	GAAGGGTCTTGCGAAGGATAGTCCGATATGATGATTCATTAG AATAACAATAAG
NbbZIP28_F1	GAAATTGAAAAACTCCACACATGG
NbbZIP28_R1	CTATATGAATACTCCATCTTCAGGTAG
NbbZIP28_R1.2	GGAAACTAACACTTGCAACCTTC
NbbZIP28_R1.3	CATTCCACCATATCTCACATTCAAC
SapI-bZIP28_F2	AGCTCTTCTATGAACAATGGCTGGGCCGATTTTG
SapI-bZIP28_R2	AGCTCTTCATGCGATCTTCAGGTAGTTACTAACGGAAC
SapI-ZIP28_R2.2	AGCTCTTCATGCGATCTACTTAGTTTTACCTCAGTCCTCT
PolyT_A1	CGATCTGCGAGCCTTAGCCGTTTTTTTTTTTTTTTTTTVN
ZT-TSP	CTGGTGTGGTCGCTTGGTATGTGGGGG[SpcC3]
ZTP_F	CTGGTGTGGTCGCTTGGTATGTG
A1_R	CGATCTGCGAGCCTTAGCCG

## 2. Preparations of primers, vectors and genomic material

### 2.1. 5'-phosphorylation of oligonucleotides

dH <sub>2</sub> O	23 µl	37°C for 30'
Oligos (100µM)	3 µl	65°C for 20'
10x T4 Ligase Buffer	3 µl	
T4 PNK (10U/µL)	1 µl	
Total volume	30 µl	

### 2.2. Dissolving dry primers

1. Spin delivered microcentrifuge types with primers down in mini centrifuge
2. Reconstitute in TE buffer for a final concentration of 100µM
3. Shake at max for 10' at up to 37°
4. Make a 10µM working dilution

### 2.3. Cloning vectors

In the first cloning round for sensor variants, pJET1.2 blunt (ThermoFisher) served as cloning vector for intermediate constructs. For the subsequent cloning of the promoter variants, we switched to the newly available universal vector pUV3. The binary vector pTRA-GG1 (8004 bp) served as final vector. It is based on one of the pTRA-vector series: pTRAc (Maclean et al. 2007). This overexpression vector has

both *E. coli* and *A. tumefaciens* origins of replication. Between the LB and RB, the T-DNA it contains a kanamycin resistance gene *nptII* under NOS promoter (Pnos), polyadenylation signal (pAnos), two copies of a scaffold attachment region (SAR) from tobacco, CaMV 35S promoter (Benfey and Chua 1990), terminator (pA35S), 5'-UTR from Chalcone synthase gene for enhanced translation and a multiple cloning site (MCS) (Komori et al. 2007). The vector was modified by adding a lacZ cassette flanked with AarI recognition sites to enable Golden-Gate assembly. We decided for this one-pot reaction due to its practical convenience by consuming low amounts of vector and allowing universal assemblies for various constructs (Engler et al. 2009). See Fig. 31 in appendix for maps of utilized plasmids.

## 2.4. Isolation of bZIP60 from PCR-based cDNA library using leaf tissue

1. Extract total RNA from 170mg of fresh leaf tissue (ground to fine powder in liquid nitrogen) with RNeasy Plant Mini Kit (Qiagen) according to manufacturer instructions;
2. Quantify RNA, assess its quality. Adjust total RNA ( $\leq 75\mu\text{g}$ ) sample volume to 100 $\mu\text{L}$  with water;
3. Incubate at 65°C for 2' to disrupt secondary structures. Place on ice;
4. Isolate mRNA from total RNA sample using 200 $\mu\text{l}$  (1mg) of Dynabeads® Oligo (dT)25 (Invitrogen) following manufacturer instructions;
5. Quantify mRNA, assess its quality. Proceed to first strand cDNA synthesis;
6. Mix:
  - mRNA – 3.2 $\mu\text{l}$  (containing 0.5 – 2 $\mu\text{g}$  in total, 1 $\mu\text{g}$  is optimal)
  - PolyT\_A1 primer (0.5 $\mu\text{g}/\mu\text{L}$ ) – 1 $\mu\text{l}$
  - dNTPs (10mM) – 1 $\mu\text{l}$
7. Incubate at 65°C for 5', then quickly place on ice for at least 1';
8. Add the following mix (4.8 $\mu\text{l}$ ):
  - Reaction Buffer (5X) – 2 $\mu\text{l}$
  - DTT (100mM) – 1 $\mu\text{l}$
  - $\text{MgCl}_2$  (25mM) – 0.8 $\mu\text{l}$
  - RNase inhibitor (40U/ $\mu\text{l}$ ) – 0.5 $\mu\text{l}$
  - SSII RT (200U/ $\mu\text{l}$ ) – 0.5 $\mu\text{l}$
9. Incubate at 50°C for 60', then lower temperature to 42°C and add the following mix (10 $\mu\text{l}$ ):
  - ddH<sub>2</sub>O – 3.1 $\mu\text{l}$
  - DTT (100mM) – 1 $\mu\text{l}$
  - Reaction Buffer (5X) – 2 $\mu\text{l}$
  - $\text{MgCl}_2$  (25mM) – 0.8 $\mu\text{l}$
  - $\text{MnCl}_2$  (100mM) – 0.6 $\mu\text{l}$
  - ZT-TSP primer (10 $\mu\text{M}$ ) – 2 $\mu\text{l}$
  - SSII RT (200U/ $\mu\text{L}$ ) – 0.5 $\mu\text{l}$
10. Incubate at 42°C for 90', then place on ice;
11. Add 2 $\mu\text{L}$  of 25mM NaOH to the RT reaction. Incubate at 68°C for 30', then place on ice;
12. Synthesize dscDNA using 11 $\mu\text{l}$  of the first strand cDNA reaction. Mix:
  - ddH<sub>2</sub>O – 18.5 $\mu\text{l}$
  - dNTPs (2mM) – 5 $\mu\text{l}$
  - 5X HF Buffer – 10 $\mu\text{l}$

- ZTP\_F primer (10μM) – 2.5μl
- A1\_R primer (10μM) – 2.5μl
- ss cDNA – 11μl
- Phusion HSII Polymerase – 0.5μl

13. Perform primer extension in a thermocycler using a program:

- 98°C – 1'
- 5 cycles:
  - 98°C – 10"
  - 68°C – 30"
  - 72°C – 3'

To isolate gene-specific cDNA, use 2-5μL of ds cDNA for subsequent PCR amplifications with gene-specific primers (e.g. bZIP60\_F1 and bZIP60\_R1 to isolate *NBbZIP60*).

## 2.5. Preparing donor plasmids for Golden-Gate Cloning

1. Precut with double cutter enzyme (Bful) (for pJET1.2-derived plasmids)
2. Dephosphorylate the linearized plasmid with SAP with subsequent deactivation
3. Load reaction mix to 1% agarose gel and let run at 55V
4. Purify with GeneJET Plasmid Miniprep kit from Thermo Scientific™

## 3. Cloning protocols for isolation and modifications of *NBbZIP60*

### 3.1. PCR reactions

with reagents from Thermo Scientific™ using primers synthesized at Sigma in Bio-Rad MJ Mini Thermo Cycler:

#### 3.1.1. General PCR reaction set-up

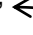
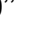

		General program:
dH <sub>2</sub> O	x μl	98°C for 1'
dNTPs (10mM)	5 μl	98°C for 10" ← Ta C for 30" — x N° of cycles 72°C for 20" —
5xHF buffer	10 μl	
P1_F (10mM)	2,5 μl	
P2_R (10mM)	2,5 μl	
template	1-5 μl	72°C for 3'
PHU polymerase	0,5 μl	14°C forever
Total reaction volume	50 μl	


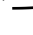
- 1<sup>st</sup> Nested PCR (Ta 56°C and 20" extension time, 35 cycles) to isolate bZIP60 with dscDNA from *N. benthamiana* as template
- Inverse PCR Ta 62, 25 cycles 1' extension using phosphorylated primers to remove the *bZIP60* intron
- Add 0,5μl DpnI to PCR mix after cycling for 30' to remove template (optional)

- Re-ligation of purified inverse PCR product
- Removing stop codons Ta 67°C, 28 cycles, by another inverse PCR

### 3.1.2. Adjusted program for overhang PCR modification:

98°C for 1'

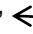
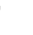
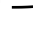
98°C for 10"  x 5  
Ta<sub>1</sub>°C for 30"   
72°C for x<sub>1</sub> 

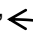

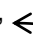

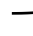
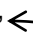
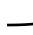
98°C for 10"  x 25  
Ta<sub>2</sub>°C for 30"   
72°C for x<sub>2</sub>

72°C for 3'

- 2nd Nested PCR (Ta 58°C and 45" extension time and 1', N1=5, N2=25) to isolate bZIP60 using PCR mix from 1<sup>st</sup> nested PCR as template
- bZIP60 length variants, Ta<sub>1</sub>=62°C x<sub>1</sub>=20", Ta<sub>2</sub>=67°C x<sub>2</sub>=1'
- GFP isolation with GFP\_bZIP60\_R and bZIP60\_GFP\_F, Ta<sub>1</sub>=62°C x<sub>1</sub>=20", Ta<sub>2</sub>=67°C x<sub>2</sub>=1' same as sensor lengths
- Adding Aarl sites to sensor variants, TM=60°C and x<sub>1</sub>=30", x<sub>2</sub>=45"
- Truncating always on sensor to F4 size, 62° 20" one step

### 3.1.3. Overlap extension PCR

dH <sub>2</sub> O	x µl	98°C for 1'
dNTPs (2mM)	5 µl	
5xGF buffer	10 µl	98°C for 10" 
P1_F (10mM)	2,5 µl	Ta C for 30" 
P2_R (10mM)	2,5 µl	72°C for 20" 
template	1-5 µl	
PHU polymerase	0,5 µl	72°C for 3'
Total reaction volume	50 µl	14°C forever

dH <sub>2</sub> O	x µl	98°C for 10" 
dNTPs (2mM)	5 µl	72°C for 1' 
5xgreen HF buffer	10 µl	
P1_F (10mM)	2,5 µl	98°C for 10" 
P2_R (10mM)	2,5 µl	Ta for 30" 
Template 1	0,5-5 µl	72°C for x 
Template 2	0,5-5 µl	
PHU polymerase	0,5 µl	98°C for 10" 
Total reaction volume	50 µl	72°C for 1' 

- Fuse GFP with bZIP60\_F2, \_F3, \_F4 with Tm=58, x=40"

### 3.2. Assembly reactions

#### 3.2.1. Blunt end ligation of insert into plasmid vector (pJET1.2 and pUV3)

dH <sub>2</sub> O	X µl	25°C for 15'
5x Quick ligation buffer	2 µl	
Insert (3x molar excess to vector)	x µl	
Vector (50ng/µl)	1 µl	
T4 ligase	0,5 µl	
Total volume	10 µl	

- *NBbZIP60* into pJET1.2: pbZIP60\_3, pbZIP60\_1

#### 3.2.2. Recircularization or ligation reaction

dH <sub>2</sub> O	7 µl	25°C for 15'
5x Quick ligation buffer	2 µl	
template	0,5 µl	
T4 ligase	0,5 µl	
Total volume	10 µl	

- pbZIP60ΔI
- pbZIP60ΔS
- pbZIP60ΔIntronΔSTOP

#### 3.2.3. Golden-Gate Assembly

dH <sub>2</sub> O	x µl	37°C for 5'	← x 10
5x Quick ligation Buffer	4 µl	25°C for 10'	
50x oligonucleotides	0,4 µl		
Donor plasmids (3x excess)	x µl	37°C for 60'	
pTRA-GG1 (50ng/µl)	1 µl	14°C forever	
AarI	0,5 µl		
T4 ligase	1 µl		
Total volume	20 µl		

- pbZIP60\_F2\_GFP=pJBE22
- pJBE5, pJBE5s

#### 3.2.4. Golden-Gate with half reaction volume

dH <sub>2</sub> O	6,1 µl	37°C for 5'	← x 10
5x Quick ligation Buffer	4 µl	25°C for 10'	
Insert (3x excess)	0,9 µl		
pUV3 (46ng/µl)	0,5 µl	37°C for 60'	
AarI	0,5 µl	14°C forever	
T4 ligase	0,5 µl		
Total volume	10 µl		



### 3.2.5. Conventional cloning (RE digest and subsequent Ligation)

dH <sub>2</sub> O	15-12-8 µl	37°C for 30''
10x Fast Digest Buffer	2 µl	
plasmids	1-4-8 µl	
PstI	1-2-2 µl	
Ascl	1-2-2 µl	
Total volume	20 µl	

dH <sub>2</sub> O	4,5 µl	25°C for 15''
10x Restriction buffer	2 µl	
plasmids	2 µl	
Inserts	1 µl	
T4 Ligase	0,5 µl	
Total volume	10 µl	

## 3.3. Purifications

### 3.3.1. Purify DNA from PCR product:

1. Load whole or aliquot of reaction with 6x Loading dye on 1-2% agarose gel containing a nucleotide dye (Biotium GelRed® Nucleic Acid Gel Stain or Invitrogen™ SYBR™ Green Nucleic Acid Gel Stain)
2. Let run in TAE buffer with Bio-Rad horizontal Electrophoresis system (or Sub-Cell® GT Cell) at 55V for 30-120'
3. Detect bands under illuminator and excise bands of expecting sizes from gel
4. Purify gel slices with GeneJET Gel Extraction Kit (Thermo Scientific™) following the given instructions
5. Measure DNA concentration (ng/ µl) with Thermo Scientific™ NanoDrop 2000

### 3.3.2. Purify DNA from bacterial cultures with kit

1. After growth over night, transfer 2ml of culture into new microcentrifuge tube
2. Purify culture according to GeneJET Plasmid Miniprep Kit (Thermo Scientific™) protocol
3. Measure DNA concentration (ng/µl) with Thermo Scientific™ NanoDrop 2000

## 3.4. Heat shock transformations

### 3.4.1. of *E. coli*

1. Thaw competent cells (DH10B *E. coli*) in ice for around 10'
  2. Add 3µl of ligation reaction to & flick microcentrifuge tube with cells
  3. Incubate on ice for 30'
  4. Heat for 30'' in 42°C warm water bath & back in ice
  5. Add 250µl of sterile SOB media
  6. Shake at 200rpm and incubate at 37°C for 60'
  7. Plate 30-40µl of culture being an aliquot or concentrate on selective agar LB plates
  8. Optional when using pTRA vector for blue-white selection: add 40µ of X-Gal and 40µ of IPTG
  9. Let colonies grow over night (16-18h) at 37°C
  10. Inoculate with single colonies 3ml culture with LB media including antibiotics
- Or make patchy plates for next-day screening through colony PCR, RE digest or cracking

### 3.4.2. of *A. tumefaciens*

1. Thaw competent cells (GV3101 pMP90RK) in ice for 20'-30'
2. Add 1µg of plasmid to & flick microcentrifuge tube with cells
3. Incubate on ice for 5'
4. Freeze in liquid N<sub>2</sub> for 5'
5. Heat for 5' in 37°C warm water bath & back in ice
6. Add 250µl of sterile YEB media
7. Shake at 200rpm and incubate at 28°C for 120'
8. Plate 30-40µl of culture being an aliquot or concentrate on selective agar YEB plates
9. Let colonies grow for 2-4 days at 28°C
10. Inoculate with single colonies 1ml culture with YEB media including antibiotics for next-day screening through colony PCR or RE digest

## 3.5. Screenings

### 3.5.1. with colony PCR using DreamTaq polymerase without proofreading function

#### Program:

dH <sub>2</sub> O	15 µl	95°C for 3'
dNTPs (2mM)	2 µl	
5xDreamTaq Green buffer	2 µl	95°C for 10" ←
P1_F (10mM)	0,4 µl	Ta C for 30" } x 29
P2_R (10mM)	0,4 µl	72°C for x" }
Singly colony = template	Dip	
DreamTaq polymerase	0,2 µl	72°C for 5'
Total reaction volume	20 µl	14°C forever

1. Load whole or aliquot of reaction with 6x Loading dye on 1-2% agarose gel containing a nucleotide dye (Biotium GelRed® Nucleic Acid Gel Stain or Invitrogen™ SYBR™ Green Nucleic Acid Gel Stain)
2. Let run in TAE buffer with Bio-Rad horizontal Electrophoresis system (or Sub-Cell® GT Cell) at 55V for 30-120'
3. Detect bands under illuminator
4. Extraction of plasmids from positive colonies using Plasmid Extraction Kit by Qiagen
5. Measure DNA concentration (ng/ µl) with Thermo Scientific™ NanoDrop 2000

### 3.5.2. with Cracking Buffer

1. Make patchy plate from plates with small single colonies
2. Pick fair amount of bacteria with sterile pipette tip from patch
3. Add to microcentrifuge tube with 50 µl of Lysis buffer with BromophenolBlue
4. Heat at 65°C for exact 5'
5. Cool on ice for exact 5'
6. Centrifuge for 10' at max speed
7. Prepare plasmid controls (100ng per lane) with loading dye
8. Load 20µl of samples omitting pellet and controls to agarose gel
9. Let run in TAE buffer with Bio-Rad horizontal Electrophoresis system (or Sub-Cell® GT Cell) at 55V for 30-120mins

3.5.3. *with Restriction enzymes (RE) digest, where at least one cuts within backbone, reagents from Thermo Scientific™*

dH <sub>2</sub> O	X µl	37°C for 15-120'
5 x FastDigest Buffer	2 µl	
Enzyme 1	0,5-1 µl	
Enzyme 2	0,5-1 µl	
Total volume	10 µl	

- BamHI, HindIII, Kpn2I, MssI, NheI, EcoRI

### 3.6. Preparation for Sanger sequencing

1. Dilute sample with MQ-H<sub>2</sub>O to absolute amount of 800 to 1200ng in 12µl
2. Add 3µl sequencing primers (10mM)
3. Label with barcode and send to Microsynth
4. Sequencing result in FASTA format and as chromatogram delivered within 48h

3.6.1. *List of samples sent to sequencing:*

Sample	Sequencing primer
bZIP60_3	JET_F
bZIP60_3	JET_R
bZIP60_1	JET_F
bZIP60_1	JET_R
bZIP60_1s	JET_F
bZIP60_1s	JET_R
bZIP60ΔSTOP_GFP_F2	JET_F
bZIP60ΔSTOP_GFP_F2	JET_R
bZIP60ΔSTOP_GFP_F3	JET_F
bZIP60ΔSTOP_GFP_F3	JET_R
bZIP60ΔSTOP_GFP_F4	JET_F
bZIP60ΔSTOP_GFP_F4	JET_R
TSF1	TRA_R
TSF2	TRA_R
TSF3	TRA_R
NS138	JET_F
NS138	JET_R

## 4. Agroinfiltration experiments

### 4.1. Induce and dilute *A. tumefaciens* cultures for infiltrations

1. Pellet 2x2ml of 1-2 day grown cultures GVK by centrifuging at 3300xg for 5'
2. Remove media & resuspend the pellet in 1ml of induction media with 100µM acetosyringone
3. Let shake for 30' at 200rpm at room temperature
4. Measure OD<sub>600</sub> with spectrophotometer
5. Dilute with ½ MS Basal Salt Mixture at pH= 5,6 to specific OD<sub>600</sub>

### 4.2. Testing sensor variants F2-F4, TSF1-4, full-length and short always-on sensors

1. Infiltrate using sterile 1ml syringes with flat tips on the underside of leaves from 5-7 weeks old *N. benthamiana* plants.
2. After 48 to 72h post-infiltration, DTT was injected to the 2<sup>nd</sup>, 3<sup>rd</sup> and 4<sup>th</sup> true leaves.
3. After 0 to 24h post-injection, the leaves were analyzed under UV light with emission of 366nm, as well as leaf parts were prepared for and observed under EFM (epi-fluorescent microscope)

### 4.3. Co-expression experiments Make mixtures of co-infiltrates

1. Infiltrate using sterile 1ml syringes with flat tips on the underside of the 2<sup>nd</sup>, 3<sup>rd</sup> and 4<sup>th</sup> true leaves from 5-7 weeks old *N. benthamiana* plants.
2. After 3 days post-infiltration, the leaves were analyzed for protein, as well as leaf parts were prepared for and observed under EFM
  - bZIP60(u) and bZIP60(s) protein content + HC and LC antibodies with p19 and DsRed
  - TSF1-4 with bZIP60(s) and bZIP28(s)

## 5. Protein extraction

1. Cut around 50mg of three infiltrated leaf
2. Pool a total of 150mg into microcentrifuge tube with 2 metal beads
3. Freeze in liquid N<sub>2</sub> & pulverize in Retschmill at max speed for 30''
4. Back into liquid N<sub>2</sub>, while preparing 1xTBS & fresh PMSF Buffer
5. Add 500µl TBS/PMSF buffer to pulverized samples on ice & vortex well
6. Incubate on ice for few minutes
7. Remove balls with magnetic stick & centrifuge at max speed for 10'
8. Make fresh 4x Laemmli Buffer by adding 400mM DTT as reducing agent
9. Transfer 200µl of supernatant to new microcentrifuge tube (= soluble proteins fraction), while avoiding to disturb the pellet
10. Discard left-over supernatant & add 1ml TBS /PMSF Buffer
11. Resuspend the pellet & centrifuge at max speed for 5'
12. Rewashing: repeat steps 10.-11. With final discard of supernatant
13. Add 400µl MQ-H<sub>2</sub>O + 100µl 4x Laemmli Buffer with DTT & resuspend the pellet
14. Heat in oven at 65°C for 30'
15. Centrifuge at max speed for 5' & transfer 200µl of supernatant to new microcentrifuge tube (= insoluble proteins fraction) & discard left-over
16. Mix 15µl of soluble proteins fraction with 5µl Laemmli Buffer, while 20µL of insoluble proteins fraction is further used

## 6. Solutions and Buffers

- TAE buffer = Tris base, acetic acid and EDTA, pH=8,3,
- TE buffer= Tris EDTA,
- 10x TBS= Tris NaCl (pH 7.5),
- PMSF=Phenylmethylsulfonyl fluoride in 1-propanol
- TBST=Tris-buffered saline, pH=7,4, Tween20 0,1% (v/v))

Recipes can be found in Cold Spring Harbor Protocols 2006 - 2019.

### 6.1. Induction media adapted from Shamloul et al. 2014

Murashige & Skoog (MS) Basal Salt Mixture	0,44g/L
MES	50mM
Glucose	0,5%
	Adjust to pH 5,6
Acetosyringone	100µM

### 6.2. 2x Lysis (Cracking) buffer

Sucrose or glycerol	20% w/v
NaOH	200mM
KCl	120mM
EDTA	10mM
SDS	0,5%
BrBlue (Bromophenol blue)	pinch

### 6.3. SOB media

Tryptone	20 g/L
Yeast Extract	5 g/L
MgSO <sub>4</sub>	02,4 g/L
NaCl	0,5 g/L
KCl	0,186 g/L

### 6.4. LB media

Tryptone	10 g/L
Yeast Extract	5 g/L
NaCl	0,5 g/L
Optional: Antibiotics	20-100 mg/L
For plates: Bacterial agarose	15 g/L

### 6.5. YEB media

Peptone	5 g/L
Yeast Extract	1 g/L
MgCl <sub>2</sub>	5 g/L

Sucrose	5 g/L
Beef extract	5 g/L
Optional: Antibiotics	20-100 mg/L
For plates: Bacterial agarose	15 g/L

#### 6.6. 4x Laemmli Sample Buffer

Tris (1.0 M, pH 6.8)	10 ml
SDS	4.0 g
Glycerol	20 ml
β-Mercaptoethanol	10 ml
BrBlue	0.1 g
dH <sub>2</sub> O	to 50 ml

#### 6.7. Developing buffer

Diethanolamine	1M
MgCl <sub>2</sub>	0,5 mM
MgSO <sub>4</sub>	Adjust to pH=9,6

### 7. Floral dip of *Arabidopsis* after Zhang et al. 2006

**Plants** should have many unopened flowers, being optimal with 2-10 cm stalks, with few already developed siliques (developed siliques may be removed)

#### Agrobacterium culture

- starter culture: inoculate 5-ml liquid LB medium (containing the appropriate antibiotics) with single *Agrobacterium* colony or from frozen stock. Incubate at 28 °C, 120 -180 rpm, for 2-3 d
- inoculate 500 ml LB (+antibiotics) with starter culture 1:1000 (e.g. 500 µl per 500 ml)
- grow for 48 hours (not 24h as in publication), to OD~ 1.5-2.0
- collect *Agrobacterium* cells by centrifugation at 4,000g for 10 min at room temperature, and gently resuspend cells in 1 volume of freshly made 5% (wt/vol) sucrose solution with a stirring bar and transfer to beaker
- add Silwet L-77 to a concentration of 0.02% (vol/vol) (e.g. 100 µl per 500 ml), mix

#### Dipping

- invert plants and dip aerial parts of plants in the *Agrobacterium* cell suspension for 10 s with gentle agitation. We dip not only inflorescences but also the rosette to soak shorter axillary inflorescences. Alternatively, after dipping one may pipette *Agrobacterium* sln on shorter axillary inflorescences which did not come into contact with *Agrobacterium* solution
- after dipping, drain plants of excess solution (dip them shortly on paper towel)

#### Afterwards

- cover dipped plants with a plastic cover (if several pots of same genetic background and dipped with same construct: lay down the treated plants on their sides into tray covered on bottom with wet paper towels; put the tray into autoclave bag and close it with tape) or wrap individual pots plastic film and lay on their side. Put them into a darkened room, at room temperature until the next day
- remove them from plastic, put them upright into growth chamber and use Aracons to protect them from cross-contamination

## Results and Discussion

Initially, the objective of this thesis was to design and clone a molecular sensor functional in plants. As base, we chose the endogenous UPR transducer bZIP60 from *N. benthamiana* (*NBbZIP60*). After confirming the *NBbZIP60* transcript, its sequence was modified in order to exploit the splicing mechanism. In a proof of concept experiment, it was shown that the double hairpin structure together with the HR domain is enough to be recognized and spliced during UPR and that the reporting system works in *N. benthamiana*.

The next objective evolved from the observation of the preliminary tests to improve the sensor. The first aim was to increase sensitivity to create a better distinction between actual signal and background by testing stress-inducible promoters. Following this, the plan was to substitute the eGFP with a modified super-bright FP in order to enable the dynamic detection of UPR. In addition, another reporter gene should be added to serve as the internal control, allowing cellular quantification of the sensor signal.

The following paragraphs describe the resulting constructs during cloning and the findings from *in planta* testings of the first two generations of sensor constructs. The promising results of the first stably transformed sensor variant in *Arabidopsis thaliana* are briefly portrayed. In addition to the main project, the effects of co-expressing UPR transducers bZIP60(u), bZIP60(s) and bZIP28(s) together with recombinant proteins of interest were deduced in co-infiltration experiments in *N. benthamiana*.

### 1. Design of sensor variants on basis of endogenous *NBbZIP60* with FP reporter

#### 1.1. Isolation of *NBbZIP60* with nested primers including overhangs

First, the sequence of the *bZIP60* gene in *N. benthamiana* had to be determined. The characterized bZIP60 protein sequence from *Arabidopsis thaliana* was taken from UniProt (Q9C7S0, in TAIR: At1g42990) and blasted against the predicted proteome from the draft genome of *N. benthamiana* published on Sol Genomics Network ([Niben.genome.v1.0.1.scaffolds.nrcontigs.fasta](#)) (Bombarely et al. 2012). There were two results: The first one, Niben101Scf24096g00018.1 annotated as “bZIP transcription factor 60”, showed highest similarities to *A. thaliana* bZIP60, while the second one showed a significantly shorter sequence. We looked into the genomic context of Niben101Scf24096g00018.1 and exported the coding sequence including 5'- and 3'-UTRs from Sol Genomics Network. Next, we decided for the common Nested PCR approach to ensure specificity while isolating *bZIP60* due to the high similarities within the bZIP family.

#### 1.2. Found second homologue

During the isolation of *NBbZIP60*, one of the bacterial clones contained a possible homologue of *bZIP60*. According to the sequencing and aligning result, the isolated sequence of this homologue was more than 98% identical to the predicted *bZIP60* sequence. However, the coding sequence strongly differed in the middle part from the sequence in Sol Genomics Network. Since the latter sequence served as a template for initial primer designs, further work with this homologue might have caused confusions.

### 1.3. Characteristics of the endogenous *NBbZIP60* sequence and its spliced isoform

The sequencing of another isolated *bZIP60* clone gave the identical sequence as found in Sol Genomics Network. Thus, our sequencing result confirmed the predicted data from the draft genome. This *bZIP60* sequence of 900bp from *N. benthamiana* (*bZIP60(u)*) was chosen as basis for the sensor. According to the characterized *bZIP60* mRNA in *A. thaliana* (Nagashima et al. 2011), the intron region which is removed during unconventional splicing is 23nt long (CTGTGCTCTTGTGGAATCCCTG). The intron is flanked by CUGCUG motifs where two cuts occur between G and C. The same motifs are found in *NBbZIP60*, indicating the intron region. The spliced mRNA sequence (*bZIP60(s)*) is predicted to be 771bp. The intron region is removed and the religated sequence experiences a frameshift resulting in premature stop codons. The splicing mechanism and premature stop codons were the main considerations while designing primers. The isolated *NBbZIP60* sequence was used as a template for several mutagenesis PCRs (see Fig. 5).

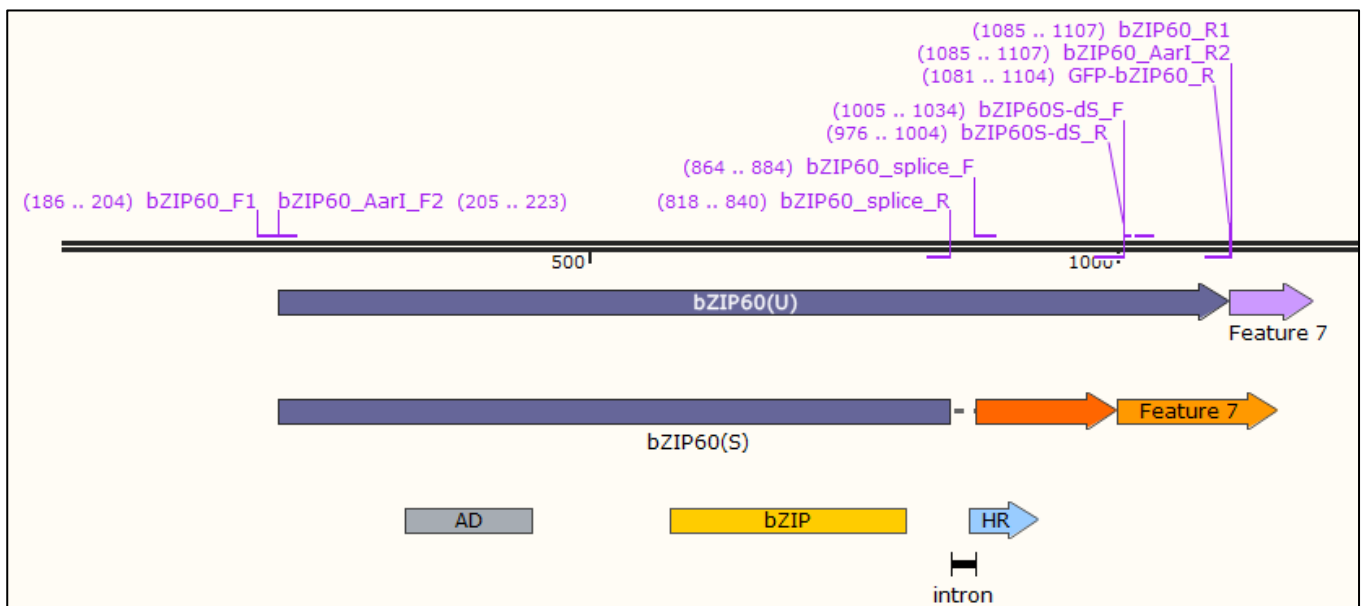


Fig. 5: Initial plan with mutagenesis primers to modify endogenous *bZIP60(u)* for sensor construct. Primer pairs *bZIP60\_F1/R1* and *bZIP60\_F2/R2* isolate the coding sequence. Outward extending primer pairs, *bZIP60\_splice\_F/R* and *bZIP60S-dS\_F/R*, are removing hindering intron and stop codons. Overhang primers are adding *AarI* cutting sites, *bZIP60\_AarI\_F/R2*, and enabling GFP fusion, *GFP-bZIP60\_R*. When *bZIP60* is spliced (*bZIP60(s)*), it leads to a shift of the ORF in the downstream sequence. The position of characterized *bZIP60* domains is indicated: activation domain (AD), *bZIP* domain, intron and hydrophobic region (HR). Generated with SnapGene.

### 1.4. Elimination of premature stop codons due to frameshift

It is assumed that 23nt are removed during unconventional splicing of *bZIP60(u)*, leading to a frameshift. Consequently, the new downstream coding sequence incorporates two new stop codons. This would provoke a premature translation stop of the *bZIP60* mRNA. Thus, the stop codons were eliminated by introducing single-point mutations, while the native downstream amino acid sequence was preserved. The first letter (T) of each stop codon (see Fig. 7) was substituted through an elongated outward primer. This was essential for the next step, where an eGFP-tag was fused to the 3' end of the *bZIP60* sequence.

### 1.5. Preparation of eGFP-tag

The main aim of the sensor was to make induced UPR visible with a fluorescent reporter protein. From the broad range of reporter systems, eGFP was chosen primarily for practical reasons: being a well-studied and common fluorescent reporter. EGFP was amplified from a sequence already available in our



lab. We designed a primer pair (bZIP60\_GFP\_F; GFP\_bZIP60\_R) with bZIP60 compatible overhangs to enable the direct fusion through Overlap Extension PCR to bZIP60 variants discussed in the following.

### 1.6. Different sensor lengths

The sensor should only report and not trigger UPR itself or neither intervene with other cellular processes in plants. Thus, we aimed to determine the shortest functional bZIP60 sequence. Moreover, *NBbZIP60* has not been extensively characterized yet. It was not known which portion of the *bZIP60* mRNA was necessary for successful splicing in plant cells. On the one hand, the *bZIP60(u)* transcript needs to be long enough including an hydrophobic region (HR) for binding to the ER membrane to get in proximity of IRE1 (Yanagitani et al. 2011; Shanmuganathan et al. 2019). On the other hand, it was unclear if the double hairpin structure of *bZIP60(u)* is sufficient for recognition and splicing by IRE1. Therefore, three different lengths of the sensor sequence were proposed. Each of them included different, potentially essential *bZIP60* domains: Activation Domain (AD) for transcriptional regulation, bZIP domain (bZIP) and transmembrane domain (TMD or HR) (Nagashima et al. 2011). All three variants were generated with different forward primers, conserving the intron followed by the HR from the bZIP60 $\Delta$ STOP sequence, where the stop codons had been already removed. The longest construct, bZIP60 $\Delta$ STOP-GFP\_F2, represents the full-length endogenous *NBbZIP60* sequence with all domains (900bp+710bp). The second, bZIP60 $\Delta$ STOP-GFP\_F3, and third length variants, bZIP60 $\Delta$ STOP-GFP\_F4, were truncated at the 5' end of *bZIP60(u)*. The middle one included the bZIP domain (585bp), while the shortest bZIP60 construct consists of only the intron, HR and downstream sequence (282bp). The fusion of eGFP (710bp) took place in the same PCR reactions as the synthesis of the different length variants by using NLS\_GFP\_R as the reverse primer and the respective forward primers by using (bZIP60\_AarI\_F2/F3/F4 and 5'-5'-20' cycling timing) (see Fig.7).

### 1.7. Conservation of intron for ER stress reporting sensor variants

For the preliminary sensor constructs, we aimed to exploit the endogenous signaling pathway of UPR. The transmembrane protein IRE1 dimerizes by the presence of unfolded proteins in the ER lumen. This activates IRE1, enabling to splice *bZIP60* mRNA present in the cytosol. The bZIP60(s) protein translocates in the nucleus, initiating the transcription of UPR genes (Zhang et al. 2015). Since bZIP60(s) is an intermediate transducer of the UPR signal, it means in consequence that the spliced form of bZIP60 is always present during UPR. In order to exploit this fact, the reporter tag was fused to the end of *bZIP60* variants; being only in frame after unconventional splicing due to UPR. As long as the bZIP60 variants in the cytosol are not activated through splicing, eGFP is not translated and no fluorescent signal should be emitted. When UPR is induced, the sensor variants are spliced enabling an eGFP signal. Therefore, it was crucial for the preliminary sensors to conserve the intron region to enable the differentiation between the unspliced and spliced form of bZIP60 variants indicating ER stress.

### 1.8. Synthetic *bZIP60(s)* serving as positive control

By synthetically removing the intron from *bZIP60(u)* while preserving the remaining sequence, the unconventional splicing event was imitated, leading to the spliced version, the *bZIP60(s)* (see Fig. 6(2)). Since the spliced bZIP60 variant would be present without the induction of UPR, we considered such constructs as always-on sensors and used them as positive controls during *in planta* experiments. In parallel, co-expression experiments were conducted to study the effect of the spliced UPR transducer on recombinant protein yields and bZIP60's role in UPR regulation. For this construct, the isolated *NBbZIP60* sequence was spliced applying outward extending primers (bZIP60\_splice\_F/R), which flanked the CUGCUG motifs of the intron. Subsequently, the stop codons were removed and the eGFP-tag was

added as in the case of the *bZIP60* length variants. The final construct bZIP60ΔIΔSTOP\_GFP\_F2 had a length of 1589bp.

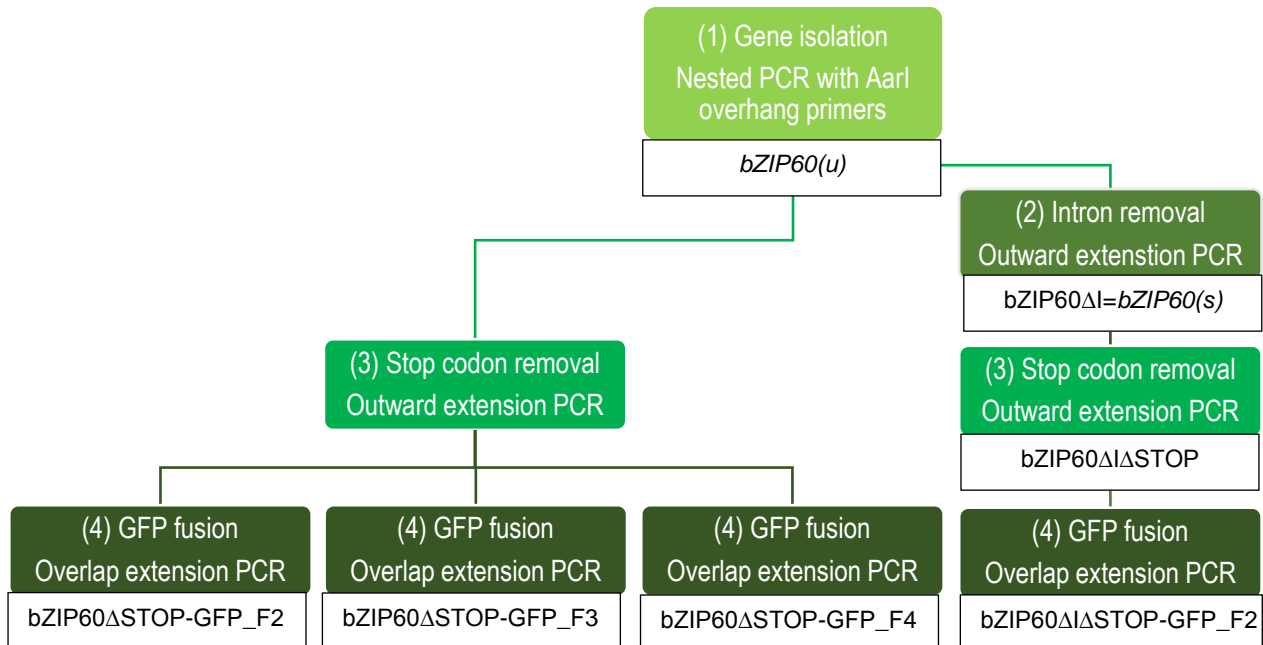


Fig. 6: Cloning steps for sensor variants starting with (1) the isolation of *bZIP60(u)*, followed by removal of (2) intron and/or (3) of stop codons with final (4) GFP fusion to length variants. Check Fig. 7 for the actual structures of length variants.

### 1.9. Additional elements of overexpression vector and final Golden-Gate assembly

The overexpression vector pTRAcK was carrying the promoter from Cauliflower Mosaic Virus 35S (CaMV35S) and the transcriptional enhancer 5'UTR from chalcone synthase gene (CHS) already. This system was described by Maclean et al. in 2007. A constitutive promoter such as CaMV35S is giving high expression levels for recombinant proteins in plants (Benfey and Chua 1990). It was considered beneficial for our initial purpose to boost *bZIP60* expression levels during transient testing. Furthermore, the native *bZIP60* incorporates an endogenous nuclear localization signal (NLS), located at the 5' end of the coding sequence. Consequently, it is missing in the two 5' end-truncated sensor variants and an additional NLS of viral origin (SV40) (Colin Dingwall et al. 1982) was installed to be at the 3' end of the sensor after eGFP. This guaranteed the targeted transport of each spliced *bZIP60* variant into the nucleus. Through this nuclear accumulation, the intensity of the fluorescent signal would be increased and more easily detected. The sensor length variants (bZIP60ΔSTOP-GFP\_F2/F3/F4) and full-length always-on sensor (bZIP60ΔIΔSTOP-GFP\_F2) were finally assembled into the prepared pTRA-GG1 vector through Golden-Gate cloning, using the type IIS restriction enzyme AarI (Fig. 7). This cloning approach represents a universal procedure, which we optimized for our purposes to generate multiple sensor variants in one-pot reactions, while saving reagents and time. Through the generalized cloning procedure, future modifications of the sensor could be conducted with reduced working steps within a moderate timeframe.



## 2. Transient testing of sensor variants

### 2.1. Proof of concept experiment demonstrates the functionality of the designed sensor

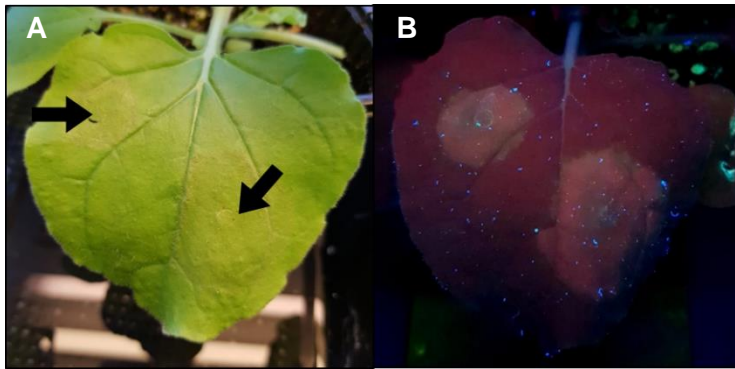


Fig. 8: Pictures taken by Stanislav Melnik. A: Leaf infiltrated with JBE20s 3dpi under normal light conditions with black arrows marking injection spots after 3dpi. B: Same leaf as A being excited with UV light at 366nm and emitting two shining spots.

In a preliminary experiment, all three-sensor length variants, plus the always-on sensor, were transiently overexpressed to evaluate their functionality. The agrobacteria containing the respective sensor variants (JBE20, JBE21, and JBE22) and the full length always-on sensor (JBE20s) were infiltrated into the leaves of *N. benthamiana* plants. The JBE20s culture, with the full-length always-on sensor, was infiltrated into three leaves, targeting two distinct areas on each of them. Three days post-infiltration (dpi), the leaves were observed under normal and UV light (Fig. 8). The partial

discolorations of the leaf were provoked by onset of necrosis, indicating where JBE20s was infiltrated earlier. Under the UV light (366nm) lamp, the whole area of the leaf showed some fluorescence. However, the untreated regions showed a weak signal, probably being autofluorescence (Croce and Bottiroli 2014) while two distinct spots were brightly shining (Fig. 8B). Since the shining spots overlap the infiltration spots (Fig. 8A), the fluorescent signal under UV light was assumed to derive from the full-length always-on sensor. This bZIP60 variant has the eGFP-tag always in-frame and is expected to give a fluorescent signal during overexpression.

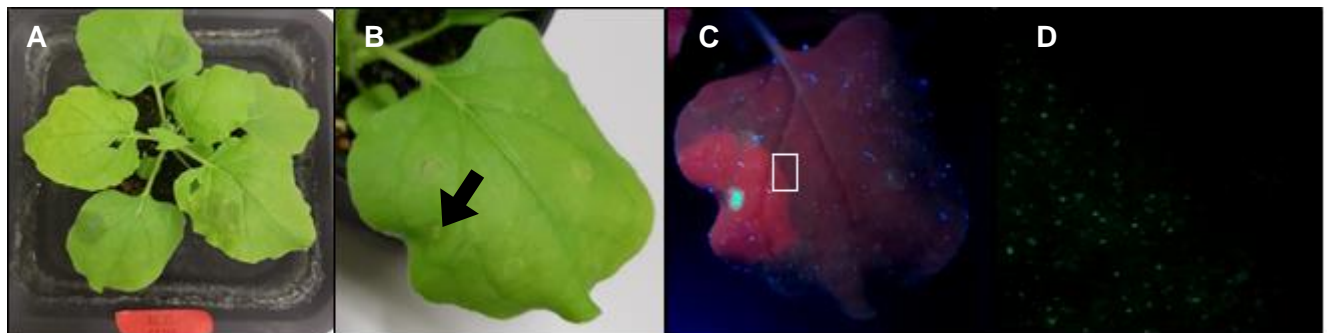


Fig. 9: Pictures taken by Stanislav Melnik. A: The three leaves after DTT infiltration. B: Leaf infiltrated with JBE22 3dpi under normal light conditions with black arrow marking 50mM DTT injection spot. C: Same leaf as B being excited with UV light at 366nm and emitting one shining spot probably indicating UPR. Tissue sample taken for subsequent analysis under EFM (white rectangle). D: Leaf sample under EFM (LEICA) showing eGFP signal of DTT treated tissue with clear interphase to untreated tissue.

Meanwhile, JBE20, JBE21 and JBE22 were each infiltrated to different leaves in duplicates. After three days, 50mM DTT was injected to distinct areas of each previously infiltrated leaf. After another half day, the treated leaves were evaluated under UV lamp (Fig. 9A/B/C for JBE22 and Fig. 32 in appendix for JBE20 and JBE21), as well as under EFM (Fig. 9D). The three leaves showed again weak fluorescence over the whole area where the sensor constructs were infiltrated. However, distinctly brighter spots were observable where DTT was injected. DTT is a known UPR inducer (Cho and Kanehara 2017). As a reductive agent, it prevents protein folding in the normally oxidative ER lumen. The unfolded proteins stimulate unconventional splicing of unspliced *bZIP60* mRNAs (Nagashima et al. 2011; Parra-Rojas et al. 2015). Our sensor variants were designed to emit a fluorescent signal derived from the eGFP-tag

when spliced. The presence of DTT was expected to lead to splicing of the *bZIP60* variants and in consequence emission of a fluorescent signal. Therefore, the bright spots under UV light were initially identified as this signal due to the apparent induction through DTT. Leaf areas with only the sensor variants emitted no signal exceeding autofluorescence. Necrotic tissues, from contact with the injection syringe, appeared bright greenish blue. Photographs were taken with a simple 13Mpix smartphone camera. To confirm the UV lamp detection results, leaf samples including tissue with and without signal, were prepared for further analysis with a epifluorescence microscope (EFM) (example: Fig. 9B white rectangle).

First, the samples were evaluated for the integrity of epidermal cells under bright light. Then, the cells were excited with a laser for GFP excitation. A homogenous distribution of the scattered eGFP signal was observed at areas infiltrated with both sensor variants and DTT, while leaf tissue infiltrated only with the sensor variants did not show any signal. A clear border was visible between DTT treated and untreated tissue (Fig. 9D). The eGFP signal was detectable with any leaf infiltrated with one of the sensor variants and subsequent DTT injection. At a larger magnification, the cellular localization of the fluorescent signal in the nucleus was clearly visible in DTT treated tissue (Fig. 10). This confirms that the eGFP-tag was translated and translocated into the nucleus. The eGFP signal indicates that the *bZIP60* variants were spliced upon UPR induction through DTT. Otherwise, it would not be expressed because it is not initially in the frame. All three sensor variants exploited the same unconventional splicing mechanism, proving that the double hairpin loop structure from *bZIP60* is a substrate of IRE1 during UPR (Howell 2013). The leaf samples from the shortest construct variant showed a comparable signal in terms of distribution and intensity to the two other length variants upon DTT injection. Hence, the intron with the HR is enough for efficient splicing. Moreover, eGFP as a fluorescent reporter seemed to also not interfere with the recognition of the double hairpin loop structure. This initial result is the proof of the concept that the unconventional splicing mechanism can be exploited in order to visualize UPR in plants.

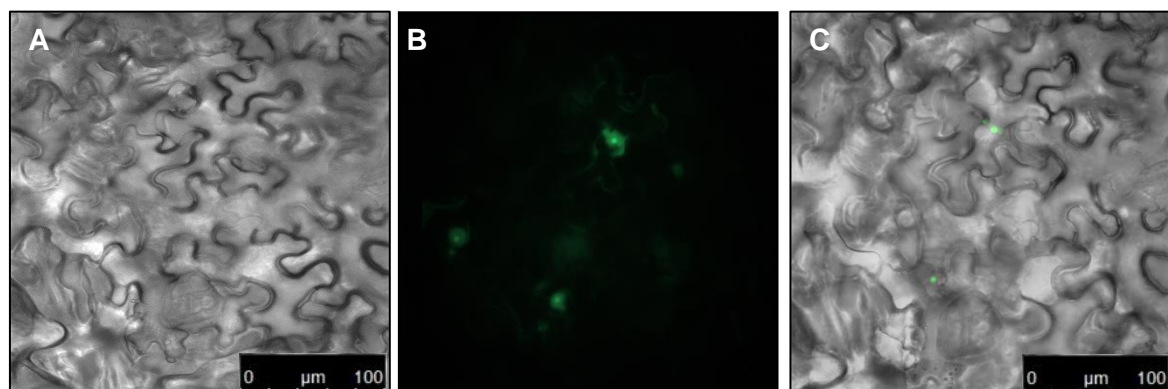


Fig. 10: Epidermal plant cells under bright light, pictures taken by Elsa Arcalis. B: Same cells as A being excited under EFM showing clear nuclear localization of eGFP signal at larger magnification. C: Overlay of A and B showing that the green signal concentrates in the nucleus of the cells.

#### 2.1.1. Negative control with sole DTT injection

By conducting sole DTT injections as negative control, the presence of 50mM and 25mM DTT in the leaf tissues revealed to induce shining under UV light. This led to the wrong assumption, that the sensor signal can be perceived through UV lamp detection (Fig. 11 and Fig. 33 in appendix).



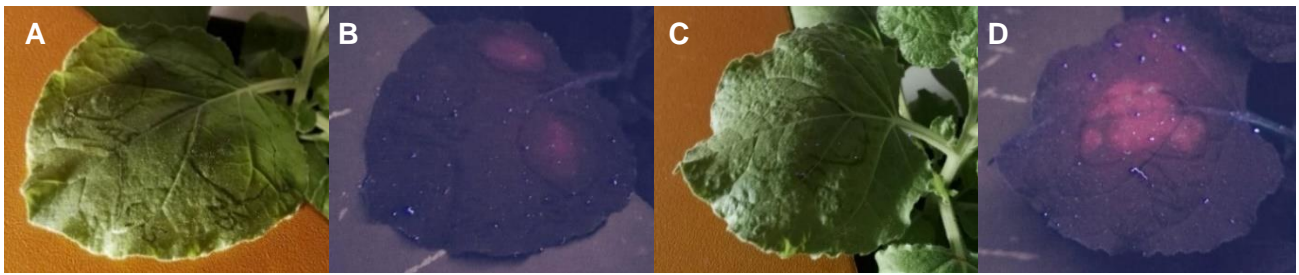


Fig. 11: A: Photos of one leaf under normal light. The left half of leaf 1 was infiltrated with JBE22, while DTT was injected to both sides. B: Under UV, both 25mM DTT injecting spots shined under UV (366nm) light indicating that DTT itself induces the shining and not the sensor. C and D: The false signal was even brighter with 50mM DTT on another leaf.

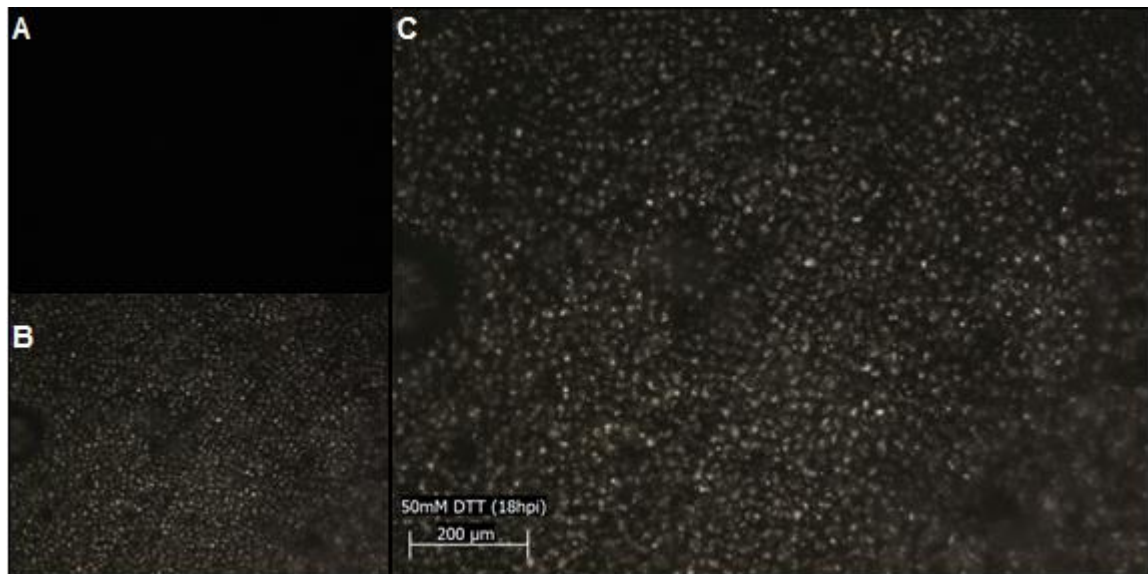


Fig. 12: Pictures of leaf tissue samples injected with only DTT under EFM (A) and under bright light (B). C: Overlay of A and B. No fluorescent signal is detected (bar=200μm).

For one negative control assay, leaves were only half infiltrated with JBE22, but 2dpi DTT was injected on both sides of these leaves. When examining 12hpi with a UV lamp, shining could be detected at the spots injected with 25mM DTT, independently from the presence of JBE22. In another assay, the same results were achieved when only 50mM DTT was injected without previous infiltration. The injection spot emitted 12hours post-infiltration (hpi), a fluorescent signal. When leaf samples were examined under EFM, leaf tissue infiltrated with only DTT, did not emit any fluorescent signal (Fig. 12). Injections of lower DTT concentrations (12,5 and 6,25mM) did not lead to fluorescence under UV lamp (data not shown). The shining spots detected under UV lamp did not correlate with actual signal detection through EFM. Therefore, previous results through UV lamp detection were false positives. In conclusion, the eGFP signal from the sensor is not strong enough to be visible on the leaf under UV light with the naked eye. High concentrations of DTT might have such an impact on plant cell integrity that autofluorescence is increased.

### 2.1.2. Always-on sensor serving as positive control

Literature and previous studies suggested that bZIP60(u) turns into its active form bZIP60(s) through splicing and translocates in the nucleus during UPR. One additional construct was cloned in order to miss the intron imitating endogenous *bZIP60(s)* and to have eGFP-tag in a reading frame, but with the minimal length (Fig. 34 in appendix). This construct, bZIP60ΔIΔSTOP-GFP\_F4 (JBE22s), provides a green fluorescent signal localized in the nucleus without UPR and was determined as a “short always-on sensor”. In order to verify that the reporting mechanism of our sensor design functions as expected, the additional construct served as a positive control to JBE22 and was also tested during the overexpression

experiments. Moreover, the outcomes from the preliminary results with the full-length always-on sensor required a re-evaluation, due to previous UV lamp detections giving false positive results. Firstly, leaves were infiltrated with JBE22s at various ODs for examination with a UV lamp 2,5dpi and 3dpi (Fig. 13).



Fig. 13: A: Leaf infiltrated with JBE20s at two distinct spots showing necrotic tissue after 3dpi. B: Same leaf as C under UV light (366nm) showing shining signal at infiltration spot. C: Leaf infiltrated with JBE22s at two distinct spots with no necrosis signs after 2,5dpi. D: Same leaf as A under UV light (366nm) not showing observable fluorescent signal despite autofluorescence.

The leaves infiltrated with JBE20s did not show any shining spots until 3dpi, when first necrosis signs also appeared (Fig. 13A/B). As previously observed, necrotic tissue emits strong autofluorescence itself. This was deduced as the cause for the shining spots being detected under the UV lamp and not fluorescence from the full-length always-on sensor. The development of necrosis through the full-length always-on sensor gives a hint that the over-expression of bZIP60(s) induces PCD leading to necrosis. This result was later replicated in a co-infiltration experiment. Meanwhile, leaves infiltrated with JBE22 did not show any observable signal and were not necrotic after several days (Fig. 13C/D). This assay with the short always-on sensor confirmed that the eGFP signal from our constructs is below the detection limit in our set-up. Considering the results from the negative control, the subsequent assays were analyzed only under microscopes in order to avoid false-positive results through UV lamp detection.

Next, leaves infiltrated with JBE22 and JBE22s were compared after 2dpi through EFM analysis (Fig. 14). While the leaf tissues infiltrated with the sensor variant JBE22 did not show any fluorescent signal, tissues with JBE22s did show a strong signal. This outcome proved that our sensor design functions as expected that only the spliced bZIP60 variant emits the signal. JBE22 expresses unspliced constructs that do not emit fluorescence. The DTT injection induces UPR in the cell, which in turn promotes the splicing of our sensor constructs.

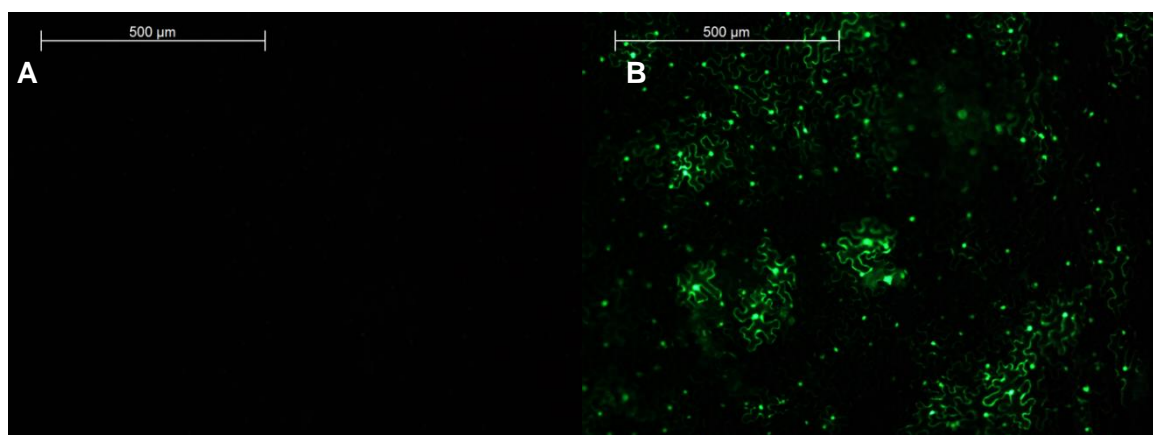


Fig. 14: Under EFM (bar =500μm) A: Leaf infiltrated with JBE22 at OD<sub>600</sub> of 0,2 after 2dpi not showing any fluorescent signal. B: Leaf infiltrated with JBE22s at same OD after 2dpi showing strong eGFP signal.

## 2.2. Further *in planta* tests to optimize conditions for transient assays

The following experiments were evaluated based on qualitative observations in order to deduce the appropriate concentrations and time for transient assays with the sensor constructs. The signal intensity could not be quantified for comparison between two samples due to the heterogeneity of leaf tissue (Bashandy et al. 2015). To enable quantification, the addition of another reporter as internal control was envisaged later on. For the subsequent development, the shortest length variant was selected, bZIP60 $\Delta$ STOP-GFP\_F4. We assumed it to be the least interfering construct regarding cellular processes. Since its endogenous *bZIP60* sequence is mostly missing, the probability that the sensor induces UPR itself should be minimized.

### 2.2.1. *In planta* testing of shortest sensor variant by varying OD and DTT concentrations

The preliminary experiment was conducted with an agrobacteria culture at an OD<sub>600</sub> of 0,4 and with 50mM DTT. This DTT concentration induced necrosis in *N. benthamiana* leaves after more than 3 days. Thus, one goal was to find lower but still suitable DTT concentrations. Additionally, we aimed to reduce the necessary amount of agrobacteria due to their influence on leaf physiology. Therefore, the first batch of experiments was conducted with different densities of JBE22 *Agrobacterium* culture, including OD<sub>600</sub>s of 0,4, 0,2 and 0,1, while varying DTT concentrations between 50mM and 6,25mM. Two to six 6-week-old plants were selected for each experiment using the third until the fifth true leaves. Each JBE22 density was infiltrated to the whole or half leaf area, while DTT was injected in marked-off areas of the same leaves after 3 days. This experiment was repeated three times. The results of the signal observations under EFM were summarized in Tab. 3.

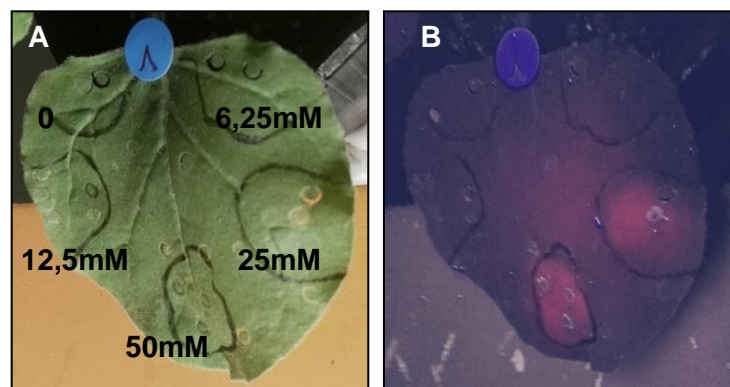


Fig. 15: A: Example of leaf infiltrated with JBE22 at OD<sub>600</sub> of 0,2 and with marked DTT injection spots. The respective DTT concentrations are indicated. 0 indicates the injection control with only H<sub>2</sub>O. B: Same leaf as A under UV light (366nm). Shining spots were observable at 25 and 50mM DTT. The same result is visible with leaves infiltrated with JBE22 at OD<sub>600</sub> of 0,1 respectively 0,4. The shining spots are due to high DTT concentrations.

The infiltrated leaves were evaluated at 12hpi of DTT. First, the leaves were always examined for necrosis signs at normal light conditions (Fig. 15A) followed by UV lamp detection at 366nm (Fig. 15B). No leaf was necrotic or showed any stress symptoms at that point in time. The applied concentrations of DTT and agrobacteria culture were appropriate for the utilized timeframe of 3dpi and 12hpi. The UV lamp detection revealed shiny areas at spots, which were injected with 25 or 50mM DTT confirming that high DTT concentrations lead to fluorescence. The shining spots could be observed at any OD of previously infiltrated JBE22. Lower DTT concentrations seemed to not induce fluorescence.

For immediate EFM analysis, leaf samples were prepared for each spot marking the DTT injection. The epidermal cells were examined under different magnifications (Fig. 16A/B/C). Samples infiltrated with JBE22 at OD<sub>600</sub>s of 0,2 to 0,4 together with 25 to 50mM DTT, revealed the best signal in terms of distribution and intensity. Leaf tissues treated with lower concentrations showed weaker signals or no



fluorescence at all (Fig. 16D/E/F). To catch any fluorescent signal, the laser intensity was set to 100%. With EFM, signals were also observed at lower OD<sub>600</sub>s and DTT concentrations (Tab. 3). The results from EFM did not confirm the observations under UV light, indicating that the shining under UV light derives from high DTT concentrations. Nevertheless, an OD<sub>600</sub> of 0,2 and 25mM DTT were determined as the best working concentrations for the follow-up experiments.

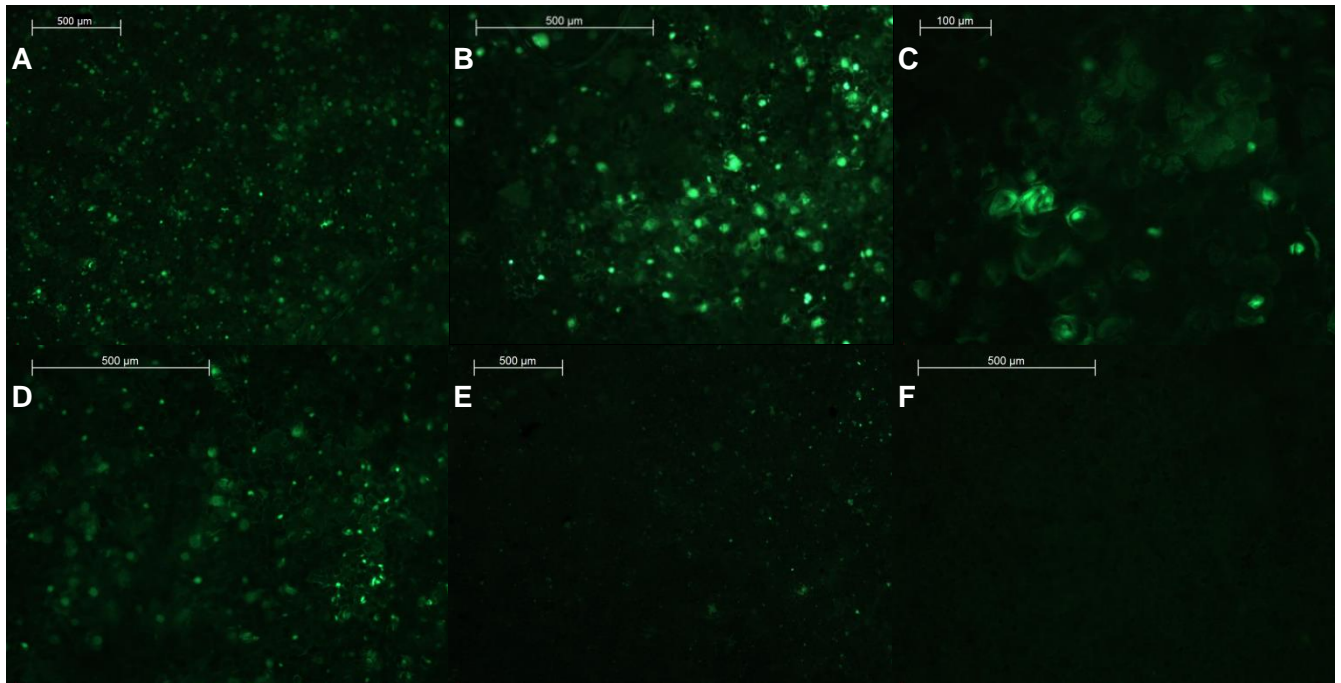


Fig. 16: Under EFM (bar=500μm except C=100μm) A: Plant epidermal tissue infiltrated with JBE22 at OD<sub>600</sub> of 0,2 and injected with 25mM DTT. This sample shows a strong signal. B and C: Same tissue as A. The eGFP signal of the spliced sensor is focused in the nuclei. D: Tissue infiltrated with JBE22 at OD<sub>600</sub> of 0,1 and injected with 25mM DTT. This shows a weaker signal. E: Same as D but injected with 12,5mM DTT emitting a very weak signal. F: No fluorescent signal detected at OD<sub>600</sub> of 0,1 and 6,25mM DTT. The laser intensity for all six pictures was maxed out.

OD <sub>600</sub>	50mM DTT	25mM DTT	12,5mM DTT	6,25mM DTT
0,4	Strong signal	Strong signal	Weaker signal	Very weak signal
0,2	Strong signal	Strong signal	Weaker signal	Very weak signal
0,1	Weaker signal	Weaker signal	Very weak signal	No signal

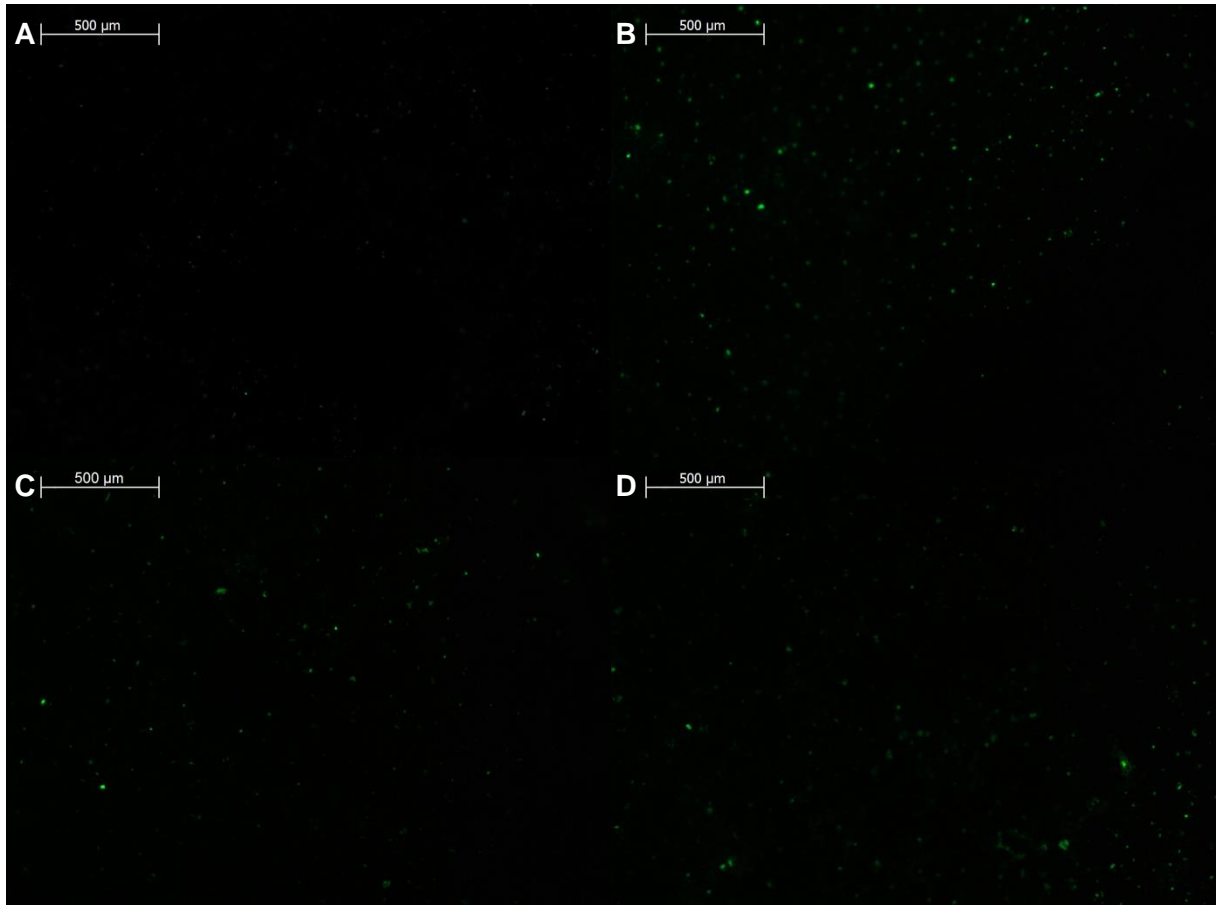
Tab. 3: Qualitative evaluation of fluorescent signal under EFM from different injection concentrations.

### 2.2.2. In planta testing of shortest sensor variant at different time points

A second objective was to determine if shorter time periods, in between injections and evaluating UPR signals, are possible. On the one hand, it would be more convenient to reduce the time between two working steps. On the other hand, in the preliminary experiment with the full-length always-on sensor JBE20s infiltrations induced necrosis starting already at the third day post-infiltration. Necrotic tissue should be avoided because it emits fluorescence under UV light and dead cells cannot be evaluated under EFM. The time period was varied between infiltrating JBE22 at OD<sub>600</sub> of 0,2 and injecting 25mM DTT after 1dpi, 2dpi, 3dpi and 4dpi. The results were evaluated under EFM, 12h upon DTT injection (Fig. 17).

For each time-period of 2, 3 or 4 days between treatments, the fluorescent signal appeared similar in terms of distribution and intensity. The period until injecting DTT was selected to be 2dpi for the next tests. The development of the signal, as well as necrosis symptoms upon DTT injection, was observed

over time. The signals could already be detected under EFM, starting 2 to 4hpi of DTT and lasting up to 24hpi until it significantly declined. The long duration of the signal enabled less strict timing of the signal evaluation. However, 20h is the measured half-life of eGFP according to He et al. 2019. This explained the observation about the signal duration of around a day. Since eGFP is so stable, the deriving fluorescent signal could outlast UPR in case the stress would be resolved. We were detecting the presence of eGFP after inducing UPR and not directly the duration of UPR itself. Real-time detection of the ER stress dynamics was not possible with this sensor variant. Therefore, a destabilization of the FP was considered to reduce its half-life (He et al. 2019).



*Fig. 17: Under EFM at 33% of laser intensity (bar=500μm) A: No signal 12hpi after injecting DTT 1dpi. B: Signal 12hpi after injecting DTT 2dpi. C: Signal intensity 12hpi after injecting DTT 3dpi. D: Signal 12hpi after injecting DTT 4dpi.*

In each assay where the leaves were fully infiltrated with the sensor, a fluorescent signal was observable after some time in tissues aside from the DTT injection sites which were marked on the leaves (data not shown). This false signal seemed to be of leaky nature leading to the assumption that some of the DTT solution leaked from the initial injection spots. Thus, this signal was determined first as leaky background signal. However, the background signal did not appear immediately when the actual signal was observable under EFM, but was delayed. After around a day, the background signal was not only observable but became also stronger with more hours passing. Therefore, the idea of DTT leaking into further tissue after injections was discarded and instead we concluded that the sensor construct itself is responsible for the background. The rising background impeded the distinction between actual and no signal lowering the reliability to correctly interpret the observed fluorescent signals.

### 2.2.1. Observations on leaf integrity during the testing

The effect on the leaf health after injecting different concentrations of DTT 2dpi was observed in each experiment. Leaves injected with the highest concentration of 50mM DTT showed necrotic signs that occurred in some cases after 18hpi, but in most cases after 24hpi. Leave tissue being infiltrated with JBE22 and injected with DTT was completely necrotic after 30hpi, whereas 25mM DTT injections seemed to be less aggressive towards leaf tissue (Fig. 18). These injection spots developed necrosis symptoms after more than 24hpi; and being completely necrotic after 72hpi. DTT concentrations of 12,5mM, or even lower rarely induced necrosis. In a few cases, first necrosis signs appeared between 72hpi and 168hpi, so after several days. The different OD<sub>600</sub> of JBE22 infiltrations had a minimal effect concerning necrosis development. The age of the leaves seemed to have the biggest influence on timing of necrosis. In general, older leaves showed a delay in the appearance of fluorescent signals, as well as necrosis symptoms.

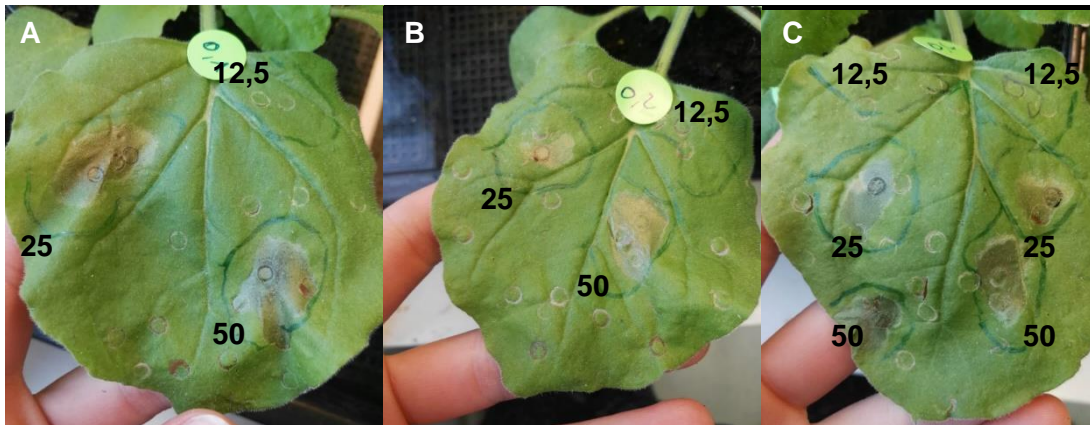


Fig. 18: Leaves one day after injecting DTT with previous infiltration of JBE22 at OD<sub>600</sub> of 0,1 (A), 0,2 (B) respectively 0,4 (C). Concentrations of DTT are indicated. 25mM and 50mM injection spots show necrotic tissue 24hpi.

### 3. Further development of sensor for better sensitivity

#### 3.1. Improving sensitivity of sensor with inducible promoters

During the testing of the shortest length sensor, a rising background signal was observable after around 24hpi of DTT and was becoming stronger over time (data not shown). A portion of bZIP60 transcripts seemed to be spliced at a basal level without the induction of UPR with DTT leading to low, but detectable background. The CaMV35S promoter was used in the first batch of sensor constructs, which leads to high expression levels (Odell et al. 1985). Consequently, the probability of basal splicing increased due to the excess of transiently expressed constructs. In order to eliminate the high expression level, it was decided to replace the constitutive CaMV35s promoter with a stress-inducible promoter; one deriving from UPR genes. Three genes involved in UPR were chosen: *BiP1*, *BiP2*, and *BiP3*. Based on experimental evidence in *Arabidopsis thaliana*, their promoters are UPR-inducible (Carolino et al. 2003). Additionally, a combination of minimal 35S promoter (mini35S) with the enhancer deriving from the promoter of *NAC103* (*NAC103e*) was cloned (Sun et al. 2013). These UPR genes, with their promoter regions are well characterized in the model plant *A. thaliana* (*BiP1-3*: Martínez and Chrispeels 2003, *NAC103*: Sun et al. 2013). For *N. benthamiana*, several homologues of said genes were found through search with BLAST in Sol Genomics Network' database. These sequence hits have not been experimentally confirmed or fully characterized yet. In addition, it would have been hard to select among the multiple genes found in *N. benthamiana* considering the low homology usually occurring in promoter regions. Isolating and testing all promoters from these homologues was unfortunately exceeding this thesis. Thus, it was decided to use the sequences deriving from *Arabidopsis*: *AtBiP1*, *AtBiP2*, *AtBiP3* and *AtNac103*. Furthermore, combining gene elements from different species increases the synthetic character of the sensor. In return, it decreases the probability to interfere with natural processes in plant cells.

To begin with, the endogenous promoter and enhancer sequences were isolated from genomic *A. thaliana* DNA using a plant gDNA isolation kit and confirmed through Sanger sequencing at Microsynth. The initial CaMV35 promoter on the pTRA-GG1 vector was substituted with the respective *BiP* promoters, or mini35S-*NAC103e* combination through conventional cloning. The four resulting vectors, pTS1-GG1, pTS2-GG1, pTS3-GG1 and pTS4-GG1, were used as backbone plasmids in Golden-Gate assembly with bZIP60 $\Delta$ I $\Delta$ STOP-GFP\_F4. The resulting promoter variants represented four different promoters, with one including an enhancer regulating the expression of an already spliced sensor (Fig. 19). Previous results showed that a pre-spliced sensor variant under CaMV35S promoter led to the expression of a fluorescent signal, without the need of inducing UPR. In the case of the inducible promoters, the hypothesis was that the spliced sensor emitting fluorescence would only be expressed upon UPR induction. Without DTT, it was expected that stress-sensitive promoters from *BiPs* would provide a sufficiently low expression in comparison to the stress activated state. The aim was to overcome the rising background signal by constricting the sensor construct to an UPR-induced expression. Other goals were to combine a strong inducible promoter with the splicing activation mechanism in order to increase specificity and to decrease unnecessary transcriptional load when not under stress. To test the effect of the chosen inducible promoters and minimal promoter with enhancer, another batch of *in planta* transient experiments was conducted with the four promoter variants.

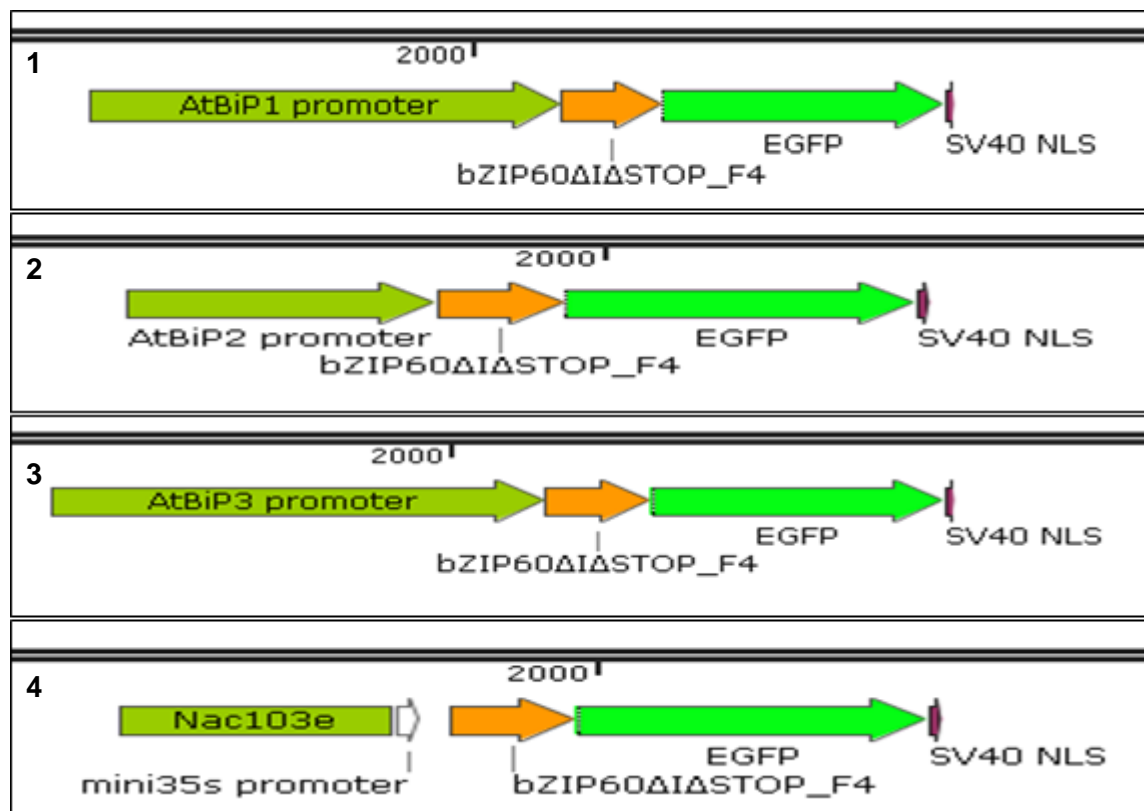


Fig. 19: Constructs of the promoter variants after Golden-Gate assembly. Each has the same sensor gene cassette: the shortest sensor variant being spliced up front with an eGFP-tag followed by SV40 NLS (bZIP60ΔIΔSTOP\_F4+eGFP+SV40NLS with length of 1003bp). 1: Variant with promoter deriving from AtBiP1 fused to sensor gene cassette. 2: Variant from AtBiP2. 3: Variant from AtBiP3. 4: Variant with combination of AtNAC103 enhancer and minimal CaMV35S promoter. 1 and 3, respectively 2 and 4 have similar sizes. Generated with SnapGene.

### 3.2. Testing of *BiP* promoter variants for UPR-sensitivity

The following *in planta* assays were executed under conditions determined from previous optimization tests with the sensor variant JBE22 and controls. The promoter variant combining mini35S and *NAC103e* required additional cloning steps, delaying its testing. Therefore, initially there were only three agrobacteria cultures, each carrying a *BiP* promoter variant (TSF1, TSF2 and TSF3). They were diluted to an OD<sub>600</sub> of 0,2 and subsequently infiltrated to the whole area of individual leaves. After 2dpi, four concentrations (50mM, 25mM, 12,5mM, 6,25mM) of DTT were injected to distinct areas of the leaves. The treated leaves were evaluated for signals under EFM. Representative micrographs are shown below (Fig. 20 to 22). The observations from several replicates were summarized in Tab. 4. Analysis under a confocal microscope was additionally performed to receive pictures with higher resolution (Fig. 23). As expected, 50 and 25mM DTT injections spots on leaves appeared brightly fluorescent under UV light (data not shown). Previous results showed that those signals can be false positive.

OD <sub>600</sub> of 0,2	50mM DTT	25mM DTT	12,5mM DTT	6,25mM DTT
TSF1	Strong signal	Strong signal	Weaker signal	Very weak signal
TSF2	Strong signal	Strong signal	Weaker signal	Very weak signal
TSF3	Strong signal	Strong signal	Strong signal	Weaker signal

Tab. 4: Summary of three replicated experiments (three plants and three leaves from each plant), with analysis of co-injected tissues under EFM.



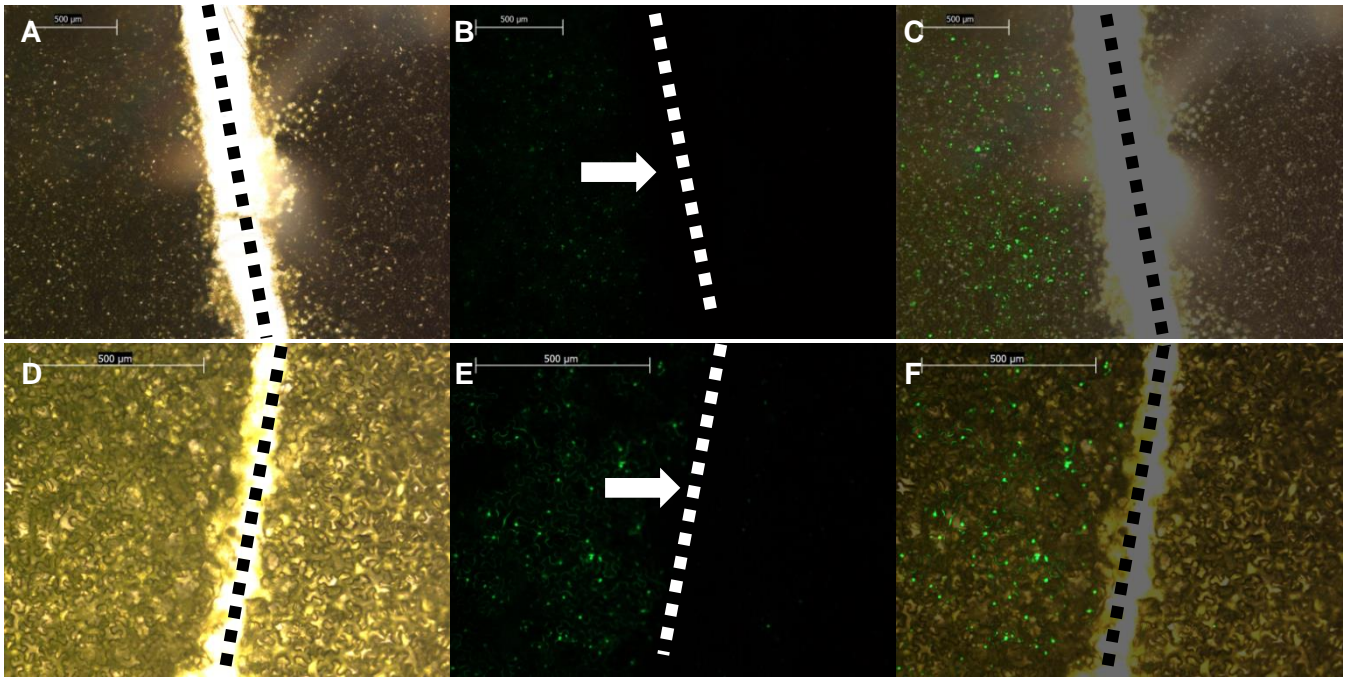


Fig. 20: Under EFM (bar=500μm). Representative pictures of samples from tissue infiltrated with TSF1-3 and DTT. A to C and D to F different magnifications. A: Bright light view of two samples from epidermal plant tissue (separated by black mark). Left is infiltrated with TSF1 2dpi at OD<sub>600</sub> of 0,2 and injected with 25mM DTT 10hpi. Right is only infiltrated with DTT. B: Same as A under EFM showing fluorescent signals covering the DTT injected tissue, while no signal with only DTT. C: Overlay of A and B. D: Bright light view of two samples. Left is infiltrated with TSF3 2dpi at OD<sub>600</sub> of 0,2 and injected with 12,5mM DTT 10hpi. Right is only infiltrated with same TSF3. E: Same as D under EFM showing fluorescent signals covering the DTT injected tissue, while signals are scattered without DTT. F: Overlay of D and E.

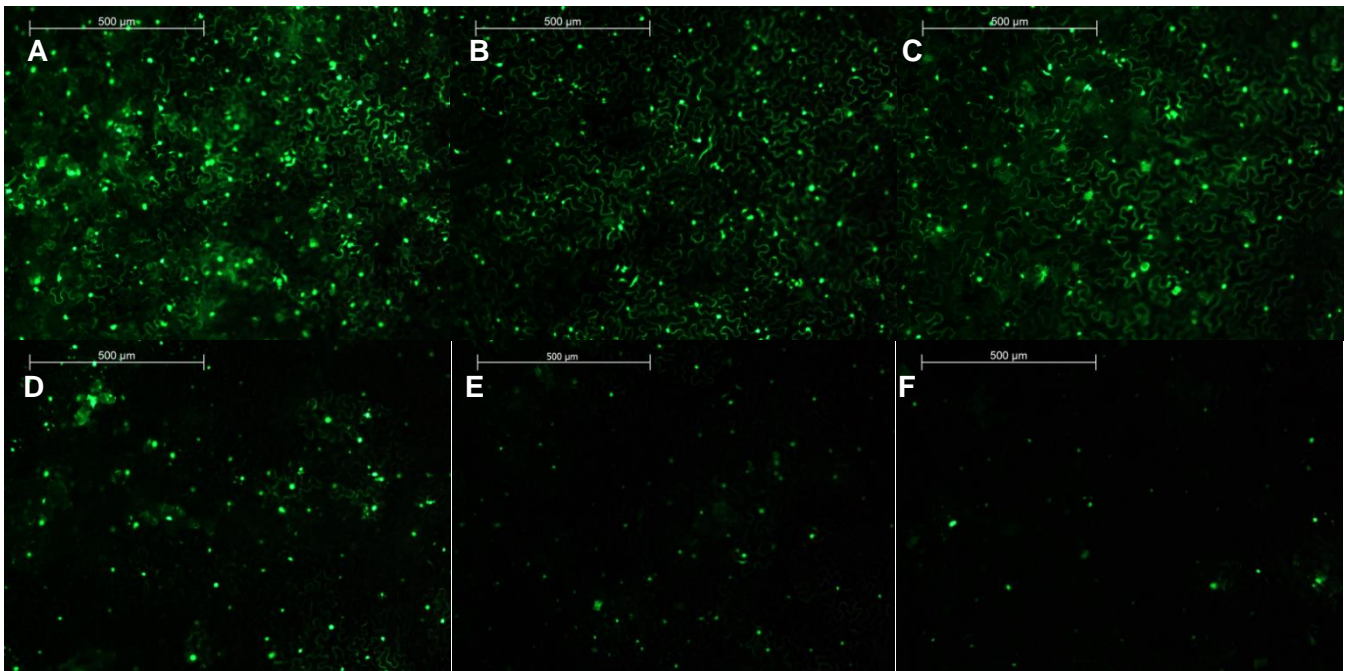


Fig. 21: Under EFM (bar=500μm). Representative pictures of epidermal plant cells for each TSF1-3 infiltration at OD<sub>600</sub> of 0,2 2,5dpi. A to C: Tissue infiltrated with TSF1 (A), TSF2 (B) respectively TSF3 (C) injected with 25mM DTT 12hpi. All three BiP promoter variants show signals in a dense pattern. D to F: Tissue infiltrated with only TSF1 (D), TSF2 (E) respectively TSF3 (F) with no DTT, as negative DTT control. The BiP promoter variants alone showed scattered signals apparently with lower intensity leading to a patchy pattern. The signals from D to F represent background signals, which differ by signal number and intensity from induced signals.

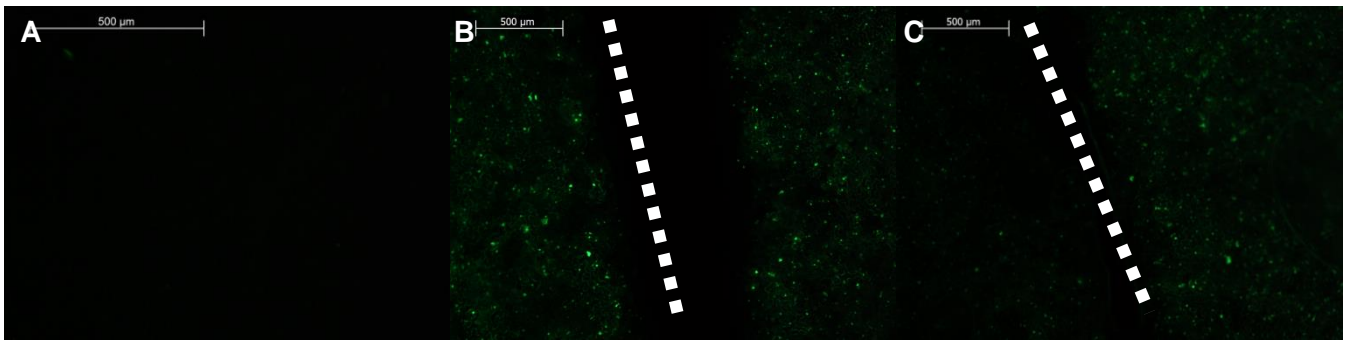
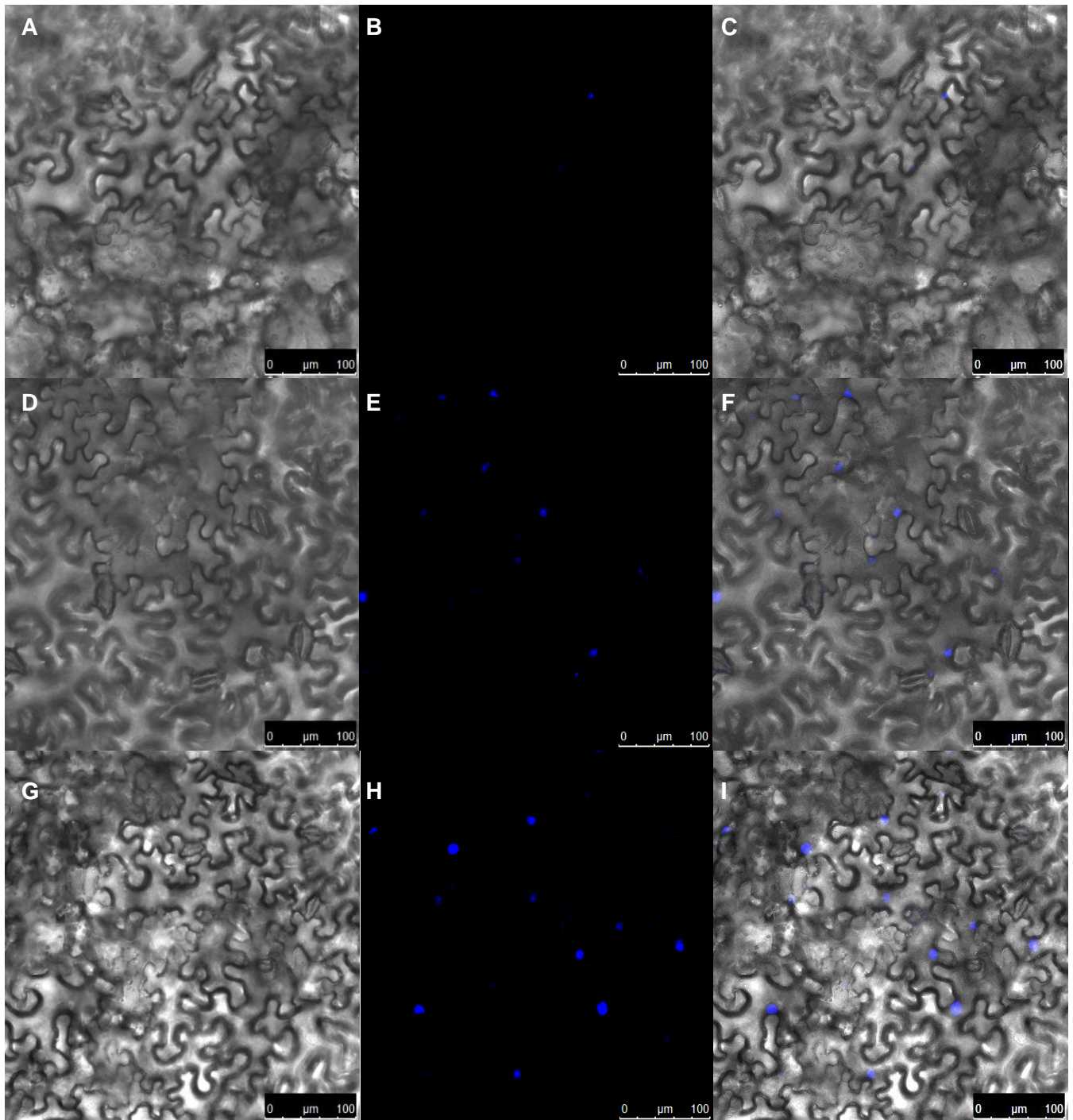


Fig. 22: Under EFM (bar=500µm). Representative pictures comparing signal intensity of different promoter variants at OD<sub>600</sub> of 0,2 after DTT injection 14hpi. A: Tissue injected with only DTT as negative TSF control. No fluorescent signal. B: Left sample injected with 25mM DTT and infiltrated with TSF1 vs right injected with 25mM DTT and infiltrated with TSF2. Left (TSF1) and right (TSF2) show similar bright signals. C: Left sample injected with 12,5mM DTT and infiltrated with TSF2 vs right injected with 12,5mM DTT and infiltrated with TSF3. Right (TSF3) is brighter than left.

All three TSFs expressed fluorescent signals with a similar dense coverage of the tissue co-infiltrated with DTT (Fig. 20, 21A/B/C and 22B/C). At a constant OD<sub>600</sub> of 0,2, the signal intensity increased with higher DTT concentrations. Leaves infiltrated with only *BiP* promoter variants served as negative DTT control (Fig. 21D/E/F). Their tissues also emitted fluorescence under EFM, but much weaker. These weak signals appeared in low numbers and were scattered, revealing a patchy pattern. This was identified as a background signal. The background was assumed to derive from the stress deriving from the basal expression of the designed *BiP* promoter variants. These constructs included a spliced *bZIP60* variant, which would result in an eGFP signal upon expression. Nevertheless, a clear distinction between DTT and non-DTT injected tissue was easily possible during the analysis of the different samples with respective TSFs (Fig. 20). This means that the induction of UPR is reported and can be differentiated from a non-UPR state, a cell being in homeostasis. These initial observations proved that the promoter variants of this second batch of constructs also function as UPR reporting sensors. During the previous tests, the sensor variants showed a rising fluorescent background after 2,5dpi. The background signal from the sensor variants had a similarly homogenous pattern as the induced signal and only differed in intensity. By combining inducible promoters with the coding sequence *bZIP60(s)*, the new variants were expressing a patchy background, which was easier to distinguish from a homogenous signal pattern. Moreover, TSF3 seemed to express the brightest signal after the 12,5mM DTT injection (Fig. 22C) and showed a weaker background signal than TSF1 or TSF2 (Fig. 21F vs 21D/E). The idea behind using inducible promoters was to make the future sensor more sensitive to stress, leading to lower or no background signal. Since the background signal from TSF3 differed the most from the induced signals, the *BiP3* promoter was proposed as one promising candidate promoter for the final sensor construct.

The EFM results from these *in planta* experiments were confirmed with confocal microscopy. Samples from the treated leaf tissues were prepared in the same way as EFM 3dpi. The epidermal cells from the leaves were observed under bright light and excited with UV light. Infiltrated tissues with different DTT concentrations were examined at 24hpi, as well as tissues with H<sub>2</sub>O instead of DTT, as injection control (Fig. 23). Injection spots of 50mM DTT showed necrosis and were excluded from further evaluation (data not shown).





*Fig. 23: Representative pictures taken by Elsa Arcalis from tissues infiltrated with TSF 1 to 3 at OD<sub>600</sub> of 0,2 taken under confocal microscope at same laser conditions 3dpi of TSFs (bar=100μm). A to C: Same tissue section infiltrated with TSF1 and 2dpi later with H<sub>2</sub>O. A: Intact cells under bright light. B: One cell is emitting weak fluorescence under UV light. C: Overlay of A and B. D to F: Same tissue section infiltrated with TSF2 and 2dpi later with 25mM DTT. D: Intact cells under bright light. E: Multiple cells showing fluorescent signals under UV light. F: Overlay of D and E. G to I: Same tissue section infiltrated with TSF3 and 2dpi later with 12,5mM DTT. G: Intact cells under bright light. H: Multiple cells emitting very strong signal under UV light. I: Overlay of G and H.*

Samples from tissues infiltrated with TSF1, and H<sub>2</sub>O as negative control showed a very low number of weak signals being scattered (Fig. 23A/B/C). The same result was observed with TSF2 and TSF3. As previously concluded, these low signals represent the background signal. In contrast, samples with TSFs and induced by DTT, emitted strong signals in terms of higher number and intensity. At cell scale (Fig. 23D/E/F), the individual signals were observed to be localized in the nucleus, emitting green fluorescence. TSF1 to 3 injected with the same DTT concentrations showed fluorescent signals similar



in intensity. However, TSF3 seemed to emit the brightest signal with 12,5mM DTT (Fig. 23G/H/I). In turn, the degree of signal coverage of the tissue was deducible at lower magnification (Fig. 35 in appendix). All three TSFs, together with DTT, showed a high number of signals with varying intensities and evenly distributed. Similar results were achieved with the other UPR inducer TM (data not shown). However, the number of strong individual signals decreased with DTT concentration. Overall, this made the samples appear less bright. Nevertheless, infiltrated tissues could be clearly distinguished due to the significant difference observed between induced and background signals. With the help of another instrument, it was demonstrated that *BiP* promoter variants are functional and report UPR. Also under the confocal microscope, TSF3 appeared to emit the brightest signal in combination with 12,5mM DTT. Its signal intensity estimated to be three times higher than that of the other two TSFs. The degree of coverage and overall distribution pattern of the fluorescent signals along the treated tissues was better to deduce at lower magnifications with EFM. Meanwhile, the confocal microscope allowed to visualize details from the cellular localization of the eGFP signal and to estimate the signal intensity.

### 3.3. Testing of *NAC103e* promoter variant for UPR-sensitivity

The same experimental set-up *in planta* was applied to test the combination of mini35S and *NAC103e* for future sensors. The construct required an additional cloning step in order to fuse the promoter and enhancer through Overlap Extension PCR. For this reason, the testing of the promoter variant was executed separately from the three *BiP* promoter variants. *Agrobacterium* cultures (TSF4) were grown carrying the fourth promoter variant. Subsequently, they were infiltrated at an OD<sub>600</sub> of 0,2 in whole leaves from different *N. benthamiana* plants as biological replicates. Samples for signal evaluation were prepared just as in previous experiments. The analysis was firstly performed with EFM (Fig. 24), then with confocal microscope (Fig. 25).

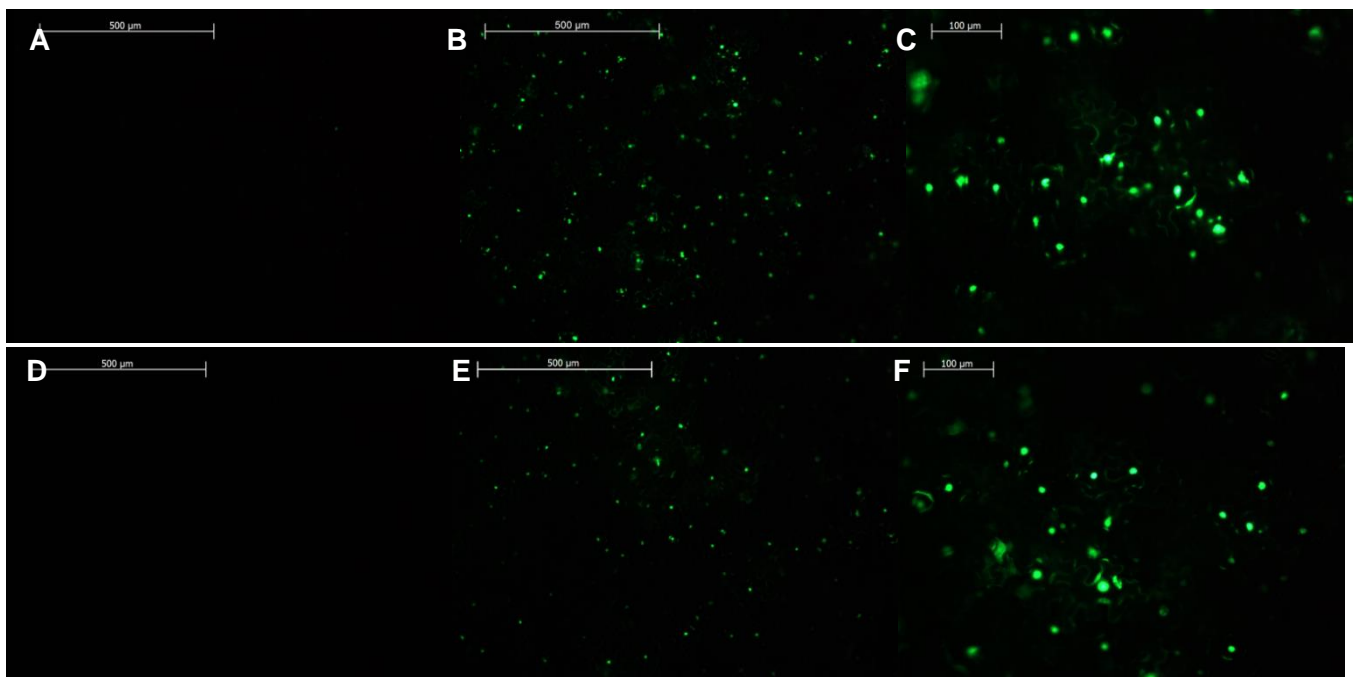


Fig. 24: Under EFM (bar=500μm except C&F=100μm) comparing signals at two time points: A to C 3dpi and D to F 4dpi. A: Sample of leaf tissue infiltrated with only TSF4 at OD<sub>600</sub> of 0,2 showing no bright signal after 3dpi. B: Same as A, but injected with 25mM DTT indicating many bright signals being well distributed. C: Same as B, but at higher magnification. D: Sample of leaf tissue infiltrated with only TSF4 at OD<sub>600</sub> of 0,2 showing no bright signal after 4dpi. E: Same as D, but injected with 25mM DTT indicating many bright signals being well distributed. F: Same as E, but at higher magnification.

Control samples of tissues infiltrated with only TSF4 showed no fluorescent signal at all (Fig. 24A/D) This means that this combinatorial promoter variant gives no basal expression and lacks a background signal. In contrast, infiltrated tissue being co-injected with DTT emitted fluorescent signals under EFM (Fig.

24B/C/E/F). The scattered signals were also observable at higher magnification. The expression signal of eGFP was scattered throughout the tissue, expressing a patchy signal pattern. This promoter variant displayed a favorable signaling behavior that was anticipated during the initial sensor designs. The idea was that when UPR occurs, the sensor should be “on” and the eGFP signal being emitted. The final sensor should visualize the switch to stress and be “off” without UPR, meaning no signal emission. Due to a missing background, it was deduced that this promoter might be exclusively UPR-driven. In parallel, the leaves were evaluated at two different time points to check if the signal intensity changes over time. Samples from same leaves were taken a day apart (Fig. 24A/B/C vs 24D/E/F) and were examined for fluorescence. There was no obvious difference in signal intensity or number when performing the analysis one day apart. The induced signal was observed between 4 and up to 48hpi, comparable to signal duration of shortest length variant from the first sensor generation.

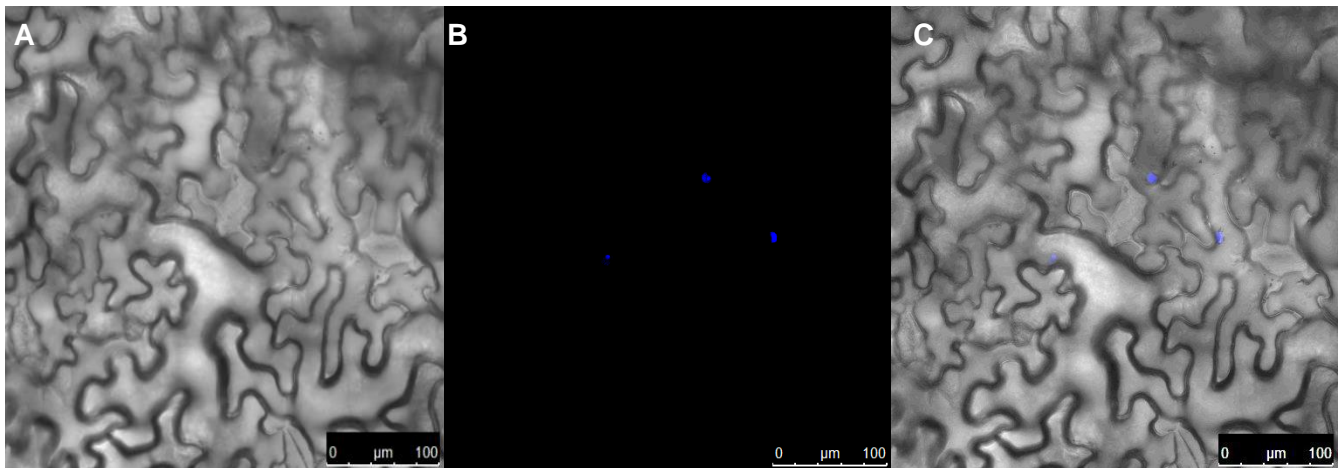


Fig. 25: Representative pictures taken by Elsa Arcalis under confocal microscope (bar=100μm). A: Sample of leaf tissue infiltrated with TSF4 at OD<sub>600</sub> of 0,2 and 25mM DTT under bright light. Epidermal cells looked intact after 3dpi. B: Same as A, but under exciting laser showing three scattered fluorescent signals. C: Overlay of A and B indicating the nuclear localization of fluorescent signals.

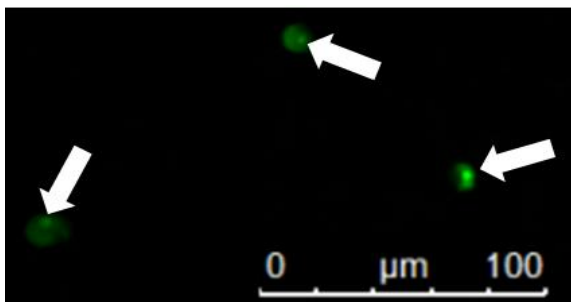


Fig. 26: Close-up of fluorescent signals localized in the nucleus in green coloration. The concentrated signals are indicating nucleoli (white arrows).

Under a confocal microscope, the fluorescent signal from the leaf tissue, treated with TSF4 and DTT, could also be detected showing a low number of scattered points (Fig. 25). Moreover, the confocal microscope allowed the visualization of more details regarding nuclear localization of the signal deriving from the *NAC103e* promoter variant. The signal seemed to be concentrated in the nucleoli (Fig. 26).

The TSF4 infiltration with later DTT injection, led to a patchy signal pattern on leaf tissues, in contrast to the evenly distributed signal pattern observed with TSF1, TSF2 and TSF3. While the three *BiP* variants were expressing a background signal without DTT induction, the *NAC103e* variant did not show any background. The minimal promoter mini35S, when compared to the full version of CaMV35S, is known to give minimal expression in plant tissues (Odell et al. 1985). Elimination of background signal was favorable concerning future sensor construct(s), but not the weakening of the induced signal. The *NAC103* enhancer seemed not to sufficiently activate the signal expression under the minimal promoter in all cells. Nevertheless, the combination of mini35S and *NAC103e* resulted in an inducible sensor variant, which gives a fluorescent signal only when UPR occurs. In comparison, the background signals from *BiP* variants were weak and scattered, but still distinguishable from their induced signals that were

evenly distributed and strong. *AtBiP3* promoter was selected for further sensor development due to its strong signal.

#### 4. Next steps in sensor development regarding reporter

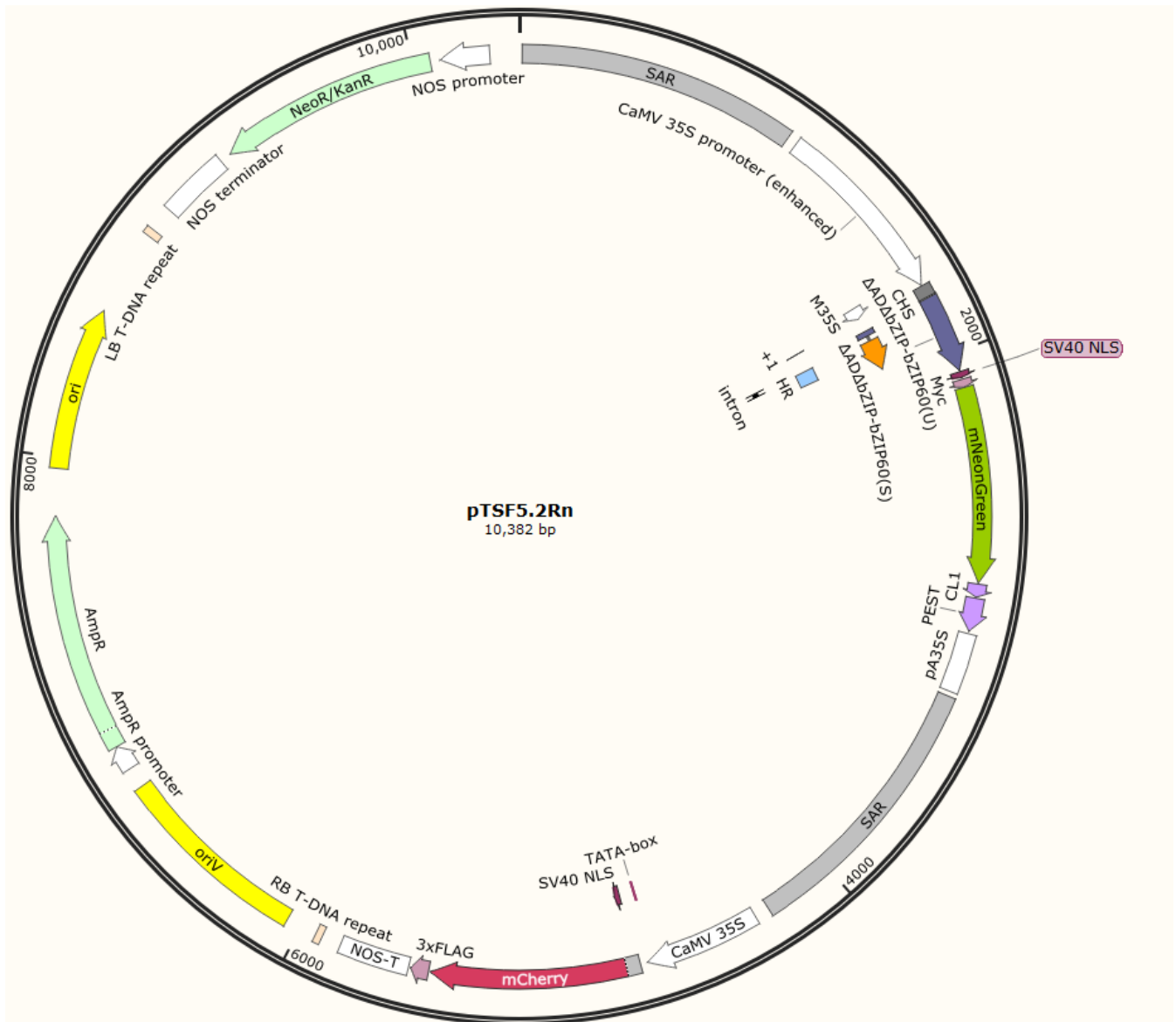


Fig. 27: Exemplary map of a sensor construct from the third generation on the basis of the shortened and modified bZIP60 sequence including a super bright FP (here mNeonGreen) with PEST degradation signal and a second reporter (here mCherry) in an independent expression cassette. Generated with SnapGene.

Due to the great stability of eGFP itself, the deriving fluorescent signal of the first sensor constructs was not reflecting the duration of UPR, but rather the half-life of the FP-tag. Studies on fluorescent tags showed that by adding a protein degradation signal, such as PEST, the signal duration from eGFP can be reduced from over 20 to 2h. This time interval is expected to be more appropriate to visualize actual UPR dynamics. However, the reduction in half-life leads also to a decrease in overall signal intensity of around 90% (He et al. 2019). In the previous *in planta* transient expression tests, the first and second generation of sensors showed a sufficient but not too bright signal. A reduction of 90% of the signal through a degradation tag would most probably reduce the signal intensity to a non-observable level under a microscope. Therefore, eGFP was envisaged to be replaced by a FP being super bright, such as LanYFP or mNeonGreen which are 4,24 and 2,76 times brighter than eGFP, respectively (Shaner et al. 2013). LanYFP is assumed to have a cytotoxic effect, hence its monomeric derivative mNeonGreen (Hostettler et al. 2017) will be tested as fluorescent reporter, too. Moreover, another FP-tag is planned to enable signal quantification. The heterogeneity of leaf tissue (Bashandy et al. 2015) and the fact that

not 100% of all cells are transformed (Menassa et al. 2012; Hwang et al. 2017) provokes a variation of signal expression when observing numerous cells of different specimens. In order to enable comparison of signals, the second reporter will be added under a constitutive promoter in an independent expression cassette. The second signal with differing emission characteristics from the actual signal should serve as reference (He et al. 2019). We chose mCherry, since it proved to be a suitable reporter in combination with green FPs, such as GFP, for *in vivo* imaging (Heppert et al. 2016). A reference signal enables to deduce if the sensor construct is present in a cell and available for expression. In addition, the ratio between actual and reference signal can be calculated and utilized to compare signal intensities between samples or even individual cells. This would allow studying the ER stress sensitivity of different plant tissues and the potential of recombinant proteins to induce UPR. Besides the two fluorescent reporters, the third generation of sensors would include the minimal length of endogenous *NbZIP60* sequence. The plasmid map illustrates such a possible sensor construct (Fig. 27). These constructs were still undergoing cloning, while this thesis was submitted. The corresponding transient expression tests in *N. benthamiana* leaves with subsequent microscopic analysis were not conducted yet and data cannot be shown.

## 5. Generation of transgenic plants carrying a sensor construct

### 5.1. First generation of *A. thaliana* transformants with bZIP60 $\Delta$ STOP-GFP\_F4 (Col0\_F4)

The overall aim for the development of the sensor was to design a construct that is universally functional among various plant species. UPR is a stress mechanism with highly conserved components (Zhang et al. 2016). Thus, a sensor on the basis of the conserved double hairpin loop structure should be recognized and spliced in any plant. Moreover, the final development step of this project foresees the generation of transgenic plants reporting UPR. To evaluate the feasibility, Col0 *Arabidopsis thaliana* plants were transformed with the shortest length variant (bZIP60 $\Delta$ STOP-GFP\_F4) from the first generation via floral dipping by following the protocol established by Zhang et al. 2006. The resulting seeds were screened on three selection plates with kanamycin. After three days of cold stratification, seedlings germinated on each plate. However, only one seedling per plate looked healthy green and developed first leaves. These three seedlings differed in appearance, but were all three transferred to new agar plates (Fig. 28A). After two weeks, only two seedlings survived and were transplanted to soil (Fig. 28B). These T1 generation plants had differing phenotypes, which was indicating that most probably only one plant is a successful transformant. Besides, the smaller plant did not develop proper flowers and turned out to be sterile.

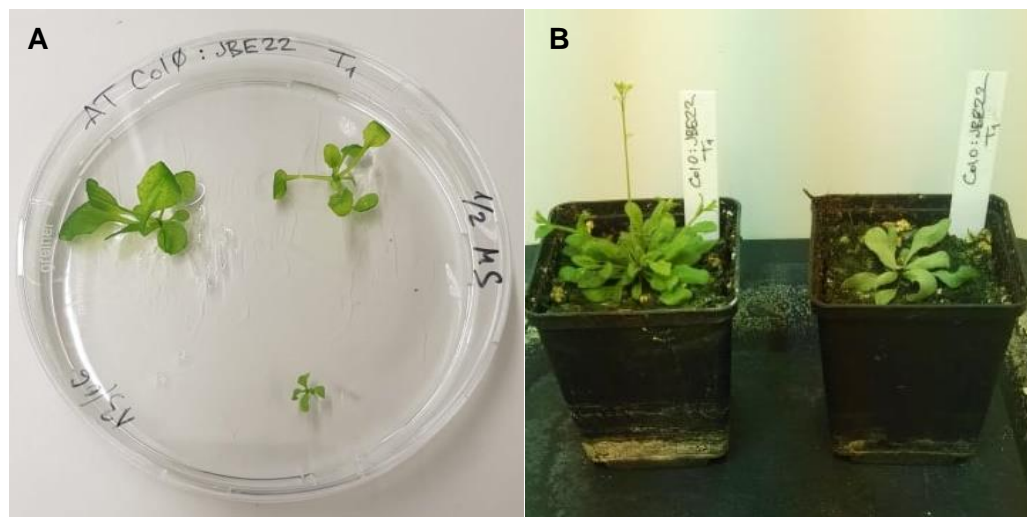


Fig. 28: A: Petri dish with seedlings being the T1 generation of Col0\_F4. The medium-sized seedling did not survive. B: T1 generation in soil being 6 weeks old.

### 5.2. Second generation of Col0\_F4

As next, the seeds of the promising transformant were harvested, sterilized and germinated on MS agar after three days of cold stratification. The resulting seedlings represent the T2 generation (Col0\_F4) and were tested for ER stress sensitivity, in turn indicating if they carry the bZIP60 $\Delta$ STOP\_GFP\_F4 construct. For the *in planta* experiment by a colleague, T2 seedlings were grown on plates with 1/2 MS solid media with 1% sucrose at 25°C. After three days, these plants were transferred to liquid media, whereas half were transferred to MS media containing 2 $\mu$ g/ml of TM and the other half to media with DMSO as control. The seedlings were incubated for six hours in dark without shaking and their roots were subsequently examined for fluorescence under EFM (Fig. 29). The transparent roots of the T2 seedlings treated with TM showed a clear green fluorescent signal being expressed in the cells. Meanwhile, the control seedlings did not show any fluorescence. This leads to the conclusion, that the T2 generation expresses bZIP60 $\Delta$ STOP\_GFP\_F4 under CaMV35S promoter and the transformed construct functions as expected by only expressing eGFP upon ER stress. The lack of any signal in the control indicates that in contrast



to transient expression in *N. benthamiana*, the stable expression of the minimal length sensor in *A. thaliana* does not lead to a background. Therefore, the first sensor generation proved to be functional as UPR reporter in plant cells emitting a clear signal and being “off” in the absence of stress. These transgenic plants allow cell-stress imaging *in vivo*.

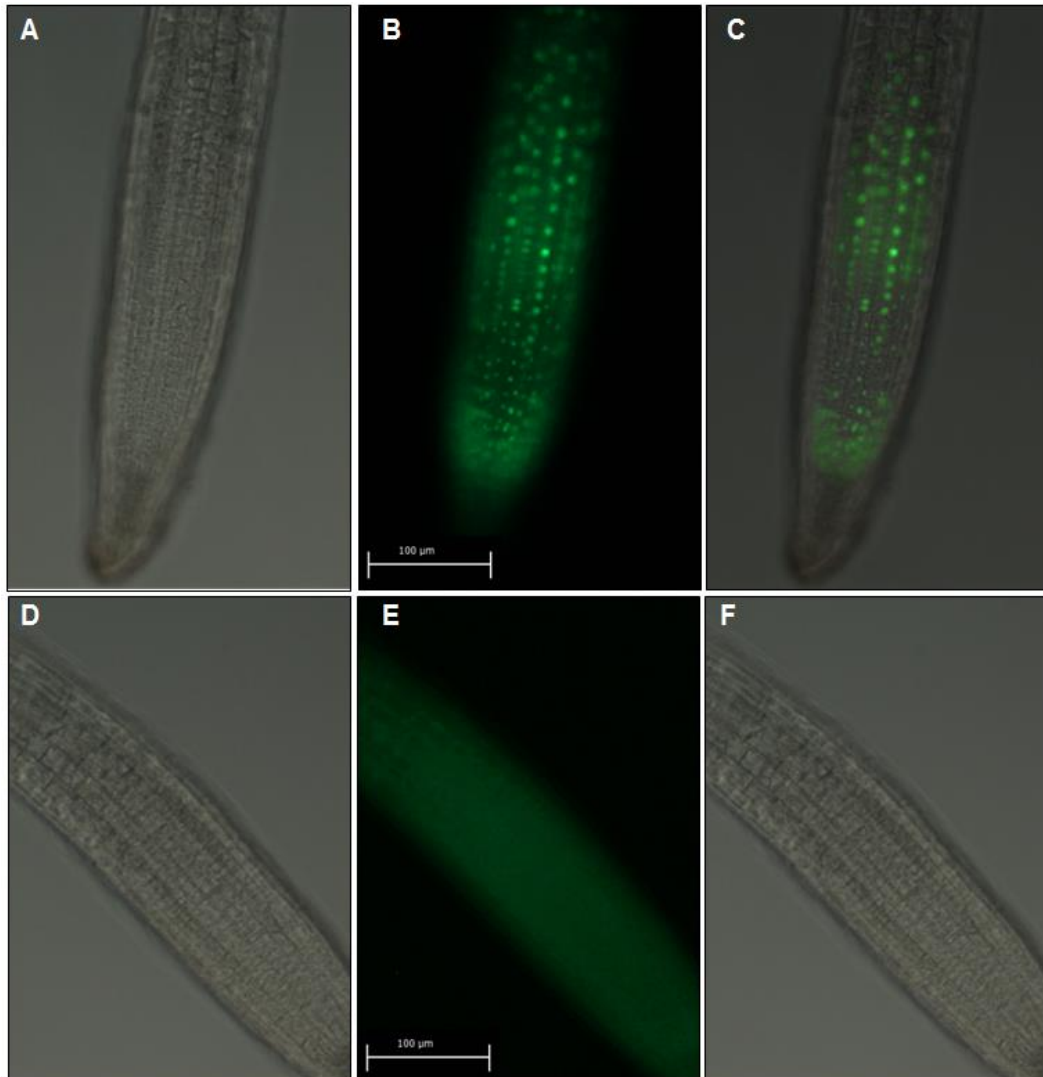


Fig. 29: *A. thaliana* roots under EFM (bar=100μm). Representative pictures taken by Julia Hilscher. A to C: Col0\_F4 treated with TM showing fluorescent signal on cellular level. D to F: Root of control Col0 seedling not expressing any fluorescent signal.

## 6. Co-expression experiments

### 6.1. Impact of *NbZIP60* on antibody expression

For his PhD thesis from 2017, Xiao Ying Chan co-expressed bZIP17, bZIP28 and bZIP60 with recombinant apoptin variants to analyze the impact of ER stress-related proteins on protein levels. As a result, the yield of soluble apoptins increased, leading the hypothesis that bZIP60(u) or bZIP60(s) could have a similar effect during co-expression with antibodies instead of apoptins. Thus, six agrobacteria cultures carrying various gene cassettes were constructed: the light (LC) and heavy chain (HC) of the human-murine hybrid IgG antibody (Melnik et al. 2018), bZIP60(u) and bZIP60(s), the RNA silencing repressor p19, as well as DsRed-KDEL. This red fluorescent protein deriving from the *Discosoma* species is constantly emitting fluorescence if driven under a constitutive promoter (Matz et al. 1999). Nine mixtures were prepared and listed in Tab. 5. The antibodies (LC+HC) were infiltrated alone or co-infiltrated with the respective two *NbZIP60*s, with and without p19. P19 is known to boost expression levels during co-expression (Lakatos et al. 2004). Similarly, DsRed-KDEL was expressed alone and together with bZIP60(u) respectively with bZIP60(s). The overexpression of co-infiltrates including bZIP60(s) showed necrosis within two days. The reasoning behind this was probably the induction of UPR leading to PCD. Therefore, leaf material was only harvested from mixtures without bZIP60(s) after 7dpi. Samples were pooled from three control leaves and from three leaves of each infiltrated mixture. Total proteins were extracted from samples and analyzed by Western Blot. When compared to p19, co-infiltrating the bZIP transducers did not significantly increase any total protein amount. Nor was a significant boost of specific LC+HC expression observed (data not shown). The results of the first co-expression experiment did not simulate the conclusions from Chan's thesis published in 2017. Co-infiltrations of bZIP variants, with the aim to influence protein yields were not pursued further.

N°	Recombinant protein	Co-infiltrates	Leaf symptoms 7dpi
1	LC+HC	none	None
2	LC+HC	p19	Slight
3	LC+HC	bZIP60(u)	Slight
4	LC+HC	bZIP60(s)	Necrosis (not harvested)
5	LC+HC	p19 + bZIP60(u)	Slight
6	LC+HC	p19 + bZIP60(s)	Necrosis (not harvested)
7	DsRed	bZIP60(u)	Slight
8	DsRed	bZIP60(s)	Necrosis (not harvested)
9	DsRed	none	None

Tab. 5: Summary of necrosis symptoms observed at the different co-infiltration spots on the leaves. bZIP60(u) and bZIP60(s) were co-infiltrated with constructs for recombinant proteins: light (LC) and heavy chain (HC) from human-murine hybrid IgG antibody, as well as DsRed.

### 6.2. Determination which UPR transducer activates *BiP* promoters and NAC103 enhancer

The unfolded protein response has two functionally overlapping branches in plants. One is mediated by bZIP60 (Zhang et al. 2015), while bZIP28 is the other UPR signal transducer in plants (Liu et al. 2007). Similar to bZIP60, it translocates the signal of unfolded proteins in the ER lumen to the nucleus (Nawkar et al. 2018). Both spliced bZIPs transcription factors regulate the expression of UPR genes, such as *BiPs* and NACs. It is assumed that the activated transcription factor bZIP60(s) binds to the promoters of *BiP1* to 3 and NAC103 leading to their activation (Iwata and Koizumi 2005; Sun et al. 2013). In order to deduce if the spliced bZIP60 or bZIP28 can activate our promoter variants, we co-expressed each spliced transducer construct together with the respective four promoter variants. Beforehand, it was observed that the three *BiP* promoter variants alone induce a leaky background signal, while the *NAC103e* variant

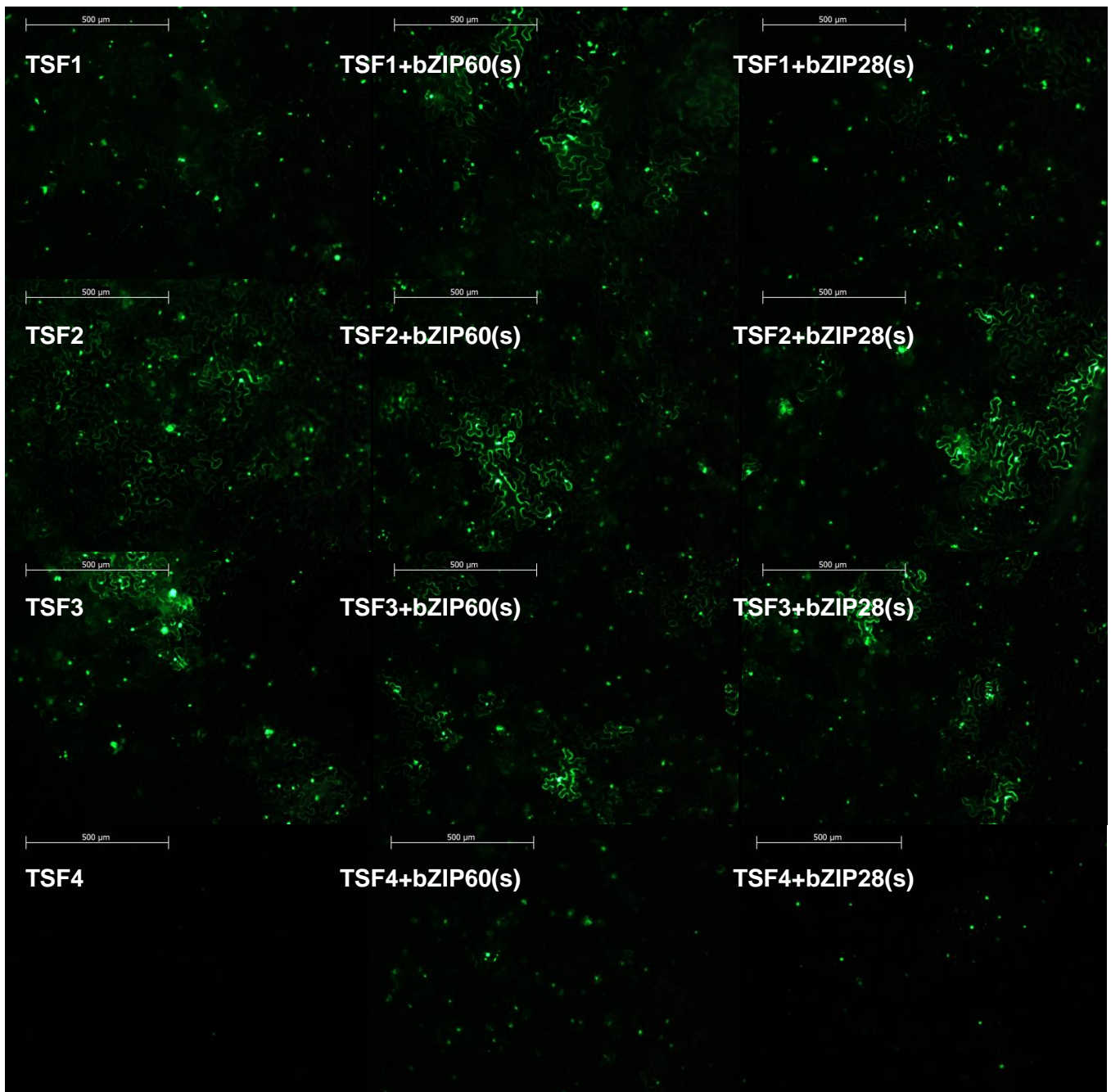


alone shows no background signal. While co-expressing with bZIP60(s) or bZIP28(s), a change in signal appearance would indicate that the respective transducer can directly regulate the given promoter variant. The co-infiltration of bZIP60(s) led to necrosis symptoms on leaves within 48h in previous co-expression experiments. Therefore, we checked the co-infiltrated plants with EFM at two earlier time points, after 12 and 24h. As expected, there were no signals observed with UV lamp detection, due to the missing DTT. Samples of the leaf tissues were checked after 12h, but no cell emitted fluorescence (data not shown). EGFP signals were detected with EFM after 24h (see Tab. 6 and Fig. 30).

N°	OD <sub>600</sub> =0,2	OD <sub>600</sub> =0,1	GFP Signal under EFM after 24h
1	TSF1	-	Scattered
2	TSF1	bZIP60(s)	Scattered, brighter than TSF1 alone
3	TSF1	bZIP28(s)	Scattered, same as TSF1 alone
4	TSF2	-	Bright scattered signal
5	TSF2	bZIP60(s)	Scattered, similar signal as TSF2 alone
6	TSF2	bZIP28(s)	Scattered, similar signal as TSF2 alone
7	TSF3	-	Scattered
8	TSF3	bZIP60(s)	Scattered, similar signal as TSF3 alone with dying cells
9	TSF3	bZIP28(s)	Scattered, similar signal as TSF3 alone
10	TSF4	-	No signal
11	TSF4	bZIP60(s)	Scattered
12	TSF4	bZIP28(s)	Scattered, less bright than TSF4 + bZIP60(s)

Tab. 6: Twelve co-expression mixtures were made with agrobacteria carrying promoter variants being diluted to an OD<sub>600</sub> of 0,2 and transducers in a density of 0,1. Control infiltrations of sole BiP promoter variants (TSF1, TSF2 and TSF3) replicated previous results showing a leaky background signal, while mini35S promoter with Nac103 enhancer variant (TSF4) alone emits no fluorescence.

While co-infiltrations with TSF2 and TSF3 showed no changes in signal (Tab. 2N°4-6), TSF1 and TSF4 showed an increase in signal when co-expressed with bZIP60(s) respectively bZIP28(s). The signal of TSF1 with bZIP60(s) (N°2) was still scattered, but significantly brighter than TSF1 alone. TSF4 with bZIP60(s) (N°11), respectively with bZIP28(s) (N°12) gave each scattered signal. However, bZIP60(s) induced in TSF4 a stronger signal by number and intensity than bZIP28(s). These observations indicated that bZIP60(s) interacts with *BiP1* promoter variant and *NAC103e* promoter variant, activating the eGFP expression. These interactions were also reported in past studies (Iwata and Koizumi 2005; Sun et al. 2013). Moreover, the *NAC103e* promoter variant also showed in co-infiltration with bZIP28(s), a slight signal. This result was expected due to past findings from co-expression experiments (Liu et al. 2007). According to literature, bZIP60 also activates *BiP2* and *BiP3* promoter (Iwata and Koizumi 2005; Henriquez-Valencia et al. 2015), but did not induce an increased in expression in TSF2 and TSF3 in our assay. Due to the heterogeneity of leaf tissues, the co-expression experiment should be repeated in order to base conclusions on a larger number of analyzed samples.



*Fig. 30: Representative pictures taken 24hpi of leaf samples using same laser settings under EFM (bar=500μm).  
 Row 1: Co-expression of TSF1+bZIP28(s) has similar signal as TSF1 expressed alone. TSF1+bZIP60(s) shows brighter signal than TSF1 alone.  
 Row 2: Co-expression of TSF2+bZIPs(s) have similar signal as TSF2 expressed alone (2A).  
 Row 3: Co-expression of TSF3+bZIPs(s) have similar signal as TSF3 expressed alone (3A).  
 Row 4: Co-expression of TSF4+bZIPs(s) show each a signal, while TSF4 expressed alone gives no signal.*

## Conclusion

Plant molecular farming is a manufacturing technology to produce proteins in plants employing genetic engineering methods. The production of secretory proteins begins with their expression in the ER in the plant cell putting this organelle into the focus of researchers. It was observed that the overexpression of proteins can affect the ER homeostasis causing UPR in some cases. For dynamic studies of UPR signaling in plants, the objective evolved to develop a molecular tool for UPR visualizations *in planta* inspired by work conducted in other organisms.

Therefore, the aim of this master's thesis was to initiate the development of a molecular sensor in plants by engineering a prototype sensor. Transient expression via agroinfiltration in *N. benthamiana* was chosen as expression system. This work describes the original design rational and initial testing of various sensor constructs for UPR visualization *in planta*. Different working parts of the sensor were deduced by cloning different length of sensors and promoter variants, with later fluorescent reporter selection. Some sensor variants showed promising performance in terms of signal intensity. Findings during the cloning and testing are in more detail below.

First, the necessary *NbZIP60* domains were identified for proper exploitation of the unconventional splicing mechanism of bZIP60. The proof-of-concept experiment illustrated that the double stem loop structure and the HR domain are essential confirming the hypothesis that translational pausing is needed for efficient *bZIP60* splicing (Yanagitani et al. 2011; Shanmuganathan et al. 2019). Before this project, previous assays with bZIP60\_GFP variants missing the HR domain did not show any signal (data not shown). Upon UPR induction with DTT, the first generation of sensor constructs led to fluorescent signal emission indicating the activation by splicing of the modified *bZIP60* sequence. This emission was detectable under EFM and confocal microscope. While testing different length variants, the minimal *bZIP60* sequence for the final sensor was identified. The minimal length sensor construct was used to determine the approximate time course of treatments (2 days) and infiltration concentrations for follow-up tests. The low ratio between actual signal intensity and background signal was seen as the greatest drawback in the transient system. Therefore, a second generation of sensor variants was designed to increase specificity of the actual signal. The second batch of sensor constructs with inducible promoters was generated and tested. Four promoters from *BiP* and *NAC103* genes, which were described to be secondary transducers of the IRE1-bZIP60 branch (Sun et al. 2013; Cho and Kanehara 2017), were isolated from *A. thaliana* and fused to the short always-on sensor variant bZIP60ΔIΔSTOP\_GFP\_F4 initially driven by CaMV35S promoter. Differing signal patterns were observed between *BiP1-3* and mini35S with *NAC103e* promoter variants. *BiP1-3* variants showed bright signals with patchy background, while UPR signal deriving *NAC103* variant was patchy with no background at all. The promoter variant based on *AtBiP3* showed the best signal ratio to background and was selected to be used for a final more sensitive sensor.

Besides the development of the sensor within *N. benthamiana*, the minimal length sensor construct from the first generation was stably transformed into *A. thaliana*. The T2 generation was experimentally tested proving that the sensor was emitting the signal upon stress induction. The signal could be *in vivo* visualized on cellular level showing a clear “on-off” pattern as desired from the initial sensor design. The result confirmed that our sensor design is suitable to report ER stress in plants.

All in all, the outcome of this thesis were several working prototypes of the molecular sensor. It was shown in numerous transient assays in *N. benthamiana* that the sensor constructs visualize UPR stress through an eGFP signal *in vivo*. Moreover, a first sensor prototype (35S:bZIP60ΔSTOP\_GFP\_F4) was stably

transformed in *A. thaliana* indicating even better performance in regards of background, being absent in the resulting transgenic plants. With this final experiment, the title of this thesis was met by generating plants, which are able to report ER stress.

Unfortunately, the initial idea to visualize the stress signal with detection under UV lamp was not possible, at least with our set-up. Also, detection trade-offs were assessed deriving from eGFP signal prevalence together with a strong background. Rigid dynamics and heterogeneity of the appearing signal emerged as biggest challenges leading to further optimization undertakings.

Thus, the development of the sensor has not been finished yet despite the promising outcomes. For the third generation of sensor constructs, the reporting system will be improved by adjusting the half-life with a degradation signal and by compensating the intensity loss with a super bright FP. This is anticipated to optimize the dynamics of the sensor allowing visualization of actual UPR occurrence in plant cells. An internal reference is planned by adding another FP-tag with another emission spectrum under a constitutive promoter. Such a „two-color biosensor“ would enable ratiometric detection allowing the quantification of the UPR signal per cell *in vivo*. The ratio between the signals from constitutively expressed and the stress-induced FP directly indicates the level of stress in cells. Thus, a better spatial and temporal resolution compared to qPCR is expected by visualizing and quantifying the UPR mechanisms *in vivo*. The overall aim is to create a complementary tool to the common UPR detection method being qPCR. In comparison to a qPCR analysis, the sensor constructs have showed already a better spatial resolution detecting UPR on a cellular level and not from whole cell pools.

Nonetheless, the feasibility of the original bZIP60 design as suitable molecular tool for cell stress visualization *in vivo*, more particular *in planta*, was demonstrated in this work. Encouraged by the intermediate results, the development of the sensor construct will be proceeded with the next optimized variants being already in the pipeline. The expression activity of the third generation of sensor variants will be in the focus, hence the sensor protein yields will be examined via Western Blot and ELISA. Eventually, the UPR signal results of the final sensor will be compared with qPCR data to validate the suitability of the new tool. A sensor with refined reporting properties would constitute an attractive tool, but this endeavor surpasses the scope of this thesis.

The final goal is the generation of a functional sensor with optimized signal half-life and sensitivity to meet actual UPR dynamics being quantifiable. The sensor would be transformed into model plants, such as *N. benthamiana* and *A. thaliana*, allowing research labs worldwide to test the UPR potential of their agroinfiltration constructs *in vivo* simply by microscopy. Besides this specific application for molecular farming, UPR sensor plants could also be interesting for basic research. UPR is an important mechanism during development, for instance the seed development under various environmental conditions may be linked to different levels and temporal patterns of UPR. A molecular sensor allowing stress imaging *in vivo* on cellular level has the potential to be a handy tool.

# Appendix

## 1. Sequencing results from *bZIP60* isolation

### 1.1. Homologue (needle alignment with Sol Genomics data):

```
# Length: 900
# Identity:      884/900 (98.2%)
# Similarity:    884/900 (98.2%)
# Gaps:          0/900 ( 0.0%)
# Score: 5190.0
#=====

Niben101Scf24      1 ATGGTGGATGACATCGATGATATCGTTGGACACATCAATTGGGACGATGT      50
| | | | | | | | | | | | | | | | | | | | | | | | | | | | | |
bZIP60_3_homo      1 ATGGTGGATGACATCGATGATATCGTTGGACACATCAATTGGGACGATGT      50

Niben101Scf24     51 AGATGACCTCTTCCACAACATTCTAGAGGATCCCGCCGACAATCTCTTCT     100
| | | | | | | | | | | | | | | | | | | | | | | | | | | | | |
bZIP60_3_homo     51 AGATGACCTCTTCCACAACATTCTAGAGGATCCCGCCGACAATCTCTTCT     100

Niben101Scf24    101 CTGCTCATGATCCGTCCGCGCCGTCTATCCAGGAGATCGAGCAGCTTCTC     150
| | | | | | | | | | | | | | | | | | | | | | | | | | | | | |
bZIP60_3_homo    101 CTGCTCATGATCCGTCCGCGCCGTCTATCCAGGAGATCGAGCAGCTTCTC     150

Niben101Scf24    151 ATGAACGATGATGAAATCGTCGGTCACGTGGCTGTCGGAGAGCCTGATTT     200
| | | | | | | | | | | | | | | | | | | | | | | | | | | | | |
bZIP60_3_homo    151 ATGAACGATGATGAAATCGTCGGTCACGTGGCTGTCGGAGAGCCTGATTT     200

Niben101Scf24    201 TCAACTTGCTGACGACTTTCTCTCCGACGTGCTAGCCGATTCTCCTGTTC     250
| | | | | | | | | | | | | | | | | | | | | | | | | | | | | |
bZIP60_3_homo    201 TCAACTTGCTGACGACTTTCTCTCCGACGTGCTGGCCGATTCTCCTGTTC     250

Niben101Scf24    251 AGTCCGATCTTTCTCACTCTGATAAAGTCATTGGATTCCCCGATTCCAAG     300
| | | | | | | | | | | | | | | | | | | | | | | | | | | | | |
bZIP60_3_homo    251 AGTCCGATCATTCTCACTCTGATAAAGTCAATGGATTCCCCGATTCCAAG     300

Niben101Scf24    301 GTTTC AAGTTGCTCAGAGGTTGATGATGACGACAAAGACAAGGAGAAGGT     350
| | | | | | | | | | | | | | | | | | | | | | | | | | | | | |
bZIP60_3_homo    301 GTTTC AAGTGGCTCCGAGGTTGATGATGACGACAAAGACAATGAGAAGGG     350

Niben101Scf24    351 TTCCCAGTCGCGGATTGACTCTAAGGACGGCTCTGACGAAC TAACTGTG     400
| | | | | | | | | | | | | | | | | | | | | | | | | | | | | |
bZIP60_3_homo    351 TTCCCAGTCGCGGACTGAGTCTAAGGACGGCTCCGACGAAC TAAACAGTA     400

Niben101Scf24    401 ATGATCCCGTCGATAAAAAGCGTAAGAGGCAATTGAGAAACAGAGATGCA     450
| | | | | | | | | | | | | | | | | | | | | | | | | | | | | |
bZIP60_3_homo    401 ACGATCCCGTCGATAAAAAGCGCAAGAGGCAATTGAGAAACAGGGATGCA     450

Niben101Scf24    451 GCTGTCAGGTCACGAGAGCGGAAGAAGTTGTATGTTAGGGATCTTGAGTT     500
| | | | | | | | | | | | | | | | | | | | | | | | | | | | | |
bZIP60_3_homo    451 GCTGTCAGGTCACGAGAGCGGAAGAAGTTGTATGTTAGGGATCTTGAGTT     500

Niben101Scf24    501 GAAGAGTAGATACTTTGAATCAGAGTGCAAGAGGTTGGGGTTAGTTCTCC     550
| | | | | | | | | | | | | | | | | | | | | | | | | | | | | |
bZIP60_3_homo    501 GAAGAGTAGATACTTTGAATCAGAGTGCAAGAGGTTGGGGTTAGTTCTCC     550

Niben101Scf24    551 AGTGCTGTCTTGCAGAAAATCAAGCTTTGCGCTTCTCTTTGCAGAAATGGC     600
| | | | | | | | | | | | | | | | | | | | | | | | | | | | | |
bZIP60_3_homo    551 AGTGCTGTCTTGCAGAAAATCAAGCTTTGCGCTTCTCTTTGCAGAAATGGC     600

Niben101Scf24    601 AATGCTAATGGTGCTTGTATGACCAAGCAGGAGTCTGCTGTGCTCTTGTT     650
| | | | | | | | | | | | | | | | | | | | | | | | | | | | | |
bZIP60_3_homo    601 AATGCTAATGGTGCTTGTATGACCAAGCAGGAGTCTGCTGTGCTCTTGTT     650

Niben101Scf24    651 GGAATCCCTGCTGTTGGGTTCCCTGCTTTGGTTCCTGGGCATCATATGCC     700
```

bZIP60_3_homo	651	 GGAATCCCTGCTGTTGGGTTCCCTGCTTTGGTTCCTGGGCATCATATGCC	700
Niben101Scf24	701	TGCTCATTCTTCCCAGCCAACCCTGGTTAATTCAGAAGAAAATCAACGA	750
bZIP60_3_homo	701	 TGCTCATTCTTCCCAGCCAACCCTGGTTAATTCAGAAGAAAATCAACGA	750
Niben101Scf24	751	AGCAGAAACCACGGTCTTCTGGTCCGATAAAGGGAGGAAATAAGGCTGG	800
bZIP60_3_homo	751	 AGCAGAAACCACGGTCTTCTGGTCCGATAAAGGGAGGAAATAAGGCTGG	800
Niben101Scf24	801	TCGGATTTTTGAGTTCCTGTCTTCATGATGGGCAAGAGATGCAAAGCTT	850
bZIP60_3_homo	801	 TCGGATTTTTGAGTTCCTGTCTTCATGATGGGCAAGAGATGCAAAGCTT	850
Niben101Scf24	851	CAAGATCGAGGATGAAGTTCAATCCCCATTCTTTGGGAATTGTTATGTGA	900
bZIP60_3_homo	851	 CAAGATCGAGGATGAAGTTCAATCCCCATTCTTTGGGAATTGTTATGTGA	900

## 1.2. *bZIP60* confirmed (needle alignment with Sol Genomics data):

```
# Length: 900
# Identity: 900/900 (100.0%)
# Similarity: 900/900 (100.0%)
# Gaps: 0/900 ( 0.0%)
# Score: 5290.0
#=====
```

Niben101Scf24	1	ATGGTGGATGACATCGATGATATCGTTGGACACATCAATTGGGACGATGT	50
bZIP60_1	1	 ATGGTGGATGACATCGATGATATCGTTGGACACATCAATTGGGACGATGT	50
Niben101Scf24	51	AGATGACCTCTTCCACAACATTCTAGAGGATCCCGCCGACAATCTCTTCT	100
bZIP60_1	51	 AGATGACCTCTTCCACAACATTCTAGAGGATCCCGCCGACAATCTCTTCT	100
Niben101Scf24	101	CTGCTCATGATCCGTCCGCGCCGTCTATCCAGGAGATCGAGCAGCTTCTC	150
bZIP60_1	101	 CTGCTCATGATCCGTCCGCGCCGTCTATCCAGGAGATCGAGCAGCTTCTC	150
Niben101Scf24	151	ATGAACGATGATGAAATCGTCGGTCACGTGGCTGTCGGAGAGCCTGATTT	200
bZIP60_1	151	 ATGAACGATGATGAAATCGTCGGTCACGTGGCTGTCGGAGAGCCTGATTT	200
Niben101Scf24	201	TCAACTTGCTGACGACTTTCTCTCCGACGTGCTAGCCGATTCTCCTGTTC	250
bZIP60_1	201	 TCAACTTGCTGACGACTTTCTCTCCGACGTGCTAGCCGATTCTCCTGTTC	250
Niben101Scf24	251	AGTCCGATCTTTCTCACTCTGATAAAGTCATTGGATTCCCCGATTCCAAG	300
bZIP60_1	251	 AGTCCGATCTTTCTCACTCTGATAAAGTCATTGGATTCCCCGATTCCAAG	300
Niben101Scf24	301	GTTTCAAGTTGCTCAGAGGTTGATGATGACGACAAAGACAAGGAGAAGGT	350
bZIP60_1	301	 GTTTCAAGTTGCTCAGAGGTTGATGATGACGACAAAGACAAGGAGAAGGT	350
Niben101Scf24	351	TCCCCAGTCGCGGATTGACTCTAAGGACGGCTCTGACGAACATAACTGTG	400
bZIP60_1	351	 TCCCCAGTCGCGGATTGACTCTAAGGACGGCTCTGACGAACATAACTGTG	400
Niben101Scf24	401	ATGATCCCGTCGATAAAAAGCGTAAGAGGCAATTGAGAAACAGAGATGCA	450
bZIP60_1	401	 ATGATCCCGTCGATAAAAAGCGTAAGAGGCAATTGAGAAACAGAGATGCA	450
Niben101Scf24	451	GCTGTCAGGTCACGAGAGCGGAAGAAGTTGTATGTTAGGGATCTTGAGTT	500
bZIP60_1	451	 GCTGTCAGGTCACGAGAGCGGAAGAAGTTGTATGTTAGGGATCTTGAGTT	500

Niben101Scf24	501	GAAGAGTAGATACTTTGAATCAGAGTGCAAGAGGTTGGGGTTAGTTCTCC	550
bZIP60_1	501	GAAGAGTAGATACTTTGAATCAGAGTGCAAGAGGTTGGGGTTAGTTCTCC	550
Niben101Scf24	551	AGTGCTGTCTTGCAGAAAATCAAGCTTTGCGCTTCTCTTGCAGAATGGC	600
bZIP60_1	551	AGTGCTGTCTTGCAGAAAATCAAGCTTTGCGCTTCTCTTGCAGAATGGC	600
Niben101Scf24	601	AATGCTAATGGTGCTTGTATGACCAAGCAGGAGTCTGCTGTGCTCTTGTT	650
bZIP60_1	601	AATGCTAATGGTGCTTGTATGACCAAGCAGGAGTCTGCTGTGCTCTTGTT	650
Niben101Scf24	651	GGAATCCCTGCTGTTGGGTTCCCTGCTTTGGTTCCTGGGCATCATATGCC	700
bZIP60_1	651	GGAATCCCTGCTGTTGGGTTCCCTGCTTTGGTTCCTGGGCATCATATGCC	700
Niben101Scf24	701	TGCTCATTCTTCCCAGCCAACCCTGGTTAATTCAGAAGAAAATCAACGA	750
bZIP60_1	701	TGCTCATTCTTCCCAGCCAACCCTGGTTAATTCAGAAGAAAATCAACGA	750
Niben101Scf24	751	AGCAGAAACCACGGTCTTCTGGTTCGATAAAGGGAGGAAATAAGGCTGG	800
bZIP60_1	751	AGCAGAAACCACGGTCTTCTGGTTCGATAAAGGGAGGAAATAAGGCTGG	800
Niben101Scf24	801	TCGGATTTTTGAGTTCCTGTCCTTCATGATGGGCAAGAGATGCAAAGCTT	850
bZIP60_1	801	TCGGATTTTTGAGTTCCTGTCCTTCATGATGGGCAAGAGATGCAAAGCTT	850
Niben101Scf24	851	CAAGATCGAGGATGAAGTTCAATCCCCATTCTTTGGGAATTGTTATGTGA	900
bZIP60_1	851	CAAGATCGAGGATGAAGTTCAATCCCCATTCTTTGGGAATTGTTATGTGA	900

# Length: 299

# Identity: 289/299 (96.7%)

# Similarity: 291/299 (97.3%)

# Gaps: 0/299 (0.0%)

# Score: 1485.0

#=====

confirmed	1	MVDDIDDIVGHINWDDVDDL FHNILED PADNLFS AHDP S APSIQEIEQLL	50
homologous	1	MVDDIDDIVGHINWDDVDDL FHNILED PADNLFS AHDP S APSIQEIEQLL	50
confirmed	51	MNDDEIVGHVAVGEPDFQLADDFLSDVLADSPVQSDLSHSDKVI GF PDSK	100
homologous	51	MNDDEIVGHVAVGEPDFQLADDFLSDVLADSPVQSDHSHSDKVN GF PDSK	100
confirmed	101	VSSCSEVDDDDKDK EKVSQSRIDSKDGSDELNCDDPVDK KRKRQLRNRDA	150
homologous	101	VSSGSEVDDDDK DNEKGSQSPTESKDGSELNSNDPVDK KRKRQLRNRDA	150
confirmed	151	AVRSRERKKLYVRDLELKSRYFESECKRLGLVLQCCLAENQALRFSLQNG	200
homologous	151	AVRSRERKKLYVRDLELKSRYFESECKRLGLVLQCCLAENQALRFSLQNG	200
confirmed	201	NANGACMTKQESAVLLLESLLLGSLLWFLGIICLLILPSQPWLIP EENQR	250
homologous	201	NANGACMTKQESAVLLLESLLLGSLLWFLGIICLLILPSQPWLIP EENQR	250
confirmed	251	SRNHGLLVPIKGGNKAGRIF EFLS FMMGKRCKASRSRMKFNPHSLGIVM	299
homologous	251	SRNHGLLVPIKGGNKAGRIF EFLS FMMGKRCKASRSRMKFNPHSLGIVM	299

(0) **Start** **EcoRI** (17) **MssI** (427) **SapI** (649) **End** (3008)

## 2. Plasmid maps

pJET\_linearized  
3008 bp

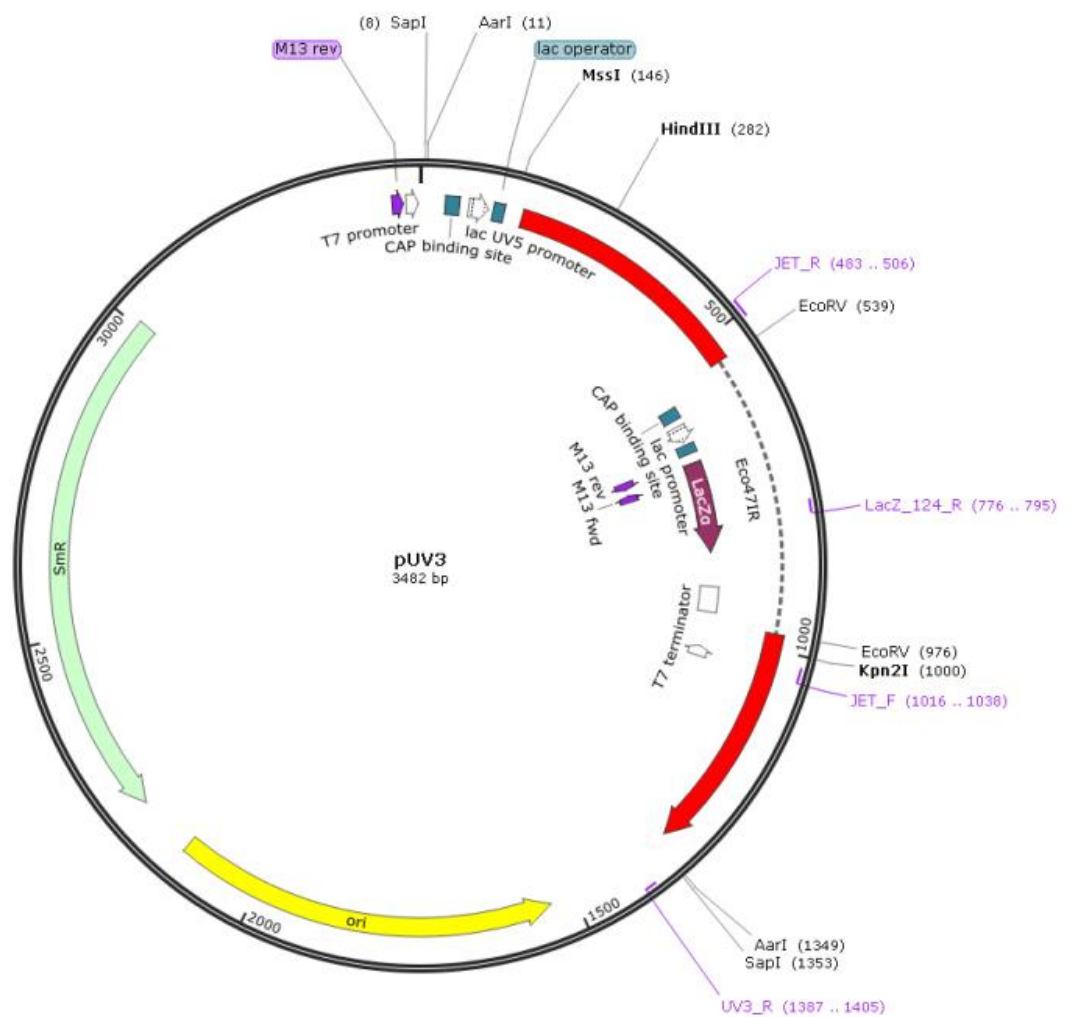
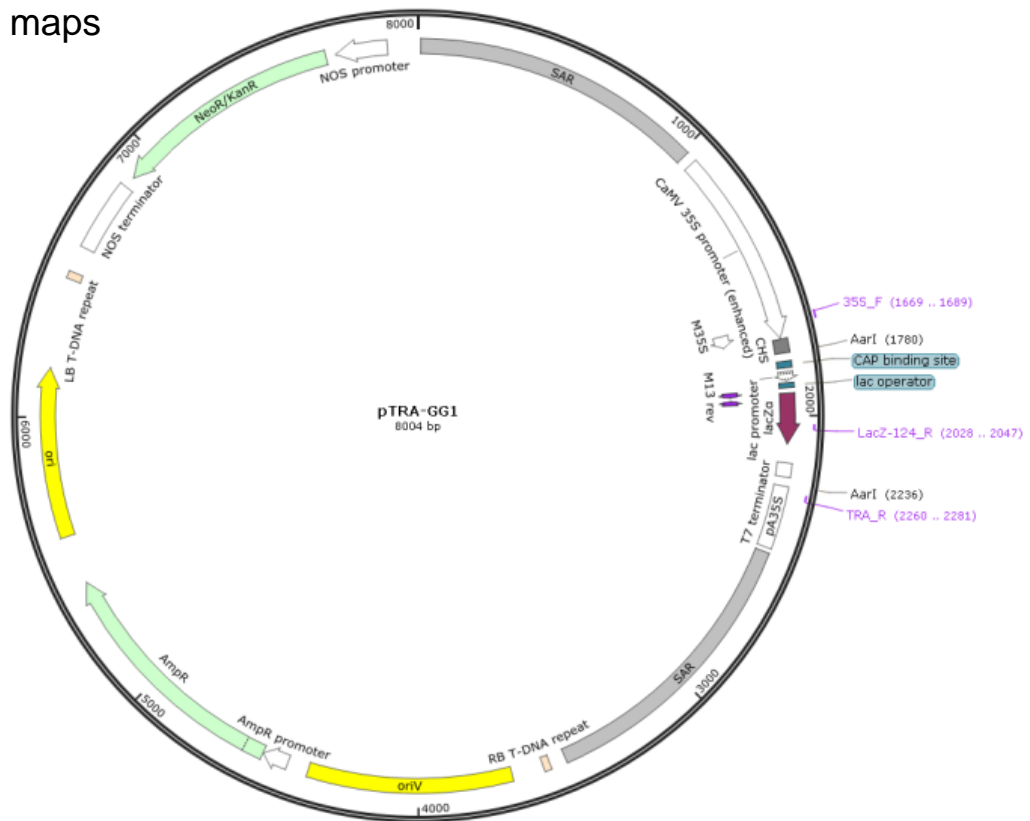


Fig. 31: Plasmid maps of utilized plasmids as vector backbones. Generated with SnapGene.



### 3. Pictures of false positive signals emitted from leaf tissue under UV lamp

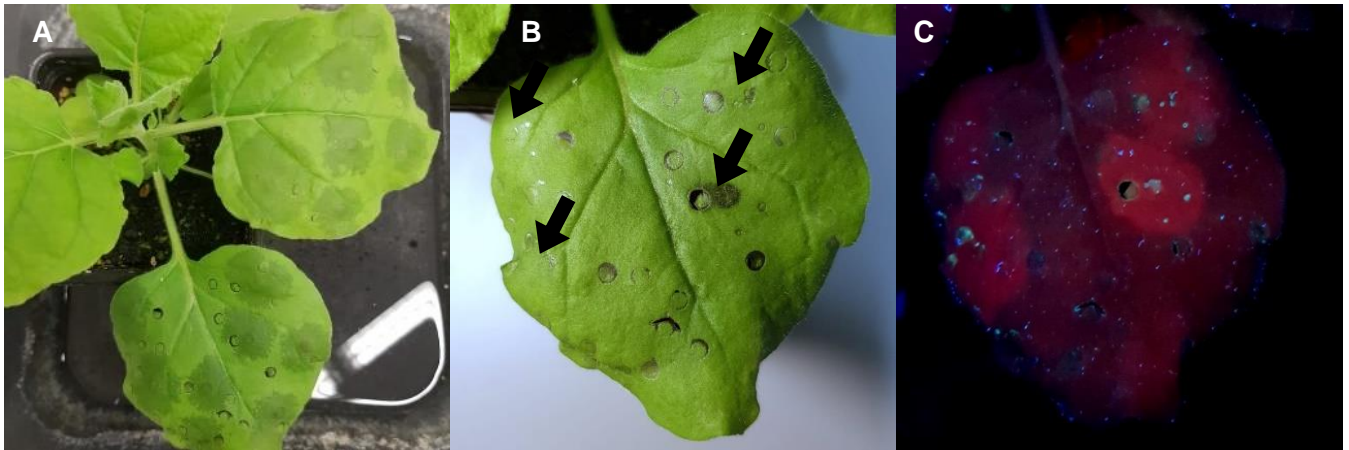


Fig. 32: A: Two leaves after infiltration with JBE20 on the leaf side and infiltrated with JBE21 on the right side. B: Leaf infiltrated with JBE20 and JBE21 3dpi under normal light conditions with black arrow marking 50mM DTT injection spot. C: Same leaf as B being excited with UV light at 366nm and emitting shining spots indicating UPR.

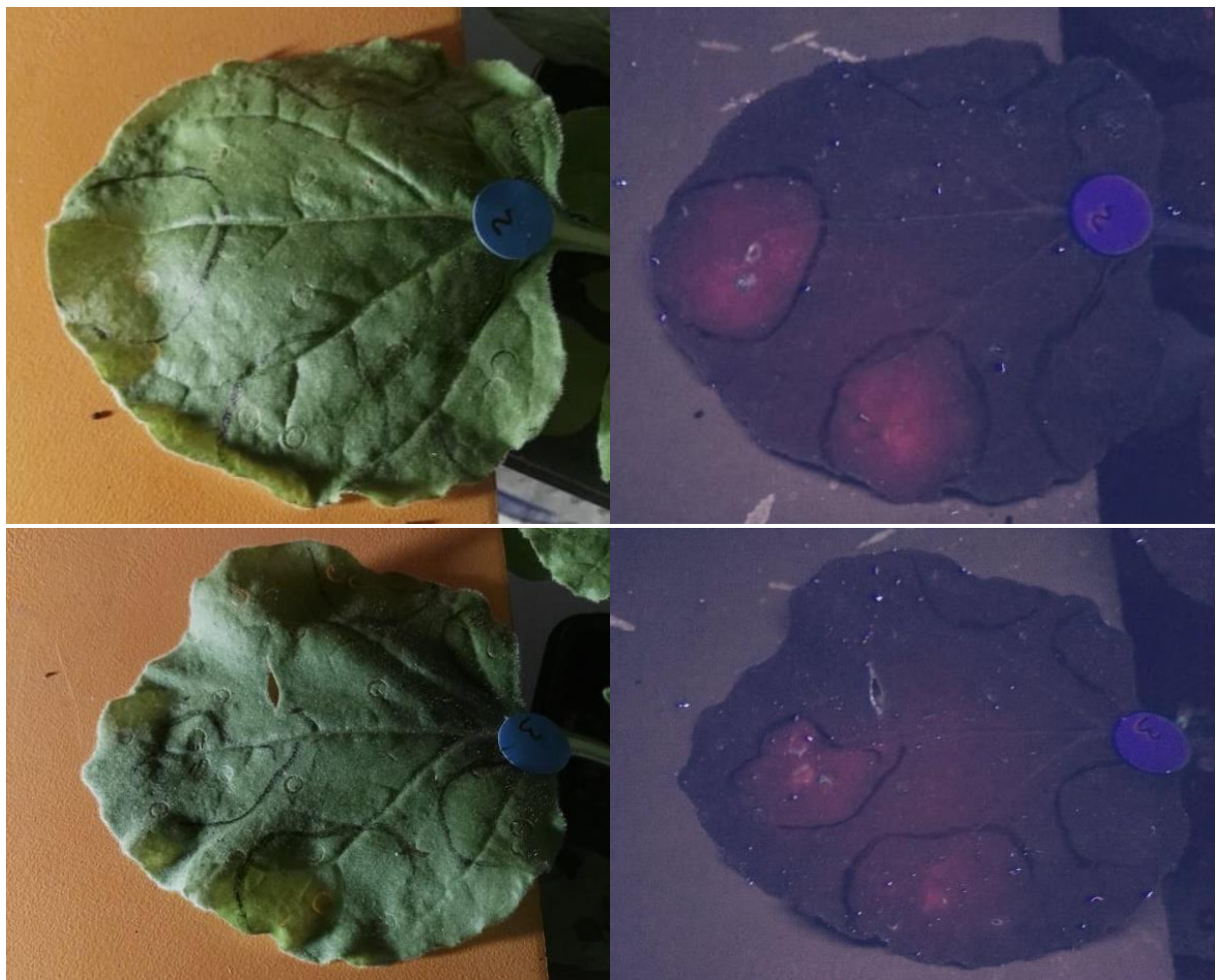


Fig. 33: False positive signal patches detected on leaves under UV lamp after DTT infiltration. Initially, it was assumed the fluorescence derives from the activated sensor construct; however, it was shown through control assays that DTT itself disturbs the tissue leading to observable autofluorescence.

#### 4. Structure of JBE22s - the second positive control sensor variant

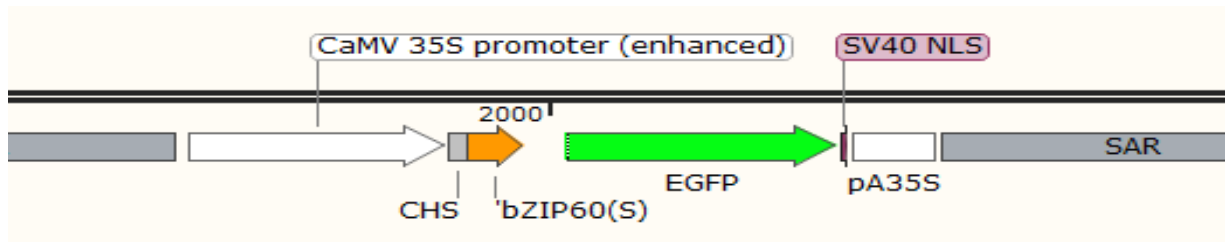


Fig. 34: Construct of the short always-on sensor with the same gene cassette as full-length always-on sensor (JBE20) except the length of bZIP60 being minimal as JBE22. Generated with SnapGene.

#### 5. Pictures from confocal microscopy

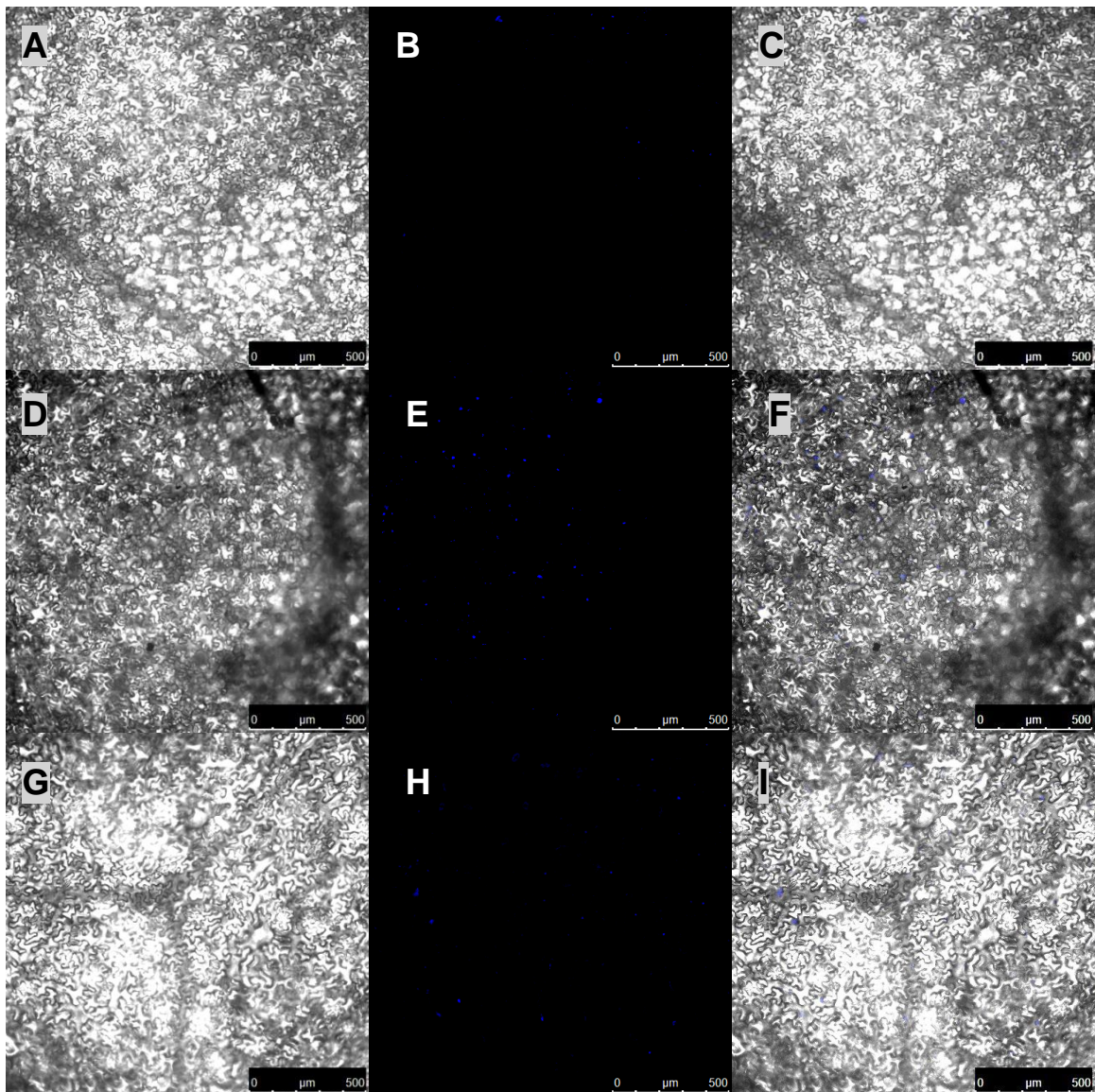


Fig. 35: Representative pictures taken by Elsa Arcalis from tissues infiltrated with TSF 1 to 3 at OD<sub>600</sub> of 0,2 under confocal microscope at same laser conditions 3dpi (bar=500μm). A to C: Same tissue section infiltrated with TSF1 and 2dpi later with H<sub>2</sub>O. A: Intact cells under bright light. B: Few cells are emitting weak fluorescence under UV light. C: Overlay of A and B. D to F: Same tissue section infiltrated with TSF1 and 2dpi later with 25mM DTT. D: Intact cells under bright light. E: Multiple cells showing fluorescence signals under UV light. F: Overlay of D and E. G to I: Same tissue section infiltrated with TSF3 and 2dpi later with 6,25mM DTT. G: Intact cells under bright light. H: Multiple cells emitting signal under UV light. I: Overlay of G and H.

## List of Figures and Tables

Fig. 1:	14
Fig. 2:	19
Fig. 3:	22
Fig. 4:	23
Fig. 5:	39
Fig. 6:	41
Fig. 7:	42
Fig. 8:	43
Fig. 9:	43
Fig. 10:	44
Fig. 11:	45
Fig. 12:	45
Fig. 13:	46
Fig. 14:	46
Fig. 15:	47
Fig. 16:	48
Fig. 17:	49
Fig. 18:	50
Fig. 19:	52
Fig. 20:	53
Fig. 21:	53
Fig. 22:	54
Fig. 23:	55
Fig. 24:	56
Fig. 25:	57
Fig. 26:	57
Fig. 27:	59
Fig. 28:	61
Fig. 29:	62
Fig. 30:	65
Fig. 31:	71
Fig. 32:	72
Fig. 33:	72
Fig. 34:	73
Fig. 35:	73
Tab. 1:	13
Tab. 2:	18
Tab. 3:	48
Tab. 4:	52
Tab. 5:	63
Tab. 6:	64



## Publication bibliography

Barta, A.; Sommergruber, K.; Thompson, D.; Hartmuth, K.; Matzke, M. A.; Matzke, A. J. (1986): The expression of a nopaline synthase - human growth hormone chimaeric gene in transformed tobacco and sunflower callus tissue. In *Plant molecular biology* 6 (5), pp. 347–357. DOI: 10.1007/BF00034942.

Bashandy, Hany; Jalkanen, Salla; Teeri, Teemu H. (2015): Within leaf variation is the largest source of variation in agroinfiltration of *Nicotiana benthamiana*. In *Plant methods* 11, p. 47. DOI: 10.1186/s13007-015-0091-5.

Benfey, P. N.; Chua, N. H. (1990): The Cauliflower Mosaic Virus 35S Promoter: Combinatorial Regulation of Transcription in Plants. In *Science (New York, N.Y.)* 250 (4983), pp. 959–966. DOI: 10.1126/science.250.4983.959.

Bombarely, Aureliano; Rosli, Hernan G.; Vrebalov, Julia; Moffett, Peter; Mueller, Lukas A.; Martin, Gregory B. (2012): A draft genome sequence of *Nicotiana benthamiana* to enhance molecular plant-microbe biology research. In *Molecular plant-microbe interactions : MPMI* 25 (12), pp. 1523–1530. DOI: 10.1094/MPMI-06-12-0148-TA.

Boss, M. A.; Kenten, J. H.; Wood, C. R.; Emtage, J. S. (1984): Assembly of functional antibodies from immunoglobulin heavy and light chains synthesised in *E. coli*. In *Nucleic acids research* 12 (9), pp. 3791–3806. DOI: 10.1093/nar/12.9.3791.

Bravo, Roberto; Gutierrez, Tomás; Paredes, Felipe; Gatica, Damián; Rodriguez, Andrea E.; Pedrozo, Zully et al. (2012): Endoplasmic reticulum: ER stress regulates mitochondrial bioenergetics. In *The international journal of biochemistry & cell biology* 44 (1), pp. 16–20. DOI: 10.1016/j.biocel.2011.10.012.

Buiatti, M.; Christou, P.; Pastore, G. (2012): The application of GMOs in agriculture and in food production for a better nutrition: two different scientific points of view. In *Genes & Nutrition* 8 (3), pp. 255–270. DOI: 10.1007/s12263-012-0316-4.

Buss, Nicholas A. P. S.; Henderson, Simon J.; McFarlane, Mary; Shenton, Jacintha M.; Haan, Lolke de (2012): Monoclonal antibody therapeutics: history and future. In *Current opinion in pharmacology* 12 (5), pp. 615–622. DOI: 10.1016/j.coph.2012.08.001.

Buyel, Johannes F. (2018): Plant Molecular Farming - Integration and Exploitation of Side Streams to Achieve Sustainable Biomanufacturing. In *Frontiers in plant science* 9, p. 1893. DOI: 10.3389/fpls.2018.01893.

Carolino, Sonia Madali Boseja; Vaez, Juliana Rocha; Irsigler, André Southernman Teixeira; Valente, Maria Anete S.; Rodrigues, Leonardo Augusto Zebral; Fontes, Elizabeth Pacheco Batista (2003): Plant BiP gene family: differential expression, stress induction and protective role against physiological stresses. In *Brazilian Journal of Plant Physiology* 15 (2), pp. 59–66. DOI: 10.1590/S1677-04202003000200001.

Castilho, Alexandra; Bohorova, Natasha; Grass, Josephine; Bohorov, Ognian; Zeitlin, Larry; Whaley, Kevin et al. (2011): Rapid high yield production of different glycoforms of Ebola virus monoclonal antibody. In *PLoS ONE* 6 (10), e26040. DOI: 10.1371/journal.pone.0026040.

Chan, Xiao Ying (2017): Molecular expression of recombinant Apoptin in planta and preliminary evaluation of biological characteristics of plant-made Apoptin on cancerous cells. PhD. University of Nottingham. Available online at <http://eprints.nottingham.ac.uk/id/eprint/42889>, checked on 9/8/2019.

Cho, Yueh; Kanehara, Kazue (2017): Endoplasmic Reticulum Stress Response in Arabidopsis Roots. In *Frontiers in plant science* 8, p. 144. DOI: 10.3389/fpls.2017.00144.

Cold Spring Harbor Protocols (2006 - 2019): Cold Spring Harbor Protocols. Archive. Edited by Richard Sever. Cold Spring Harbor Laboratory Press. Available online at <http://cshprotocols.cshlp.org/>.

Colin Dingwall; Stephen V. Sharnick; Ronald A. Laskey (1982): A polypeptide domain that specifies migration of nucleoplasmin into the nucleus. In *Cell* 30 (2), pp. 449–458. DOI: 10.1016/0092-8674(82)90242-2.

Croce, A. C.; Bottiroli, G. (2014): Autofluorescence spectroscopy and imaging: a tool for biomedical research and diagnosis. In *European journal of histochemistry : EJH* 58 (4), p. 2461. DOI: 10.4081/ejh.2014.2461.

Deng, Yan; Srivastava, Renu; Howell, Stephen H. (2013): Endoplasmic reticulum (ER) stress response and its physiological roles in plants. In *International journal of molecular sciences* 14 (4), pp. 8188–8212. DOI: 10.3390/ijms14048188.

Donini, Marcello; Marusic, Carla (2019): Current state-of-the-art in plant-based antibody production systems. In *Biotechnology letters* 41 (3), pp. 335–346. DOI: 10.1007/s10529-019-02651-z.

Engler, Carola; Gruetzner, Ramona; Kandzia, Romy; Marillonnet, Sylvestre (2009): Golden gate shuffling: a one-pot DNA shuffling method based on type IIs restriction enzymes. In *PLoS ONE* 4 (5), e5553. DOI: 10.1371/journal.pone.0005553.

Fischer, Rainer; Schillberg, Stefan; Buyel, Johannes F.; Twyman, Richard M. (2013): Commercial aspects of pharmaceutical protein production in plants. In *Current pharmaceutical design* 19 (31), pp. 5471–5477. DOI: 10.2174/1381612811319310002.

Gachon, Claire; Mingam, Annaïck; Charrier, Bénédicte (2004): Real-time PCR: what relevance to plant studies? In *Journal of experimental botany* 55 (402), pp. 1445–1454. DOI: 10.1093/jxb/erh181.

Gomord, Véronique; Fitchette, Anne-Catherine; Menu-Bouaouiche, Laurence; Saint-Jore-Dupas, Claude; Plasson, Carole; Michaud, Dominique; Faye, Loïc (2010): Plant-specific glycosylation patterns in the context of therapeutic protein production. In *Plant biotechnology journal* 8 (5), pp. 564–587. DOI: 10.1111/j.1467-7652.2009.00497.x.

Goulet, Marie-Claire; Gaudreau, Linda; Gagné, Marielle; Maltais, Anne-Marie; Laliberté, Ann-Catherine; Éthier, Gilbert et al. (2019): Production of Biopharmaceuticals in *Nicotiana benthamiana*-Axillary Stem Growth as a Key Determinant of Total Protein Yield. In *Frontiers in plant science* 10, p. 735. DOI: 10.3389/fpls.2019.00735.

Hamorsky, Krystal Teasley; Kouokam, J. Calvin; Jurkiewicz, Jessica M.; Nelson, Bailey; Moore, Lauren J.; Husk, Adam S. et al. (2015): N-glycosylation of cholera toxin B subunit in *Nicotiana benthamiana*: impacts on host stress response, production yield and vaccine potential. In *Scientific reports* 5, p. 8003. DOI: 10.1038/srep08003.

He, Li; Binari, Richard; Huang, Jiuhong; Falo-Sanjuan, Julia; Perrimon, Norbert (2019): In vivo study of gene expression with an enhanced dual-color fluorescent transcriptional timer. In *eLife* 8. DOI: 10.7554/eLife.46181.

Henriquez-Valencia, Carlos; Moreno, Adrian A.; Sandoval-Ibañez, Omar; Mitina, Irina; Blanco-Herrera, Francisca; Cifuentes-Esquivel, Nicolas; Orellana, Ariel (2015): bZIP17 and bZIP60 Regulate the Expression of BiP3 and Other Salt Stress Responsive Genes in an UPR-Independent Manner in *Arabidopsis thaliana*. In *Journal of cellular biochemistry* 116 (8), pp. 1638–1645. DOI: 10.1002/jcb.25121.

Heppert, Jennifer K.; Dickinson, Daniel J.; Pani, Ariel M.; Higgins, Christopher D.; Steward, Annette; Ahringer, Julie et al. (2016): Comparative assessment of fluorescent proteins for in vivo imaging in an animal model system. In *Molecular Biology of the Cell* 27 (22), pp. 3385–3394. DOI: 10.1091/mbc.E16-01-0063.

Hiatt, Andrew; Caffferkey, Robert; Bowdish, Katherine (1989): Production of antibodies in transgenic plants. In *Nature* 342 (6245), pp. 76–78. DOI: 10.1038/342076a0.

Holtz, Barry R.; Berquist, Brian R.; Bennett, Lindsay D.; Kommineni, Vally J. M.; Munigunti, Ranjith K.; White, Earl L. et al. (2015): Commercial-scale biotherapeutics manufacturing facility for plant-made pharmaceuticals. In *Plant biotechnology journal* 13 (8), pp. 1180–1190. DOI: 10.1111/pbi.12469.

Hostettler, Lola; Grundy, Laura; Käser-Pébernard, Stéphanie; Wicky, Chantal; Schafer, William R.; Glauser, Dominique A. (2017): The Bright Fluorescent Protein mNeonGreen Facilitates Protein Expression Analysis In Vivo. In *G3 (Bethesda, Md.)* 7 (2), pp. 607–615. DOI: 10.1534/g3.116.038133.

Howell, Stephen H. (2013): Endoplasmic reticulum stress responses in plants. In *Annual review of plant biology* 64, pp. 477–499. DOI: 10.1146/annurev-arplant-050312-120053.

Hudson, P. J. (1999): Recombinant antibody constructs in cancer therapy. In *Current opinion in immunology* 11 (5), pp. 548–557.

Hwang, Hau-Hsuan; Yu, Manda; Lai, Erh-Min (2017): Agrobacterium-mediated plant transformation: biology and applications. In *The arabidopsis book* 15, e0186. DOI: 10.1199/tab.0186.

Icon Genetics (1/28/2010): Bayer starts clinical Phase I study with personalized vaccine from tobacco plants Idiotypic vaccination in the treatment of non-Hodgkin's lymphoma. Leverkusen (Germany). online.

Available online at <https://www.icongenetics.com/bayer-starts-clinical-phase-i-study-with-personalized-vaccine-from-tobacco-plants-idiotypic-vaccination-in-the-treatment-of-non-hodgkins-lymphoma/>, checked on 8/20/2019.

Iwata, Yuji; Koizumi, Nozomu (2005): An Arabidopsis transcription factor, AtbZIP60, regulates the endoplasmic reticulum stress response in a manner unique to plants. In *Proceedings of the National Academy of Sciences of the United States of America* 102 (14), pp. 5280–5285. DOI: 10.1073/pnas.0408941102.

Iwawaki, Takao; Akai, Ryoko; Kohno, Kenji; Miura, Masayuki (2004): A transgenic mouse model for monitoring endoplasmic reticulum stress. In *Nature medicine* 10 (1), pp. 98–102. DOI: 10.1038/nm970.

Jakoby, Marc; Weisshaar, Bernd; Dröge-Laser, Wolfgang; Vicente-Carbajosa, Jesus; Tiedemann, Jens; Kroj, Thomas; Parcy, François (2002): bZIP transcription factors in Arabidopsis. In *Trends in Plant Science* 7 (3), pp. 106–111. DOI: 10.1016/S1360-1385(01)02223-3.

Keshavareddy, G.; Kumar, A.R.V.; S. Ramu, Vemanna (2018): Methods of Plant Transformation- A Review. In *Int.J.Curr.Microbiol.App.Sci* 7 (07), pp. 2656–2668. DOI: 10.20546/ijcmas.2018.707.312.

Komarova, Tatiana V.; Baschieri, Selene; Donini, Marcello; Marusic, Carla; Benvenuto, Eugenio; Dorokhov, Yuri L. (2010): Transient expression systems for plant-derived biopharmaceuticals. In *Expert review of vaccines* 9 (8), pp. 859–876. DOI: 10.1586/erv.10.85.

Komori, Toshiyuki; Imayama, Teruyuki; Kato, Norio; Ishida, Yuji; Ueki, Jun; Komari, Toshihiko (2007): Current status of binary vectors and superbinary vectors. In *Plant physiology* 145 (4), pp. 1155–1160. DOI: 10.1104/pp.107.105734.

Kunert, Renate; Reinhart, David (2016): Advances in recombinant antibody manufacturing. In *Applied Microbiology and Biotechnology* 100 (8), pp. 3451–3461. DOI: 10.1007/s00253-016-7388-9.

Kwon, Kwang-Chul; Verma, Dheeraj; Singh, Nameirakpam D.; Herzog, Roland; Daniell, Henry (2013): Oral delivery of human biopharmaceuticals, autoantigens and vaccine antigens bioencapsulated in plant cells. In *Advanced drug delivery reviews* 65 (6), pp. 782–799. DOI: 10.1016/j.addr.2012.10.005.

Lajoie, Patrick; Fazio, Elena N.; Snapp, Erik L. (2014): Approaches to imaging unfolded secretory protein stress in living cells. In *Endoplasmic reticulum stress in diseases* 1 (1), pp. 27–39. DOI: 10.2478/ersc-2014-0002.

Lakatos, Lóránt; Szittya, György; Silhavy, Dániel; Burgyán, József (2004): Molecular mechanism of RNA silencing suppression mediated by p19 protein of tombusviruses. In *The EMBO journal* 23 (4), pp. 876–884. DOI: 10.1038/sj.emboj.7600096.

Lambertz, Camilla; Garvey, Megan; Klinger, Johannes; Heesel, Dirk; Klose, Holger; Fischer, Rainer; Commandeur, Ulrich (2014): Challenges and advances in the heterologous expression of cellulolytic enzymes: a review. In *Biotechnology for biofuels* 7 (1), p. 135. DOI: 10.1186/s13068-014-0135-5.

Largent, Emily A. (2016): EBOLA and FDA: reviewing the response to the 2014 outbreak, to find lessons for the future. In *Journal of law and the biosciences* 3 (3), pp. 489–537. DOI: 10.1093/jlb/lsw046.

Leite, Michel L.; Sampaio, Kamila B.; Costa, Fabrício F.; Franco, Octávio L.; Dias, Simoni C.; Cunha, Nicolau B. (2019): Molecular farming of antimicrobial peptides: available platforms and strategies for improving protein biosynthesis using modified virus vectors. In *Anais da Academia Brasileira de Ciencias* 91 (suppl 1), e20180124. DOI: 10.1590/0001-3765201820180124.

Leuzinger, Kahlin; Dent, Matthew; Hurtado, Jonathan; Stahnke, Jake; Lai, Huafang; Zhou, Xiaohong; Chen, Qiang (2013): Efficient agroinfiltration of plants for high-level transient expression of recombinant proteins. In *Journal of visualized experiments : JoVE* (77). DOI: 10.3791/50521.

Liu, Jian-Xiang; Srivastava, Renu; Che, Ping; Howell, Stephen H. (2007): An endoplasmic reticulum stress response in Arabidopsis is mediated by proteolytic processing and nuclear relocation of a membrane-associated transcription factor, bZIP28. In *The Plant cell* 19 (12), pp. 4111–4119. DOI: 10.1105/tpc.106.050021.

Lu, Yuwen; Yin, Mingyuan; Wang, Xiaodan; Chen, Binghua; Yang, Xue; Peng, Jiejun et al. (2016): The unfolded protein response and programmed cell death are induced by expression of Garlic virus X p11 in *Nicotiana benthamiana*. In *The Journal of general virology* 97 (6), pp. 1462–1468. DOI: 10.1099/jgv.0.000460.

Ma, Julian K-C; Barros, Eugenia; Bock, Ralph; Christou, Paul; Dale, Philip J.; Dix, Philip J. et al. (2005): Molecular farming for new drugs and vaccines. Current perspectives on the production of pharmaceuticals in transgenic plants. In *EMBO reports* 6 (7), pp. 593–599. DOI: 10.1038/sj.embor.7400470.

Ma, Julian K-C; Christou, Paul; Chikwamba, Rachel; Haydon, Hugh; Paul, Mathew; Ferrer, Merardo Pujol et al. (2013): Realising the value of plant molecular pharming to benefit the poor in developing countries and emerging economies. In *Plant biotechnology journal* 11 (9), pp. 1029–1033. DOI: 10.1111/pbi.12127.

Ma, Julian K-C; Drossard, Jürgen; Lewis, David; Altmann, Friedrich; Boyle, Julia; Christou, Paul et al. (2015): Regulatory approval and a first-in-human phase I clinical trial of a monoclonal antibody produced in transgenic tobacco plants. In *Plant biotechnology journal* 13 (8), pp. 1106–1120. DOI: 10.1111/pbi.12416.

Maclean, J.; Koekemoer, M.; Olivier, A. J.; Stewart, D.; Hitzeroth, I. I.; Rademacher, T. et al. (2007): Optimization of human papillomavirus type 16 (HPV-16) L1 expression in plants: comparison of the suitability of different HPV-16 L1 gene variants and different cell-compartment localization. In *The Journal of general virology* 88 (Pt 5), pp. 1460–1469. DOI: 10.1099/vir.0.82718-0.

Martínez, Immaculada M.; Chrispeels, Maarten J. (2003): Genomic analysis of the unfolded protein response in Arabidopsis shows its connection to important cellular processes. In *The Plant cell* 15 (2), pp. 561–576. DOI: 10.1105/tpc.007609.



Martinis, Domenico de; Rybicki, Edward P.; Fujiyama, Kazuhito; Franconi, Rosella; Benvenuto, Eugenio (2016): Editorial: Plant Molecular Farming: Fast, Scalable, Cheap, Sustainable. In *Frontiers in plant science* 7, p. 1148. DOI: 10.3389/fpls.2016.01148.

Matoba, Nobuyuki; Davis, Keith R.; Palmer, Kenneth E. (2011): Recombinant protein expression in *Nicotiana*. In *Methods in molecular biology (Clifton, N.J.)* 701, pp. 199–219. DOI: 10.1007/978-1-61737-957-4\_11.

Matz, M. V.; Fradkov, A. F.; Labas, Y. A.; Savitsky, A. P.; Zarsky, A. G.; Markelov, M. L.; Lukyanov, S. A. (1999): Fluorescent proteins from nonbioluminescent Anthozoa species. In *Nature biotechnology* 17 (10), pp. 969–973. DOI: 10.1038/13657.

Melnik, Stanislav; Neumann, Anna-Cathrine; Karongo, Ryan; Dirndorfer, Sebastian; Stübler, Martin; Ibl, Verena et al. (2018): Cloning and plant-based production of antibody MC10E7 for a lateral flow immunoassay to detect 4-argininemicrocystin in freshwater. In *Plant biotechnology journal* 16 (1), pp. 27–38. DOI: 10.1111/pbi.12746.

Menassa, Rima; Ahmad, Adil; Joensuu, Jussi J. (2012): Transient Expression Using Agrobacterium Infiltration and Its Applications in Molecular Farming. In Aiming Wang, Shengwu Ma (Eds.): *Molecular farming in plants. Recent advances and future prospects* / Aiming Wang, Shengwu Ma, editors, vol. 27. Dordrecht, London: Springer, pp. 183–198.

Montero-Morales, Laura; Steinkellner, Herta (2018): Advanced Plant-Based Glycan Engineering. In *Frontiers in bioengineering and biotechnology* 6, p. 81. DOI: 10.3389/fbioe.2018.00081.

Mor, Tsafir S. (2015): Molecular pharming's foot in the FDA's door: Protalix's trailblazing story. In *Biotechnology letters* 37 (11), pp. 2147–2150. DOI: 10.1007/s10529-015-1908-z.

Moustafa, Khaled; Makhzoum, Abdullah; Trémouillaux-Guiller, Jocelyne (2016): Molecular farming on rescue of pharma industry for next generations. In *Critical reviews in biotechnology* 36 (5), pp. 840–850. DOI: 10.3109/07388551.2015.1049934.

Nagashima, Yukihiro; Mishiba, Kei-Ichiro; Suzuki, Eiji; Shimada, Yukihiro; Iwata, Yuji; Koizumi, Nozomu (2011): Arabidopsis IRE1 catalyses unconventional splicing of bZIP60 mRNA to produce the active transcription factor. In *Scientific reports* 1, p. 29. DOI: 10.1038/srep00029.

Nandi, Somen; Kwong, Aaron T.; Holtz, Barry R.; Erwin, Robert L.; Marcel, Sylvain; McDonald, Karen A. (2016): Techno-economic analysis of a transient plant-based platform for monoclonal antibody production. In *mAbs* 8 (8), pp. 1456–1466. DOI: 10.1080/19420862.2016.1227901.

Nawkar, Ganesh M.; Lee, Eun Seon; Shelake, Rahul M.; Park, Joung Hun; Ryu, Seoung Woo; Kang, Chang Ho; Lee, Sang Yeol (2018): Activation of the Transducers of Unfolded Protein Response in Plants. In *Frontiers in plant science* 9, p. 214. DOI: 10.3389/fpls.2018.00214.

Nelson, P. N.; Reynolds, G. M.; Waldron, E. E.; Ward, E.; Giannopoulos, K.; Murray, P. G. (2000): Monoclonal antibodies. In *Molecular pathology : MP* 53 (3), pp. 111–117. DOI: 10.1136/mp.53.3.111.

Niazian, M.; Sadat Noori, S. A.; Galuszka, P.; Mortazavian, S.M.M. (2017): Tissue culture-based Agrobacterium-mediated and in planta transformation methods. In *Czech J. Genet. Plant Breed.* 53 (No. 4), pp. 133–143. DOI: 10.17221/177/2016-CJGPB.

Odell, J. T.; Nagy, F.; Chua, N. H. (1985): Identification of DNA sequences required for activity of the cauliflower mosaic virus 35S promoter. In *Nature* 313 (6005), pp. 810–812. DOI: 10.1038/313810a0.

Owczarek, B.; Gerszberg, A.; Hnatuszko-Konka, K. (2019): A Brief Reminder of Systems of Production and Chromatography-Based Recovery of Recombinant Protein Biopharmaceuticals. In *BioMed Research International* 2019, p. 4216060. DOI: 10.1155/2019/4216060.

Parra-Rojas, Juan; Moreno, Adrian A.; Mitina, Irina; Orellana, Ariel (2015): The Dynamic of the Splicing of bZIP60 and the Proteins Encoded by the Spliced and Unspliced mRNAs Reveals Some Unique Features during the Activation of UPR in *Arabidopsis thaliana*. In *PLoS ONE* 10 (4). DOI: 10.1371/journal.pone.0122936.

Paul, Matthew J.; Thangaraj, Harry; Ma, Julian K-C (2015): Commercialization of new biotechnology: a systematic review of 16 commercial case studies in a novel manufacturing sector. In *Plant biotechnology journal* 13 (8), pp. 1209–1220. DOI: 10.1111/pbi.12426.

Pujol, Merardo; Gavilondo, Jorge; Ayala, Marta; Rodríguez, Meilyn; González, Ernesto M.; Pérez, Lincidio (2007): Fighting cancer with plant-expressed pharmaceuticals. In *Trends in biotechnology* 25 (10), pp. 455–459. DOI: 10.1016/j.tibtech.2007.09.001.

Rademacher, Thomas; Sack, Markus; Blessing, Daniel; Fischer, Rainer; Holland, Tanja; Buyel, Johannes (2019): Plant cell packs: a scalable platform for recombinant protein production and metabolic engineering. In *Plant biotechnology journal* 17 (8), pp. 1560–1566. DOI: 10.1111/pbi.13081.

Rosales-Mendoza, Sergio; Tello-Olea, Marlene Anahí (2015): Carrot cells: a pioneering platform for biopharmaceuticals production. In *Molecular biotechnology* 57 (3), pp. 219–232. DOI: 10.1007/s12033-014-9837-y.

Roy, Gargi; Zhang, Shu; Li, Lina; Higham, Eileen; Wu, Herren; Marelli, Marcello; Bowen, Michael A. (2017): Development of a fluorescent reporter system for monitoring ER stress in Chinese hamster ovary cells and its application for therapeutic protein production. In *PLoS ONE* 12 (8), e0183694. DOI: 10.1371/journal.pone.0183694.

Sack, Markus; Hofbauer, Anna; Fischer, Rainer; Stoger, Eva (2015): The increasing value of plant-made proteins. In *Current opinion in biotechnology* 32, pp. 163–170. DOI: 10.1016/j.copbio.2014.12.008.

Schillberg, Stefan; Raven, Nicole; Spiegel, Holger; Rasche, Stefan; Buntru, Matthias (2019): Critical Analysis of the Commercial Potential of Plants for the Production of Recombinant Proteins. In *Frontiers in plant science* 10, p. 720. DOI: 10.3389/fpls.2019.00720.

Shamloul, Moneim; Trusa, Jason; Mett, Vadim; Yusibov, Vidadi (2014): Optimization and utilization of *Agrobacterium*-mediated transient protein production in *Nicotiana*. In *Journal of visualized experiments : JoVE* (86). DOI: 10.3791/51204.

Shaner, Nathan C.; Lambert, Gerard G.; Chammass, Andrew; Ni, Yuhui; Cranfill, Paula J.; Baird, Michelle A. et al. (2013): A bright monomeric green fluorescent protein derived from *Branchiostoma lanceolatum*. In *Nature methods* 10 (5), pp. 407–409. DOI: 10.1038/nmeth.2413.

Shanmuganathan, Vivekanandan; Schiller, Nina; Magoulopoulou, Anastasia; Cheng, Jingdong; Braunger, Katharina; Cymer, Florian et al. (2019): Structural and mutational analysis of the ribosome-arresting human XBP1u. In *eLife* 8. DOI: 10.7554/eLife.46267.

Sijmons, P. C.; Dekker, B. M.; Schrammeijer, B.; Verwoerd, T. C.; van den Elzen, P J; Hoekema, A. (1990): Production of correctly processed human serum albumin in transgenic plants. In *Bio/technology (Nature Publishing Company)* 8 (3), pp. 217–221.

Sone, Michio; Zeng, Xiaomei; Larese, Joseph; Ryoo, Hyung Don (2012): A modified UPR stress sensing system reveals a novel tissue distribution of IRE1/XBP1 activity during normal *Drosophila* development. In *Cell Stress & Chaperones* 18 (3), pp. 307–319. DOI: 10.1007/s12192-012-0383-x.

Song, Ilchan; Kang, YangJoo; Lee, Young Koun; Myung, Soon-Chul; Ko, Kisung (2018): Endoplasmic reticulum retention motif fused to recombinant anti-cancer monoclonal antibody (mAb) CO17-1A affects mAb expression and plant stress response. In *PLoS ONE* 13 (9), e0198978. DOI: 10.1371/journal.pone.0198978.

Stoger, Eva; Fischer, Rainer; Moloney, Maurice; Ma, Julian K-C (2014): Plant molecular pharming for the treatment of chronic and infectious diseases. In *Annual review of plant biology* 65, pp. 743–768. DOI: 10.1146/annurev-arplant-050213-035850.

Strasser, Richard; Altmann, Friedrich; Steinkellner, Herta (2014): Controlled glycosylation of plant-produced recombinant proteins. In *Current opinion in biotechnology* 30, pp. 95–100. DOI: 10.1016/j.copbio.2014.06.008.

Sun, Ling; Yang, Zheng-Ting; Song, Ze-Ting; Wang, Mei-Jing; Le Sun; Lu, Sun-Jie; Liu, Jian-Xiang (2013): The plant-specific transcription factor gene NAC103 is induced by bZIP60 through a new cis-regulatory element to modulate the unfolded protein response in *Arabidopsis*. In *The Plant journal : for cell and molecular biology* 76 (2), pp. 274–286. DOI: 10.1111/tpj.12287.

Topp, Edward; Irwin, Rebecca; McAllister, Tim; Lessard, Martin; Joensuu, Jussi J.; Kolotilin, Igor et al. (2016): The case for plant-made veterinary immunotherapeutics. In *Biotechnology advances* 34 (5), pp. 597–604. DOI: 10.1016/j.biotechadv.2016.02.007.

Tschofen, Marc; Knopp, Dietmar; Hood, Elizabeth; Stöger, Eva (2016): Plant Molecular Farming: Much More than Medicines. In *Annual review of analytical chemistry (Palo Alto, Calif.)* 9 (1), pp. 271–294. DOI: 10.1146/annurev-anchem-071015-041706.

Tusé, Daniel; Ku, Nora; Bendandi, Maurizio; Becerra, Carlos; Collins, Robert; Langford, Nyla et al. (2015): Clinical Safety and Immunogenicity of Tumor-Targeted, Plant-Made Id-KLH Conjugate Vaccines for Follicular Lymphoma. In *BioMed Research International* 2015. DOI: 10.1155/2015/648143.

Virdi, Vikram; Depicker, Ann (2013): Role of plant expression systems in antibody production for passive immunization. In *The International journal of developmental biology* 57 (6-8), pp. 587–593. DOI: 10.1387/ijdb.130266ad.

West, Robert (2017): Tobacco smoking: Health impact, prevalence, correlates and interventions. In *Psychology & health* 32 (8), pp. 1018–1036. DOI: 10.1080/08870446.2017.1325890.

Williams, Brett; Verchot, Jeanmarie; Dickman, Martin B. (2014): When supply does not meet demand-ER stress and plant programmed cell death. In *Frontiers in plant science* 5, p. 211. DOI: 10.3389/fpls.2014.00211.

Yanagitani, Kota; Kimata, Yukio; Kadokura, Hiroshi; Kohno, Kenji (2011): Translational pausing ensures membrane targeting and cytoplasmic splicing of XBP1u mRNA. In *Science (New York, N.Y.)* 331 (6017), pp. 586–589. DOI: 10.1126/science.1197142.

Yao, Jian; Weng, Yunqi; Dickey, Alexia; Wang, Kevin Yueju (2015): Plants as Factories for Human Pharmaceuticals: Applications and Challenges. In *International journal of molecular sciences* 16 (12), pp. 28549–28565. DOI: 10.3390/ijms161226122.

Yokota, Jun-Ichi; Shiro, Daisuke; Tanaka, Mizuki; Onozaki, Yasumichi; Mizutani, Osamu; Kakizono, Dararat et al. (2017): Cellular responses to the expression of unstable secretory proteins in the filamentous fungus *Aspergillus oryzae*. In *Applied Microbiology and Biotechnology* 101 (6), pp. 2437–2446. DOI: 10.1007/s00253-016-8086-3.

Zeitlin, Larry; Pettitt, James; Scully, Corinne; Bohorova, Natasha; Kim, Do; Pauly, Michael et al. (2011): Enhanced potency of a fucose-free monoclonal antibody being developed as an Ebola virus immunoprotectant. In *Proceedings of the National Academy of Sciences of the United States of America* 108 (51), pp. 20690–20694. DOI: 10.1073/pnas.1108360108.

Zhang, Lingrui; Chen, Hui; Brandizzi, Federica; Verchot, Jeanmarie; Wang, Aiming (2015): The UPR branch IRE1-bZIP60 in plants plays an essential role in viral infection and is complementary to the only UPR pathway in yeast. In *PLoS genetics* 11 (4), e1005164. DOI: 10.1371/journal.pgen.1005164.

Zhang, Lingrui; Zhang, Changwei; Wang, Aiming (2016): Divergence and Conservation of the Major UPR Branch IRE1-bZIP Signaling Pathway across Eukaryotes. In *Scientific reports* 6, p. 27362. DOI: 10.1038/srep27362.

Zhang, Xiuren; Henriques, Rossana; Lin, Shih-Shun; Niu, Qi-Wen; Chua, Nam-Hai (2006): Agrobacterium-mediated transformation of *Arabidopsis thaliana* using the floral dip method. In *Nature protocols* 1 (2), pp. 641–646. DOI: 10.1038/nprot.2006.97.